CFD Analysis of Airflow Patterns and Heat Transfer in Small, Medium, and Large Structures

Michael Francis Detaranto

Thesis submitted to the faculty of the Virginia Polytechnic Institute and State University in partial fulfillment of the requirements for the degree of

Master of Science

In

Mechanical Engineering

Francine Battaglia, Chair

Javid Bayandor

Scott T. Huxtable

September 26, 2014

Blacksburg, VA

Keywords: CFD, Natural Ventilation, cross-ventilation, single-sided ventilation

CFD Analysis of Airflow Patterns and Heat Transfer in Small, Medium, and Large Structures

Michael Francis Detaranto

ABSTRACT

Designing buildings to use energy more efficiently can lead to lower energy costs, while maintaining comfort for occupants. Computational fluid dynamics (CFD) can be utilized to visualize and simulate expected flows in buildings and structures. CFD gives architects and designers the ability to calculate the velocity, pressure, and heat transfer within a building. Previous research has not modeled natural ventilation situations that challenge common design rules of thumb used for cross-ventilation and single-sided ventilation. The current study uses a commercial code (FLUENT) to simulate cross-ventilation in simple structures and analyzes the flow patterns and heat transfer in the rooms. In the Casa Giuliana apartment and the Affleck house, this study simulates passive cooling in spaces well-designed for natural ventilation. Heat loads, human models, and electronics are included in the apartment to expand on prior research into natural ventilation in a full-scale building. Two different cases were simulated. The first had a volume flow rate similar to the ambient conditions, while the second had a much lower flow rate that had an ACH of 5, near the minimum recommended value Passive cooling in the Affleck house is simulated and has an unorthodox ventilation method; a window in the floor that opens to an exterior basement is opened along with windows and doors of the main floor to create a pressure difference. In the Affleck house, two different combinations of window and door openings are simulated to model different scenarios. Temperature contours, flow patterns, and the air changes per hour (ACH) are explored to analyze the ventilation of these structures.

Acknowledgements

I would like to thank the people who helped me towards this point in my academic career. First, I would like to thank Dr. Francine Battaglia. Without her, I would have been lost beginning and finishing the past year. She supported me from the beginning to the end of my research and always made time to help guide me to where I am today.

I would like to thank Prof. Ulrike Passe for her contributions to the project and her graduate student Suncica Jasarovic for creating the complex models that I worked with. I would also like to thank Dr. Bayandor and Dr. Huxtable for serving on my graduate committee.

Thank you to my co-workers and fellow students in the CREST lab: Jeff, Santhip, David, Bahareh, Elizabeth, Lu, and Rob. They all helped me through my classes and my research and made sure I was able to get through all the bumps in the road. Thank you, Jeff, for helping me with all the small problems along the way, and dealing with the nuances of working with the larger models.

Lastly, I would like to thank my family and friends. Thank you to my parents, Peggy and Frank, who continuously support me in school and life. Thank you to my fiancé, Carmi, for making sure I worked hard while ensuring I didn't forget to enjoy Blacksburg and my time there. And thank you to all my friends who were always there for me.

Table of Contents

List of Figures

List of Tables

List of Variables

Variables

Gr	Grashof Number
Ra	Rayleigh Number
Pr	Prandtl Number
Re	Reynolds Number
g	Gravity
T	Temperature
l	Length Scale
V	Velocity
μ	Dynamic Viscosity
t	Time
p	Pressure
E	Total Energy
S	Source Terms
k	Conductivity, Turbulent Kinetic Energy
h	Enthalpy
c_p	Specific Heat Capacity

Greek

$\underline{\beta}$	Thermal Expansion Coefficient
v	Kinematic Viscosity
α	Thermal Diffusion Coefficient
ρ	Density

$\bar{\bar{\tau}}$	Stress Tensor
Θ	Non-dimensional Temperature
ε	Turbulent Dissipation Rate

Subscript

0	Reference
∞	Atmospheric
s	Surface
t	Turbulence
k	Due to mean velocity gradients
b	Due to Buoyancy
P	Present Cell
i	Initial

Superscript

*	Non-dimensional value
‘	Correction

Chapter 1 Introduction

The energy to cool and ventilate buildings is expected to grow, and with the energy increase comes a rise in costs and a buildings carbon footprint. As more of the world develops into economically strong regions, the amount of energy needed to ventilate buildings will increase worldwide, as economically strong regions use 25 times more energy than impoverished regions. With the increases in energy use and cost, it is important to design buildings to have ventilation systems that are energy efficient, cost effective, and maintain occupants' comfort.

1.1 Motivation

Energy usage in buildings for space cooling and heating has been increasing over time and consequently, there is an additional cost increase. The cost to cool and ventilate buildings is expected to increase more as the population of developing countries increases, and people in economically strong regions of the world use 25 times more energy than the impoverished regions [1]. The total energy consumption for space cooling is expected to increase in the United States during the next three decades due to an increased migration to the warmer southern climates [2]. Natural ventilation can be utilized to decrease the amount of energy needed to heat and cool buildings. Naturally ventilated buildings use 40% less energy than a mechanically air-conditioned building [3]. It is most effective when the outdoor temperature is within thermal comfort levels.

While there are caveats to implementing natural ventilation, the principles can also be applied to buildings that utilize mechanical ventilation. Surveys have shown that occupants have a preference for open windows and natural light [4]. Natural ventilation has lower maintenance costs and installation costs, and buildings that are designed for natural ventilation have a reduced need for electrical and mechanical complexity and a reduced environmental impact. There is also

a connection to outdoor temperatures, which conforms to the occupant's expectations of thermal comfort. Natural ventilation is driven by wind around a building, which causes pressure differences, temperature differences between the indoor and outdoor environments, and a combination of both.

The projects in this study were conceived by Ulrike Passe, Associate Professor of Architecture at Iowa State University as an effort to study the flow patterns resulting from natural ventilation. The rooms are designed for cross-ventilation and single-sided ventilation and match common rules of thumb and are used to view the ventilation and flow through common structures. The extension of this idea to simulate cross-ventilation in a real building that employs natural ventilation principles, specifically the Casa Giuliana apartment, can be attributed to Prof. Passe. The situation that will be simulated is a common scenario of a hot summer day where an apartment is closed off from the outside until a person returns from work. A similar scenario will be simulated in the Affleck House, a Frank Lloyd Wright home in the Midwest. The models and scenarios in this study came about through collaboration with Prof. Passe and her graduate student, Suncica Jasarovic, who provided the architectural CAD files.

1.2 Background

Natural ventilation is effective in improving air quality, thermal comfort, and reducing energy consumption when utilized properly. It is most effective in climates where there is low noise, low pollution, and where the outdoor temperature is within comfort levels. Appropriate air velocities and thermal comfort levels can be found in ASHRAE standard 55 [5]. Air flow into buildings can be driven by wind velocities, buoyancy, mixing, and temperature differences.

In the design of buildings that utilize natural ventilation, architects employ certain rules of thumb. These rules originated in the Chartered Institution of Buildings Services Engineers

(CIBSE) in the UK BRE Digest [4]. The rules of thumb include recommendations for cross-ventilation and single-sided ventilation. Cross-ventilation is expected to be effective with a depth-to-height ratio (DH) of 5:1 and with an unrestricted flow path. For single-sided ventilation with only one opening, the rule of thumb is a DH of 2. If there are two openings, this ratio is 2.5. While it is unclear, it appears the rules of thumb are for moderate to high heat gains of 20-50 W/m^2. It is expected that with lower heat gains, the buildings can be naturally ventilated irrespective of size.

Two principles that are important when designing buildings for natural ventilation are thermal comfort and air quality. Recommendations for thermal comfort and maximum air velocities are prescribed in the ASHRAE standard 55 [5]. Thermal comfort is determined from conditions where 80% of the occupants find the environment acceptable. Moving air leads to an increase in the acceptable temperature. The thermal conditions and corresponding temperatures increase with air speed, and are summarized in Table 1.1 and Table 1.2 [5]. The upper limit of air speed for light activity is approximately 0.9 m/s.

Table 1.1. Thermal comfort conditions from ASHRAE Standard 55.

Outdoor Air Temperature	10°C		33.5°C	
	Lower Limit	Upper Limit	Lower Limit	Upper Limit
90% acceptable	17.5°C	23.5°C	23°C	30.5°C
80% acceptable	18.5°C	24.5°C	26°C	31°C

Table 1.2. Increase in acceptable temperature due to moving air.

Air Speed (m/s)	Temperature Increase (°C)
0.6	1.2
0.9	1.8
1.2	2.2

Designing buildings using different methods to analyze thermal comfort and air flow patterns can increase building efficiency and reduce ventilation costs. Approaches to model air flow in and around buildings include experimental methods such as wind tunnel measurements and field measurements; empirical and analytical methods; multi-zone and zonal methods; and computational fluid dynamics (CFD). CFD can be utilized to help design and analyze cooling and heating of buildings. For the purposes of this paper, the focus will be on CFD methods. CFD methods allow for a low cost alternative analysis that can model the entire building and the velocity and temperature fields within the building. A major advantage of CFD is the ability to visualize the movement of air and the heat transfer patterns in the entire structure.

Several studies have used CFD to predict natural ventilation flows. Using single-sided ventilation with one large opening, Park [6] measured heat transfer in a single room with a heater. Other studies such as Asfour et al. [7] have investigated cross-ventilation within a small structure using different sized rooms and wind angles. In Ayad, [8] cross-ventilation was studied and it was found that upstream turbulence and the placement of openings have an effect on the interior room velocity. Allocca et al. [3] simulated flow in a single-sided ventilated room and a building with heat sources, and they found that the effects of buoyancy were higher at lower wind speeds around the building and the effect decreased with higher wind speeds. The computational model used a large domain, and Allocca et al. [3] found that convergence was difficult when buoyancy effects were great.

There are few CFD investigations of full scale buildings, as large amounts of memory and computation time are needed to complete the studies. In Stoakes et al. [9,10], passive cooling and heating were investigated in the Viipuri Library and Esherick House. Stoakes et al. used windows

and doors as designated inlets and outlets to simulate the environment and the flow into the building.

1.3 Objectives

The objectives of this study are to explore and simulate the ventilation of multiple structures and to give recommendations to architects and engineers based on the results. Ansys Fluent will be employed to model and simulate air flow patterns and heat transfer in structures that utilize cross-ventilation and single-sided ventilation. Ventilation in simple structures will be modeled using different sized rooms and different sized window openings and locations. A full-scale apartment and house will also be modeled.

There are two simple structures that will be investigated in this study: a long room with two openings representing windows on each side for cross-ventilation, and a short room with two openings on one side for single-sided ventilation. The structures for cross-ventilation are designed to have a DH of 5 to match the rule of thumb. Another structure will be modeled with a DH of 7, to challenge the rule of thumb.

A combination of opening sizes will be used to investigate the effect of inlet and outlet sizes on cross-ventilation. Three rooms will be used: Room 1.1, which has a small inlet and a large outlet; Room 2.1, which has a large inlet and a small outlet; Room 1.3, which has a small inlet and a small outlet. Using these three rooms, passive cooling and passive heating will be modeled. The effects of boundary conditions will be explored to find the differing flow patterns and heat transfer in the rooms. The investigation will be done to find potential regions of stagnant or stale air, examine the overall air quality, and to make recommendations in the design of rooms that utilize cross-ventilation.

Single-sided ventilation will be investigated with two rooms: Room 2.1, which has openings on one side of the room near the lower and upper walls, and Room 2.2, which has openings on one side near center of the wall. The structures are designed to match a DH of 2.5 to match the rule of thumb and a DH of 3 to challenge the rule. The air flow patterns and overall air quality will be explored to make recommendations in the overall design utilizing single-sided ventilation. A rectangular model for a human figure is included in Room 2.1 to examine the effects on thermal stratification, air flow patterns, and air quality.

Full scale buildings will also be included in the study to model natural ventilation in real buildings designed with natural ventilation potential. The first structure is an apartment from the Casa Giuliana building in Italy. The apartment has a deck that is wind-facing and outlet windows that are mostly unaffected by the outside, a very open interior layout, and is well designed for cross-ventilation. The building is located near a lake, which drives a cool breeze into the town. Passive cooling with and without furniture, human models, and heat loads will be modeled. The overall climate and conditions of the region where the apartment is located, combined with the layout of the apartment, match a situation where natural ventilation is expected to be effective. Conditions late on a hot summer day, late at night after the exterior temperature has dropped, is simulated to examine the efficacy of natural ventilation in a real building and in a situation that challenges the effectiveness of natural ventilation.

A second building, the Affleck house, is a structure where passive cooling will be modeled. The Affleck house's main section is cooled with a window located in the floor that is above an exterior basement that is shaded by the house. The air flow into the home will be analyzed to determine the overall air quality in the house. The home is complicated and has many windows

and doors, and will be modeled with two different scenarios that are used to simulate normal cooling situations.

The current study looks to expand upon previous studies of a full scale building by modeling air flow into buildings using false surfaces to model areas where air flow is expected, while not prescribing flow rate directly into the buildings. The false surface represents a location in space where a physical boundary does not exist. An inlet is prescribed at a location where air flow from wind is expected to exist. Also, heat loads are included in the Casa Giuliana apartment to simulate a more realistic situation.

Chapter 2 Fundamental Principles

An overview of the principles of natural ventilation, the effect of a human heat load, and a measure of air quality will discussed in this chapter.

2.1 Driving Forces behind Natural Ventilation

A major force behind natural ventilation is buoyancy. Buoyancy is driven by a temperature difference between the indoor and outdoor density difference. When buoyancy is the dominant force, the flows will have an upward flow, as hot air moves upward and cold air replaces it underneath. When the temperature difference is smaller, leading to a reduced buoyancy force, the flow is downward, as air moves from top to bottom [11]. Once there is a negligible temperature difference, the stack pressure is reduced to near zero and buoyancy effects are less pronounced.

Buoyancy effects are determined by the ratio of buoyancy forces to viscous forces, known as the Grashof (Gr) number:

$$Gr = \frac{g\beta\Delta T l^3}{\nu^2} \tag{2.1}$$

where g is gravity, β is the thermal expansion coefficient, ΔT is a temperature difference, l is a length scale, and ν is the kinematic viscosity. Transition to turbulent flow approximately occurs when the Rayleigh (Ra) number is Ra = 10^9 [12]:

$$Ra = GrPr \tag{2.2}$$

where Pr is the Prandtl (Pr) number:

$$Pr = \frac{\nu}{\alpha} \tag{2.3}$$

and α is the thermal diffusivity.

Wind-driven flow is due to a pressure difference between the openings. In cross-ventilation, the pressure difference is often created by wind on the windward side. The flow creates a higher pressure on the windward side of the building and a lower pressure on the leeward side, driving flow from windward to leeward [13]. Other driving forces in wind-driven flow are turbulence effects and the opening size. The effect of wind-driven flow is measured using the Reynolds (Re) number:

$$Re = \frac{\rho V l}{\mu} \tag{2.4}$$

where ρ is the density, V is a velocity, and μ is the fluid dynamic viscosity.

Most flows have a combination of buoyant forces and wind driven forces. The relationship Gr/Re^2 is used to determine the dominant effect. If $Gr/Re^2 << 1$ buoyancy effects are negligible, $Gr/Re^2 >> 1$ buoyancy effects are dominant, and $Gr/Re^2 \sim 1$, the effects can be determined as mixed conditions.

2.2 Human Heat Load

An important aspect of designing for natural ventilation is whether the design can handle heat loads and specifically human heat loads. Analysis of human heat loads has been done previously for HVAC purposes and for natural ventilation. Craven and Settles [14] used experiments to obtain images and temperature stratification in a room and compared the data to CFD results. While the human thermal plume is due to radiation, convection, evaporation, and respiration, Craven and Settles [14] modeled the human using only a heat flux. The results were comparable between experimental and CFD results, and both showed a thermal plume above the head and thermal stratification throughout the room. Using only a heat flux in the thermal model

is more efficient than including a radiation model. Also, Stamou and Katsins [15] showed that in experimental and computational studies of a human in mechanically-ventilated and naturally-ventilated rooms, there exists a thermal plume and air flow impinges on the ceiling above the human.

An overview of heating and cooling for buildings can be found in [16]. Various metabolic rates for different human activities can be found. A standing average sized male, corresponds to a metabolic rate of approximately 160 W total, with 75 W from sensible heat.

2.3 Rules of Thumb

Architectural design for natural ventilation is determined using rules of thumb from CIBSE BRE [4]. These rules are used for moderate to high heat gains of 20-50 W/m^2 and are used to avoid summertime overheating and to make sure the structure has reasonable air distribution. While there is little explanation or research connected to the rules of thumb, Edwards [17] investigated their origins and found that the conditions and assumptions made for the rules of thumb are not well defined. In a study of single-sided ventilation, Walker and White [18] found that air speeds and unmixed air from the exterior of the building can penetrate deeper than the generally accepted depth of 6 meters, and that the fresh air was distributed throughout the structure.

The general rules of thumb are for cross-ventilation and single-sided ventilation. For cross-ventilation the rule is a depth-to-height ratio (DH) of 5:1. For single-sided ventilation with one opening the ratio is 2:1 and with two openings it is 2.5:1. The rules have a depth-to-height ratio because it is expected that with increased floor to ceiling height, the temperature is more stratified and pollutants are lifted above the occupied space.

2.4 Air Quality

A measure of air quality in a room or space and an often used rule of thumb for ventilation design is the air change rate (ACH). The ACH is the volumetric flow rate into a room divided by its volume and is most commonly used as air changes per hour with units of 1/hr. The ACH can be used to determine the overall air quality of a room and whether it meets the expectations of ASHRAE with a minimum of 0.35.

Effective heat removal from a space is a requirement to ensure ventilation. In [19], the ACH to remove heat is approximately 2-15. A minimum of 2 air changes per hour is used as a general rule to ensure a room or space does not overheat due to the heat loads.

Chapter 3 Numerical Methodologies

The numerical approach that the physical solution will use is explained in this chapter. Fluent 14.5 [20] is used for all simulations. The governing equations, a non-dimensional approach, and a grid resolution study will be presented in the following chapter.

3.1 Governing Equations

Computational fluid dynamics solves partial differential equations that describe the movement of a fluid. The velocity and temperature are solved with the three-dimensional Navier-Stokes equations and the energy transport equation. The equations use a finite volume of fluid and apply basic laws for mass, momentum, and energy. The partial differential equation for conservation of mass is:

$$\frac{\partial \rho}{\partial t} + \vec{\nabla} \cdot (\rho \vec{V}) = 0 \tag{3.1}$$

where t represents time, ρ is density, and $\vec{V}$ is the velocity vector:

$$\vec{V} = u\hat{\imath} + v\hat{\jmath} + w\hat{k} \tag{3.2}$$

where $\vec{\nabla}$ in a Cartesian coordinate system is:

$$\vec{\nabla} = \frac{\partial}{\partial x}\hat{\imath} + \frac{\partial}{\partial y}\hat{\jmath} + \frac{\partial}{\partial z}\hat{k} \tag{3.3}$$

The conservation of momentum is:

$$\frac{\partial}{\partial t}(\rho \vec{V}) + \vec{\nabla} \cdot (\rho \vec{V}\vec{V}) = -\vec{\nabla} p + \vec{\nabla} \cdot \bar{\bar{\tau}} + \rho \vec{g} \tag{3.4}$$

where p is static pressure, $\bar{\bar{\tau}}$ is the stress tensor, and $\vec{g}$ is the gravitational body force vector. The first term on the left side is the unsteady term and the second is the momentum convection term. For a Newtonian fluid $\bar{\bar{\tau}}$ is:

$$\bar{\bar{\tau}} = \mu[(\vec{\nabla}\vec{V} + \vec{\nabla}\vec{V}^T)] \tag{3.5}$$

The buoyancy effects are solved using the Boussinesq model. This approximation is valid because temperature and velocity differences are small, so the density differences are small. The thermal expansion coefficient, β, is:

$$\beta = -\frac{1}{\rho}\left(\frac{\partial\rho}{\partial T}\right)_p \approx \frac{1}{\rho_0}\frac{\rho_0 - \rho}{T_0 - T} \tag{3.6}$$

The Boussinesq approximation can be represented as:

$$(\rho_0 - \rho) \approx \rho_0\beta(T_0 - T) \tag{3.7}$$

where ρ_0 and T_0 are reference values. Using these equations, density is solved and substituted into (3.4). Other density terms are constant and equal to ρ_0.

Conservation of energy equation is:

$$\frac{\partial}{\partial t}(\rho E) + \vec{\nabla}\cdot\left[\vec{V}(\rho E + p)\right] = \vec{\nabla}\cdot k_{eff}\vec{\nabla}T + \vec{\nabla}\cdot\left(\bar{\bar{\tau}}_{eff}\cdot\vec{V}\right) + S_h \tag{3.8}$$

where E is the total energy and k_{eff} is the effective conductivity, which is the sum of the fluid thermal conductivity and the turbulent thermal conductivity. The second term from the right is included as the viscous heating term and S_h is for volumetric heat sources. The total internal energy of the fluid is:

$$E = h - \frac{p}{\rho} + \frac{V^2}{2}$$

(3.9)

where h is the sensible enthalpy:

$$h = \int_{T_0}^{T} c_p dT$$

(3.10)

and T_0 is the reference temperature and c_p is the constant specific heat. The final forms of the incompressible conservation equations are:

$$\vec{\nabla} \cdot \vec{V} = 0$$

(3.11)

$$\frac{\partial \vec{V}}{\partial t} + \vec{V} \cdot \vec{\nabla}\vec{V} = -\frac{1}{\rho_0}\vec{\nabla}p + \frac{\mu}{\rho_0}\vec{\nabla}^2\vec{V} + \vec{g} - \beta(T - T_0)\vec{g}$$

(3.12)

$$\frac{\partial T}{\partial t} + \vec{V} \cdot \vec{\nabla}T = \alpha\vec{\nabla}^2 T$$

(3.13)

3.2 Non-Dimensional Equations

The equations are non-dimensionalized to assess the importance of each term in the governing equations. This is done using l, u_0, and ρ with all the variable and a superscript * will indicate the non-dimensional quantity:

$$t^* = \frac{tu_0}{l}$$

(3.14)

$$\vec{\nabla}^* = \vec{\nabla} l$$

(3.15)

$$\vec{V}^* = \frac{\vec{V}}{u_0}$$

(3.16)

$$p^* = \frac{p}{\rho {u_0}^2}$$

(3.17)

$$g^* = \frac{gL}{{u_0}^2}$$

(3.18)

$$\theta^* = \frac{T - T_\infty}{T_s - T_\infty}$$

(3.19)

Equations 14-19 are substituted into 11-13 to produce a non-dimensional set of equations.

$$\vec{\nabla}^* \cdot \vec{V}^* = 0$$

(3.20)

$$\frac{\partial \vec{V}^*}{\partial t^*} + \vec{V}^* \cdot \vec{\nabla}^* \vec{V}^* = -\vec{\nabla} p^* + \frac{1}{Re} \vec{\nabla}^{*2} \vec{V}^* + \vec{g}^* - \frac{Gr}{Re^2} \theta^*$$

(3.21)

$$\frac{\partial \theta^*}{\partial t^*} + \vec{V}^* \cdot \vec{\nabla}^* \theta^* = \frac{1}{RePr} \vec{\nabla}^{*2} \theta^*$$

(3.22)

3.3 Turbulence Models

Most indoor airflow has been found to be turbulent [3] and therefore must be modeled in CFD. The standard k-ε model has been found to be sufficient for natural ventilation flow fields [21], while the realizable k-ε model is recommended in Fluent. The realizable k-ε satisfies mathematical constraints on the Reynolds stresses that the standard k-ε model does not. The transport equations are:

$$\frac{\partial}{\partial t}(\rho k) + \vec{\nabla} \cdot (\rho k \vec{V}) = \vec{\nabla} \cdot \left[\left(\mu + \frac{\mu_t}{\sigma_\varepsilon}\right)\vec{\nabla}\kappa\right] + G_k + G_b - \rho\varepsilon - Y_M + S_k \tag{3.23}$$

and

$$\frac{\partial}{\partial t}(\rho\varepsilon) + \vec{\nabla} \cdot (\rho\varepsilon \vec{V}) = \vec{\nabla} \cdot \left[\left(\mu + \frac{\mu_t}{\sigma_\varepsilon}\right)\vec{\nabla}\varepsilon\right] + \rho C_1 S_\varepsilon + \rho C_2 \frac{\varepsilon^2}{k + \sqrt{\nu\varepsilon}} - \rho\varepsilon + C_{1\varepsilon}\frac{\epsilon}{k} C_{3\varepsilon} G_b + S_\varepsilon \tag{3.24}$$

where G_k is the production of turbulent kinetic energy due to mean velocity gradients, G_b is the generation of turbulent kinetic energy due to buoyancy, Y_m is the contribution of of the fluctuating dilation in compressible turbulence, and S is the source terms. The constants and source terms are defined as:

$$C_1 = \max\left[0.43, \frac{\eta}{\eta + 5}\right] \tag{3.25}$$

$$\eta = S\frac{k}{\epsilon} \tag{3.26}$$

$$S = \sqrt{2S_{ij}S_{ij}} \tag{3.27}$$

and the constant are summarized in Table 3.1.

Table 3.1. Constants for the Turbulence Models used in Fluent

$C_{1\epsilon}$	1.44
C_2	1.9
σ_k	1.0
σ_ϵ	1.2

3.4 Discretization Methods

The pressure-based Navier Stokes (PBNS) solver is used in this study. Fluent uses a finite control volume approach and the dependent variables are solved at the center of each cell. The variables at the center are used at the cell faces to compute fluxes. The semi-implicit method SIMPLE is used to couple pressure and velocity. In the current study, a second-order upwind scheme is used to solve momentum, energy, and turbulent kinetic and dissipation rate. The second-order upwind scheme uses a Taylor expansion of the upstream cell about the cell-centered data. The least squares cell based (LSCB) and PRESTO! spatial discretization are used for the gradient and pressure, respectively. Time is discretized using a first-order implicit method.

The SIMPLE algorithm is the PBNS solver used in the current study to couple pressure and velocity. The SIMPLE algorithm uses a given pressure field, p^*, to solve the velocity field $\vec{V}^*$. The final solution for the velocity field must satisfy the continuity equation. The final velocity field and pressure are:

$$\vec{V} = \vec{V}^* + \vec{v}' \tag{3.28}$$

$$p = p^* + p' \tag{3.29}$$

where $\vec{V}'$ and p' are the velocity field and pressure correction, respectively. The solution for the velocity field is:

$$\vec{V}' = -\frac{1}{A_P}\sum_l A_l \vec{V}_l' - \frac{1}{A_P}\nabla p'|_P \tag{3.30}$$

where A_p and A_l are coefficient from the discretized momentum equation. The subscript P represents the cell being solved and l represents the neighbor points. The velocity fields and pressure are updated using Eqs. (3.28) and (3.29) once the velocity and pressure have been corrected [22].

3.5 Grid Resolution

A grid resolution study was used to determine the appropriate grid for natural ventilation purposes. Previous natural ventilation studies using large and small scale models [6,9,10] were used to get an appropriate range of cell sizes. The room used in this study is shown in Figure 3.1. The room is approximately 3 m x 3.25 m x 3 m. Initially, the room is at 36.85˚ C. The two openings in the room represent a door and window, where the door is specified as a velocity inlet and the window as a pressure outlet. The conditions at the inlet are a velocity of 2 m/s and a temperature at 16.85˚ C. The outlet is specified as zero gauge pressure. To achieve a temperature distribution through the room at steady state, the ceiling is held at a temperature equal to the initial temperature of 36.85˚ C. All other walls are designated as non-slip walls and are adiabatic.

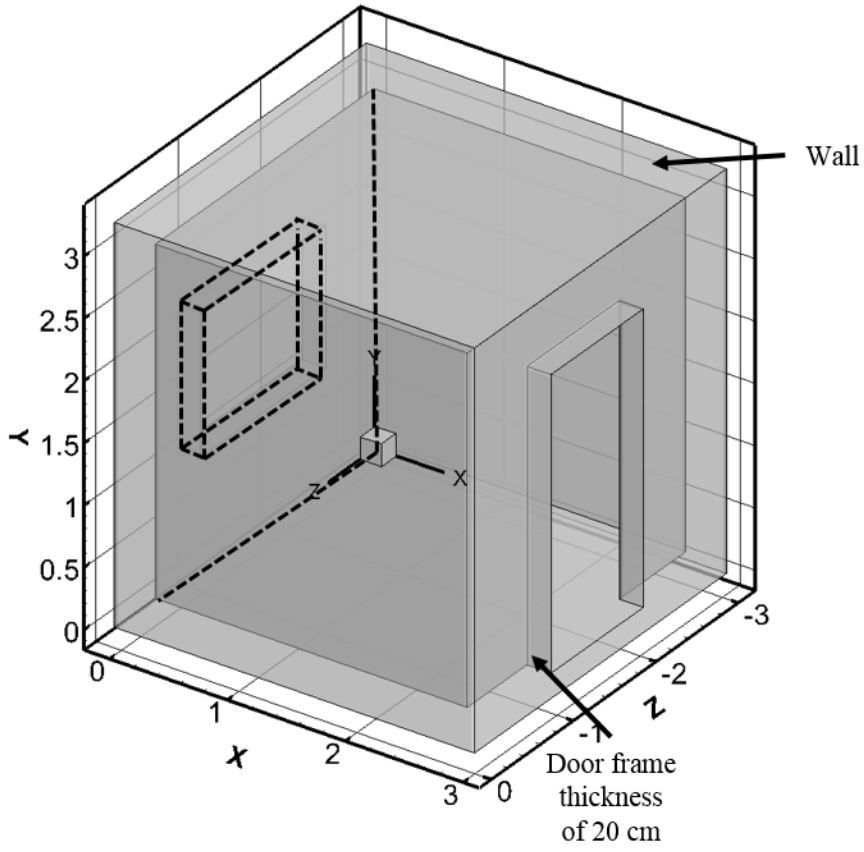

Figure 3.1. Geometry used to simulate natural-ventilation to define the proper grid.

The proper grid resolution was determined using multiple uniform grids of different cell volumes and the results are shown in Figure 3.2. The uniform grid distributions used were 3 cm, 4 cm, 5 cm, 6 cm, and 10 cm. The temperature profile and the u-velocity and v-velocity profiles are shown in Figure 3.2a, b, and c respectively. To compare temperature and velocity profiles, a vertical line 0.3 m from the center of the window was used. While the overall profiles were captured throughout the middle portion of the room for all cell sizes, the recirculation zone at the bottom (near y=0 on Figure 3.2b and c) was not captured with the coarse grids (10 cm and 6 cm). The medium grid (5 cm) did capture this zone, but did not match the solutions of the fine (4 cm and 3 cm) grids. The fine grids converged to a similar solution.

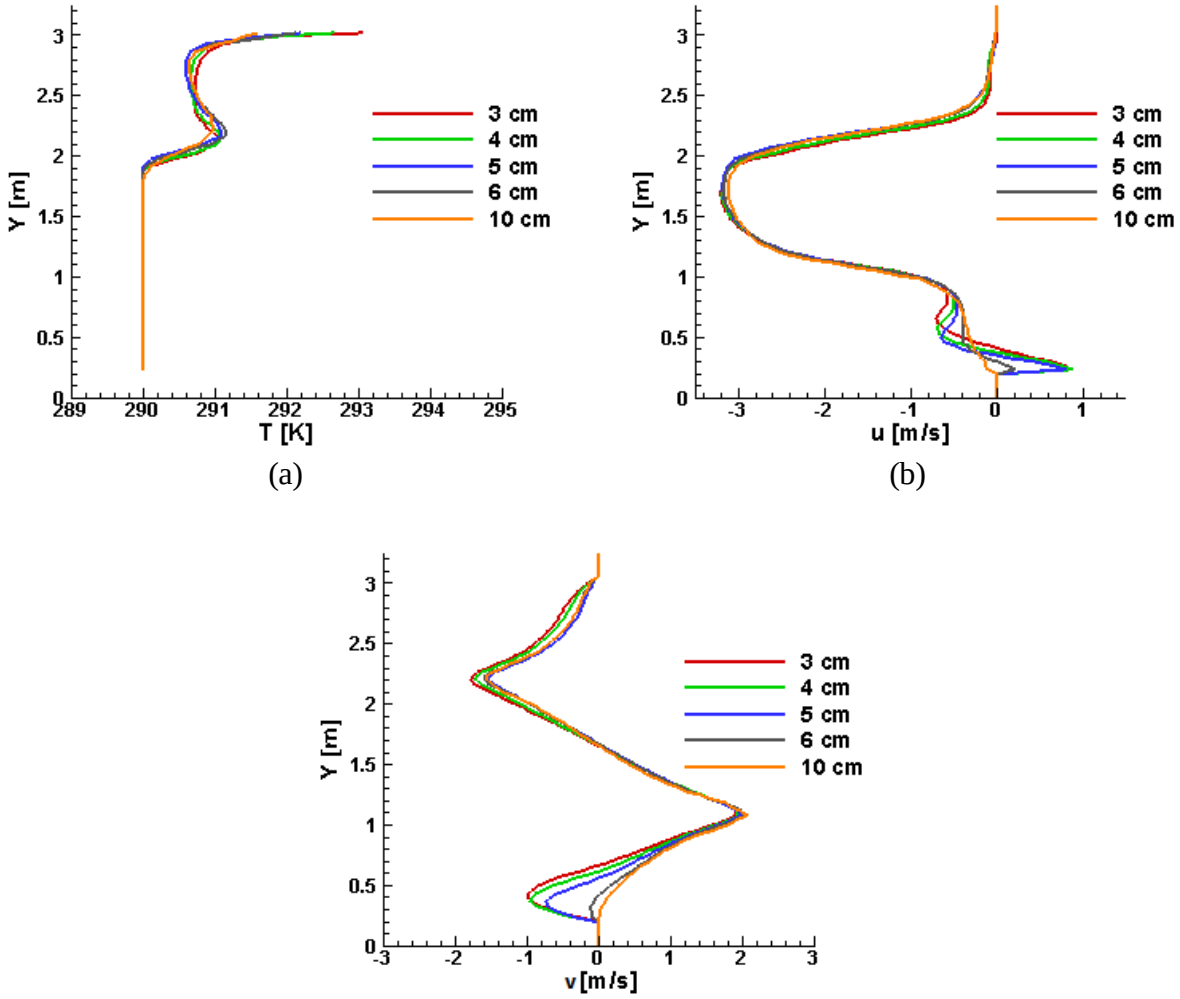

Figure 3.2. Profiles at 0.3 meters from the center of the window for (a) temperature (b) u-velocity and (c) v-velocity

In an effort to minimize the computation time while maintaining the integrity of the results, a hybrid grid was utilized and can be seen in Figure 3.3. The region where the coarse grid did not provide accurate results was in a region 1 m from the wall. At the wall, a grid resolution of 3 cm was used. There was a uniform increase from the wall to 1 m from the wall. At one meter from the wall and throughout the middle region of the interior, a uniform 10 cm grid distribution was used. The compression added along the walls allow a coarse grid to be used in the regions where it was

appropriate while using refined cells near the walls to capture the recirculation zones near the wall. The physical walls are meshed and are about 0.2 m thick, but are designated as adiabatic.

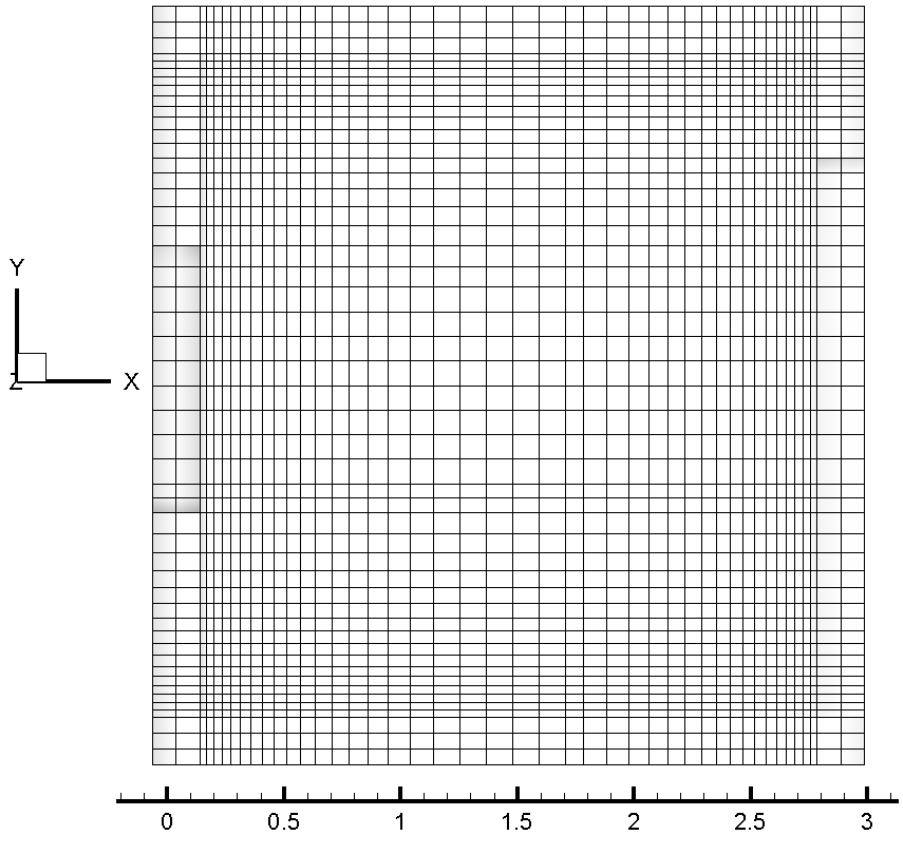

Figure 3.3. Side view of the hybrid mesh showing the compression near the walls. The walls surrounding the interior zone have a cell size of 10 cm, unless affected by the compression within the room.

The results for the hybrid grid were very similar to the results for the fine grids and are compared in Figure 3.4. The middle region, where the uniform coarse mesh was used, has approximately the same profile as the fine grids. The hybrid grid is adequate for regions farther from the wall, even with coarse cells. The regions near the wall where the recirculation zones occur are also well represented by the hybrid mesh thus the hybrid mesh resolves the wall regions using a refined mesh that uniformly increases to a coarse distribution throughout the middle region. As

the structures used to simulate ventilation in simple structures are large, this will dramatically decrease computation time while providing accurate results over the flow field.

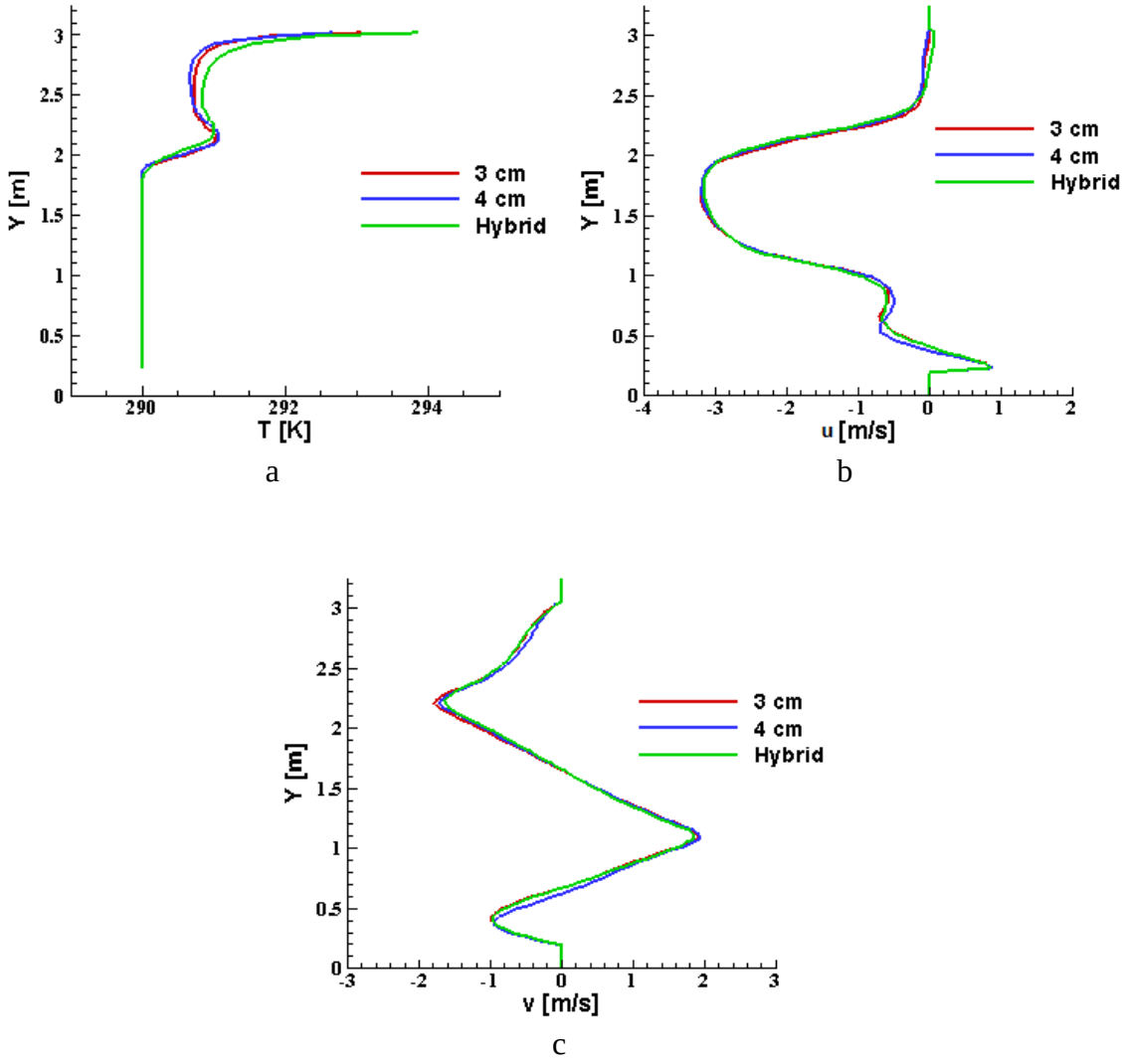

Figure 3.4. Results comparing the profiles for (a) temperature (b) u-velocity (c) v-velocity

The absolute error of u and v velocities for each grid was used to quantify the error with the chosen mesh. The absolute errors can be seen in Table 3.2. The solution was determined from the fine mesh, 3 cm. As the cell sizes decreased, from 10 cm to 4 cm, the absolute error decreased as well. The coarse mesh had an absolute error of 18% and 17% for the u and v velocity components, while a mesh with cell sizes of 4 cm had absolute errors of 7% and 5% for the velocity

components. Using the hybrid grid, which has a near wall cell size of 3 cm and a cell size of 10 cm a meter away from the walls, the u and v velocity error was 5% and 3%, respectively.

Table 3.2. Absolute error for the u and v velocity components.

Grid mesh	Absolute Error %	
	u component	v component
10 (cm)	18	20
6 (cm)	17	18
5 (cm)	15	15
4 (cm)	7	5
Hybrid	5	3

The law of the wall for the hybrid grid was used to ensure accurate solutions. The dimensionless wall distance, y^+ [20] is:

$$y^+ = \frac{u_* y_*}{\nu} \tag{3.31}$$

where u_* is the friction velocity, y_* is the distance from the wall to the node, and ν is the kinematic viscosity. Fluent [20] recommends the first cell is located within the log-log layer, $30 < y^+ < 300$. At the wall, there is a cell size of 3 cm. At this location the majority of cells are within a range of $40 < y^+ < 120$, while a very small range of 0.2 m is between $20 < y^+ < 30$.

3.6 Mesh Generation

The geometries used in the simulations were provided by colleagues at Iowa State University. The files were received as SAT format and imported into Ansys ICEM. The meshes were built in ICEM and then exported to Fluent. They were built by using blocking to get a reasonable imprint of the fluid interior of the structures. The small structures used the hybrid grid, with all walls receiving compression. The mesh for the larger buildings were built to have an

average cell length of 10 cm, which was appropriate for the flow profiles. A more complex grid for the full-scale buildings was not possible due to the size and complexity of the buildings.

Chapter 4 Cross-Ventilation

In this chapter, cross-ventilation is predicted in a simple structure with openings on opposing faces. Cross-ventilation is predicted for passive cooling and passive heating using three different combinations of opening sizes. Two different combinations of boundary conditions are modeled: a velocity inlet and pressure outlet and both pressure boundaries. The velocity inlet simulates wind-driven flow, where ventilation is driven by a combination of forced air and a temperature difference between ambient and internal air. Pressure boundaries simulate a condition with quiescent ambient air and ventilation is driven by the temperature difference. The effectiveness of cross-ventilation is determined by comparing flow patterns, temperature contours, and the ACH for each case.

4.1 Geometry and Conditions

Cross-ventilation is modeled using three different base rooms shown in Figure 4.1. These rooms have different combinations of opening sizes that represent windows at opposite walls. The room configurations and dimensions were recommended by Prof. Passe to demonstrate the importance of the rules of thumb. Room 1.1 has a small inlet and a large outlet, Room 1.2 has a large inlet and a small outlet, and Room 1.3 has a small inlet and outlet. The rooms are approximately 3 m tall by 3 m wide by 15 m long, corresponding to the 5:1 depth-to-height ratio (DH) from the rules of thumb for cross-ventilation and to test the effectiveness of the rule, a room with a DH of 7 is modeled for rooms 1.2 and 1.3. The windows are placed in the middle of the walls. The smaller opening is 1.05 m by 0.9 m and the larger opening is 2.1 m by 1.8 m. The conditions are similar to a set of case studies from Ghass and Allard [1].

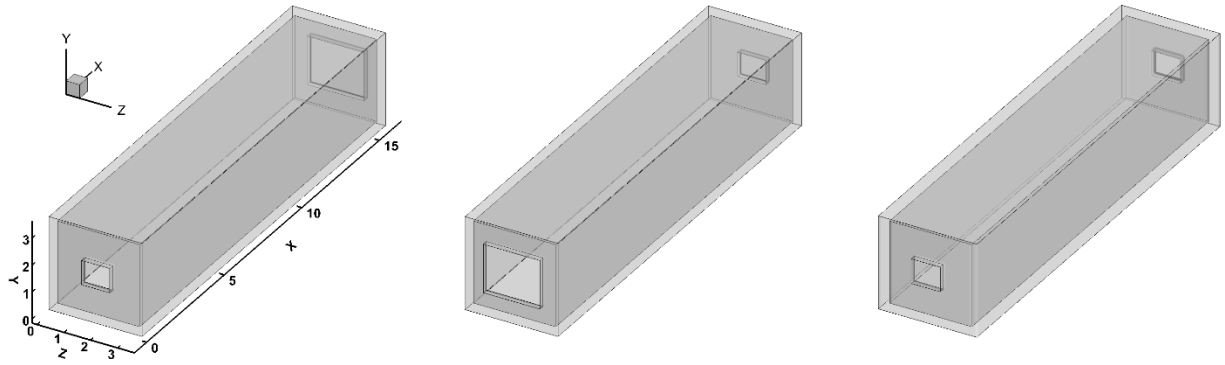

(a) Room 1.1 (b) Room 1.2 (c) Room 1.3

Figure 4.1. Base rooms used for cross-ventilation. Dimensions in m.

Velocity inlets and pressure outlets are used to model wind-driven cross-ventilation flow for both passive cooling and passive heating. There is an initial 4 °C temperature difference between the interior and ambient conditions for cooling and heating cases. All wind-driven cases with a velocity inlet are simulated as transient until steady-state is reached. The time step is determined from the stability criterion using the Courant-Friedrichs-Levy (CFL) number:

$$CFL = \frac{V\Delta t}{\Delta \mathrm{x}} \tag{4.1}$$

where V is a velocity, usually assumed to be the inlet velocity, Δx is the minimum cell size, and Δt is the appropriate time step. To maintain stability, the CFL number should be near or below unity. Convergence is determined when a majority of time steps reached residuals of 10^{-6}.

When using pressure boundaries for all openings, convergence and stability are more difficult to determine. The convergence criterion is decreased to 10^{-5} for the continuity equation. An adaptive time step is used to decrease simulation time, increase convergence, and allow for the time step to be larger when possible.

A steady-state solution was difficult to achieve using pressure boundaries from a fully transient simulation, so different strategies were utilized to reach steady-state. When possible, a fully steady-state simulation was run to convergence criteria of 10^{-6}. If the steady simulation did not converge to the appropriate criteria, the steady simulation was continued for a number of iterations, and then changed to run as a transient case. The transient time steps converge to 10^{-6}, and steady-state was determined by either a steady volume flow rate or a quasi-steady volume flow rate where the solution was time-averaged over a period.

Results from simulations show symmetry across the mid-plane in the z-axis. A comparison between the results using a full geometry and a half geometry indicated a symmetric boundary was appropriate. These results can be seen in Appendix A. The half geometry is used to reduce computation time as the number of cells is decreased by 50%. Adiabatic walls are also used to decrease computation time and the meshed wall zones are not included in the simulation.

The simulation for Room 1.1 did not converge to the criteria as the other two rooms did. Convergence is difficult to achieve due to backflow, presented in Figure 4.2, at the pressure outlet and was greatly increasing simulation time preventing the desired computational accuracy. The backflow does not allow the solution to converge to the same criteria as the other simulations and leads to a less accurate result. To remedy the problem, a "false room" is added to the end of the room with an exit equal to the size of the inlet. A comparison of the geometries is shown in Figure 4.3. The added false room alleviates the convergence problem and the simulation subsequently successfully reaches steady state.

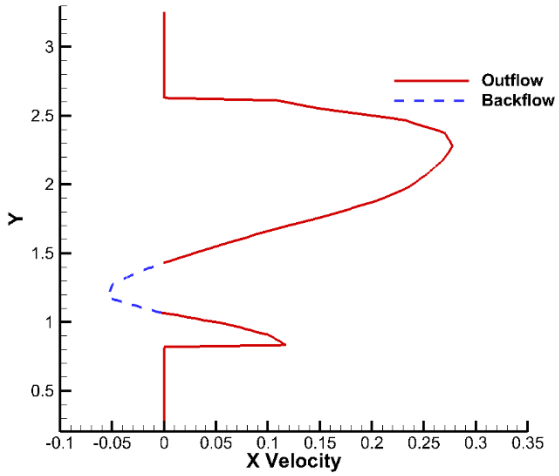

Figure 4.2. Velocity profile at the outlet of Room 1.1

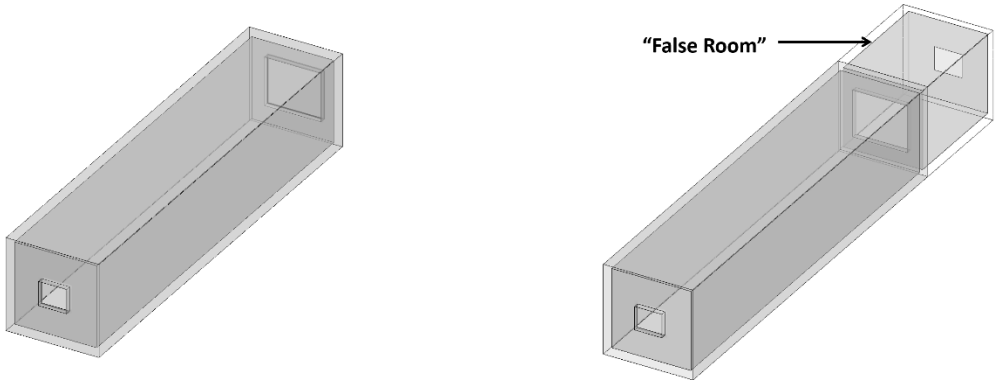

(a) Room 1.1 (b) Room 1.1 (false room)

Figure 4.3. Geometry for (a) Room 1.1 and (b) Room 1.1 with a false room

The results for Room 1.1 and Room 1.1 with a false room are shown in Figure 4.4, represented with temperature contours and streamlines, at 300 seconds. The major flow features in the two geometries are similar, with a minor difference at the outlet. The simulation for Room 1.1 did not converge and contributes to an inaccurate solution. For future reference, the geometry with the false room is used for Room 1.1.

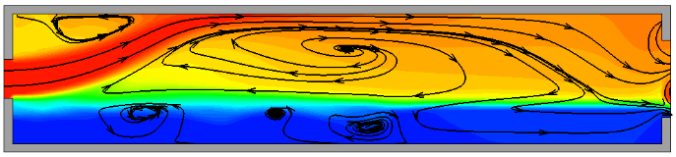

(a) Room 1.1

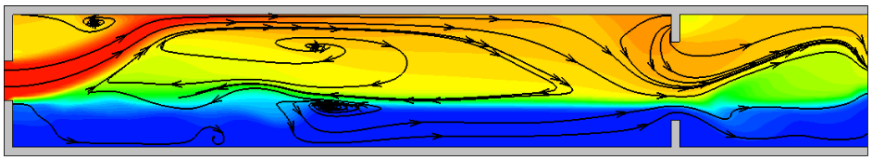

(b) Room 1.1 with False Room

Figure 4.4. Temperature contour with overlaying streamlines for Room 1.1.

The results for Room 1.1 and Room 1.3 are extremely similar. The results at 300 seconds for Room 1.3 can be seen in Figure 4.5 and the results for Room 1.1 are shown in Figure 4.4a. The flow patterns and temperature stratification throughout the rooms were nearly identical. The similarity of the results showed that the flow patterns and thermal stratification are dominated by the inlet size and not the outlet. This allowed further simulations to only be run on Room 1.3. This reduces the amount of cases to run and subsequently the total computational time for the study.

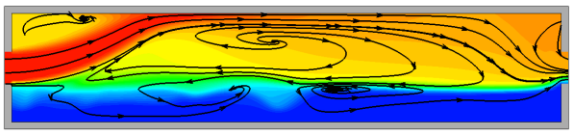

Figure 4.5. Passive heating temperature contours and overlaying streamlines for Rom 1.3.

4.2 Results for Passive Heating and Cooling in Cross-Ventilation

Passive heating and cooling are simulated using a velocity inlet and a pressure outlet. Two different velocities are specified: 0.5 m/s and 5 m/s. The relationship between buoyancy effects and viscous forces is presented in Table 4.1. Ventilation for the low velocity cases was mixed, with both buoyancy forces and forced air effects influencing the flow patterns. The relationship

Gr/Re^2 is near unity, which is an indication of mixed flow. The medium velocity cases are forced air dominated, with Gr/Re^2 much less than unity, indicating that buoyancy effects are negligible.

Table 4.1. Cross-ventilation Reynolds and Grashof numbers and the relationship between buoyancy and forced flow

	Room	Velocity	Re	Gr	Gr/Re^2
Cooling	Room 1.2	0.5 m/s	5.77×10^4	3.17×10^9	0.95
		5 m/s	5.77×10^5	3.17×10^9	0.0095
	Room 1.3	0.5 m/s	2.89×10^4	4.00×10^8	0.48
		5 m/s	2.89×10^5	4.00×10^8	0.0048
Heating	Room 1.2	0.5 m/s	5.62×10^4	3.00×10^9	0.94
	Room 1.3	0.5 m/s	2.81×10^4	3.70×10^8	0.47

The buoyancy effects can be seen when the warm, less dense air rises above the cold, denser air. The time-sequences of temperature with overlaying streamlines at the mid-plane in the z-axis are shown in Figure 4.6. When low speed flow is modeled, the effect of buoyancy can be easily viewed over time, as the warm ambient air moves into the room (t_1). The warm air moves through the upper region of the room towards the outlet (t_2). The larger opening in Room 1.2 warms the air significantly faster and fills the entire room with warm air, while the smaller opening in Room 1.3 has a smaller warm air field and is not as effective in filling the room (t_3).

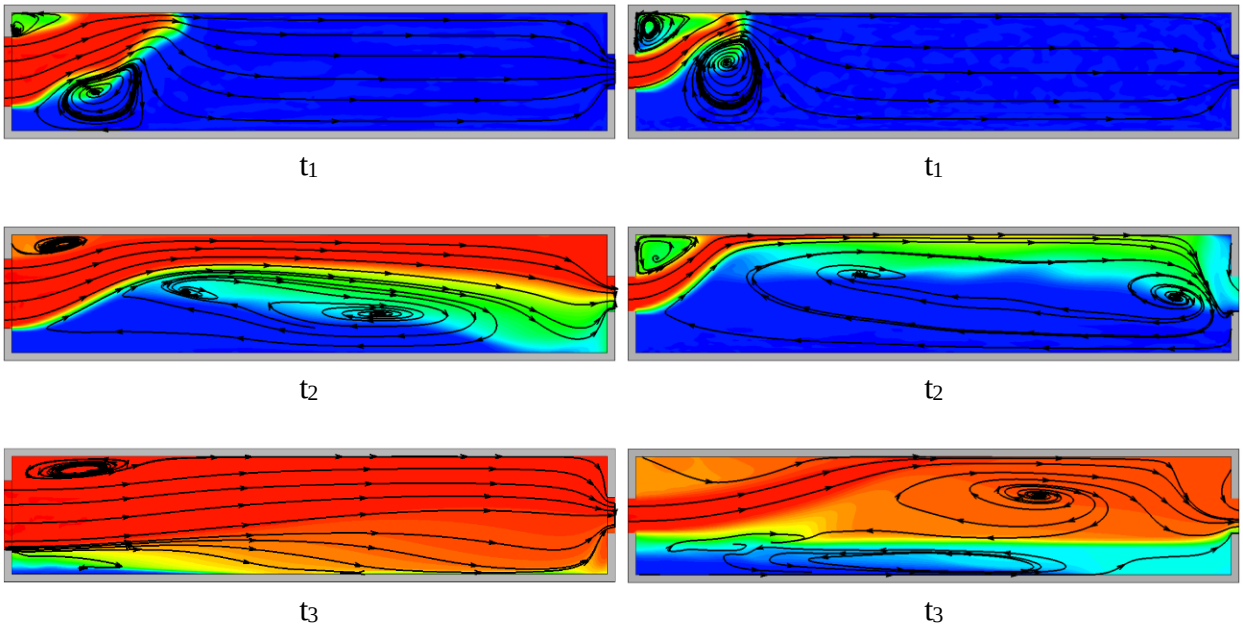

(a) Room 1.2 (b) Room 1.3

Figure 4.6. Buoyancy-driven flow for passive-heating in cross-ventilation comparing temperature and streamlines: t_1 = 10s, t_2 = 60s, t_3 = 600s

The comparison of Grashof and Reynolds number using Gr/Re^2 for Room 1.2 and Room 1.3 are 0.95 and 0.475 respectively. The steady-state results in Figure 4.7 show this small difference very well with velocity vectors and streamlines. While both rooms have mixed conditions, the effects due to buoyancy in Room 1.2 are greater. Over time, shown previously in Figure 4.6, the warm air moving into the room impinges on the ceiling closer to the inlet. This effect remains throughout time and is apparent in the steady-state results. Both rooms have recirculation zones above and below the incoming flow, but the location and size of the recirculation zones are different. In Room 1.3, the upper zone is much larger than the lower, and the zones are a distance about one-third of the room length downstream of the inlet. In Room 1.2, the recirculation zones are near the inlet and are much smaller than those of Room 1.3. The warm ambient air moves into the room and impinges on the ceiling earlier in the flow, as the contribution of the forced air effects are lower. This effect remains even when the room is at a constant

temperature. As the recirculation zones are close the inlet, the ambient air appears to "fill" the entire room. The flow patterns presumably allow for better ventilation of the entire space than with the smaller opening in Room 1.3.

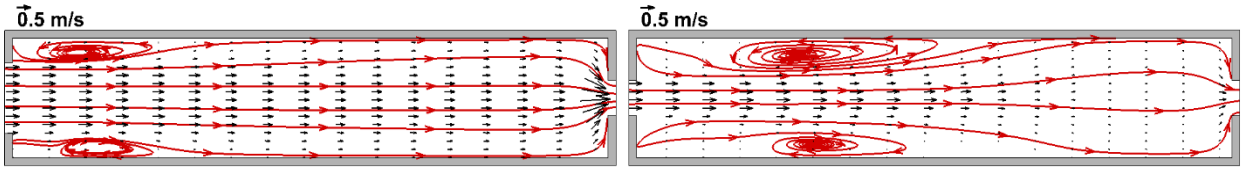

(a) Room 1.2 (b) Room 1.3

Figure 4.7. Steady-state flow fields for passive heating represented by streamlines and vectors in cross-ventilation with a low inlet velocity.

Passive heating and passive cooling have extremely similar results. Passive cooling is shown in Figure 4.8 and Figure 4.7a for passive heating (Room 1.2). The resulting streamlines are the same but they are flipped about the midplane of the y-axis. The cooling effect has a larger eddy at the lower portion of the room, while passive heating has the same size eddy at the upper half of the room. Opposing the larger eddy is a smaller eddy on the other side of the inflow.

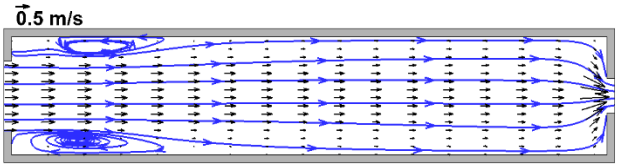

Figure 4.8. Steady-state flow fields for passive cooling for a low inlet velocity. Room 1.2

The difference between mixed flow and flow dominated by forced air are most visible when comparing inlet velocities. A velocity of 0.5 m/s corresponds to a $Gr/Re^2 = 0.951$, which is a mixed condition (Room 1.2). A velocity of 5 m/s corresponds to Gr/Re^2 of 0.00951, which has very weak buoyancy effects and is dominated by the air velocity (Room 1.2). The results are shown in Figure 4.9 for Room 1.2 represented with velocity vectors and streamlines. As previously explained for Figure 4.7a, a flow that has mixed effects has a very large eddy near the upper wall

of the room during passive heating and a smaller eddy near the lower wall. When the flow is dominated by forced air, eddies above and below the incoming flow appear to be very equal in size and are generally equally distributed.

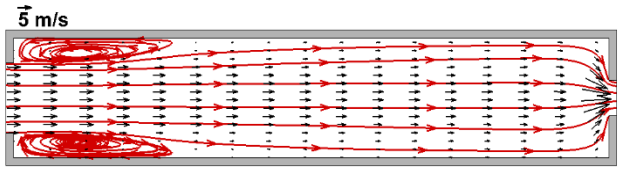

Figure 4.9. Steady-state flow fields for passive heating represented by streamlines and vectors for medium velocity inlet conditions for Room 1.2.

Air quality can be determined by the air change rate (ACH), which measures the amount of volume changes the room has per hour. A minimum of 0.35 ACH is recommended [23] to maintain air quality of a room. To remove heat, a minimum of 2 ACH is needed [19]. Using velocity inlets with a 0.5 m/s and 5 m/s velocity, cross-ventilation is very effective at removing heat and maintaining air quality in a room. The velocity of the ambient external air is difficult to model as the real conditions change over time and would not have a constant velocity over the entire surface for an extended period of time, but 0.5 m/s is a velocity within comfort standards and is a reasonable air velocity in a room. However, 5 m/s leads to an uncomfortable environment, and the ACH corresponding with 5 m/s is unreasonable to achieve while keeping the room comfortable for the occupants. The ACH is presented in Table 4.2.

Table 4.2. ACH for forced air conditions in cross-ventilation

Room	Room 1.2		Room 1.3	
Inlet Velocity (m/s)	0.5	5	0.5	5
Volumetric Flow Rate (m^3/hr)	6804	68040	1701	17010
ACH (1/hr)	48	480	12	120

4.3 Investigation of the Effect of Different Boundary Conditions

The previous results modeled flow with a velocity inlet and a pressure outlet. It is difficult to equate the velocity modeled with a meteorological wind speed outside the room as the current models that equate the two are derived empirically and are for specific circumstances. The velocities chosen were compared to an analysis in [1] for an ACH study as a reference. Cross-ventilation will be simulated with both openings as ambient pressure boundaries, which effectively models cross-ventilation when the ambient air is stationary. The corresponding airflow represents the minimum air velocity when temperature differences exist between the exterior and interior air.

The air flow using a velocity versus pressure boundary conditions produce different patterns and effects, shown with instantaneous temperature contours and streamlines in Figure 4.10. While forced air has a large and well defined flow field moving from the inlet to the outlet, the openings with pressure boundaries induce air flow patterns that are less organized. A specified velocity inlet forces air from one opening to the other. Pressure boundaries allow the flow to develop based on the temperature differences and other pressure differences, based on opening size. The eddies and recirculation zones with forced air appear at locations along the inflow and where large temperature gradients exist. With pressure boundaries, shown in Figure 4.10b, the recirculation zones appear throughout the flow field, not necessarily corresponding to the inflow or the temperature gradients in the room.

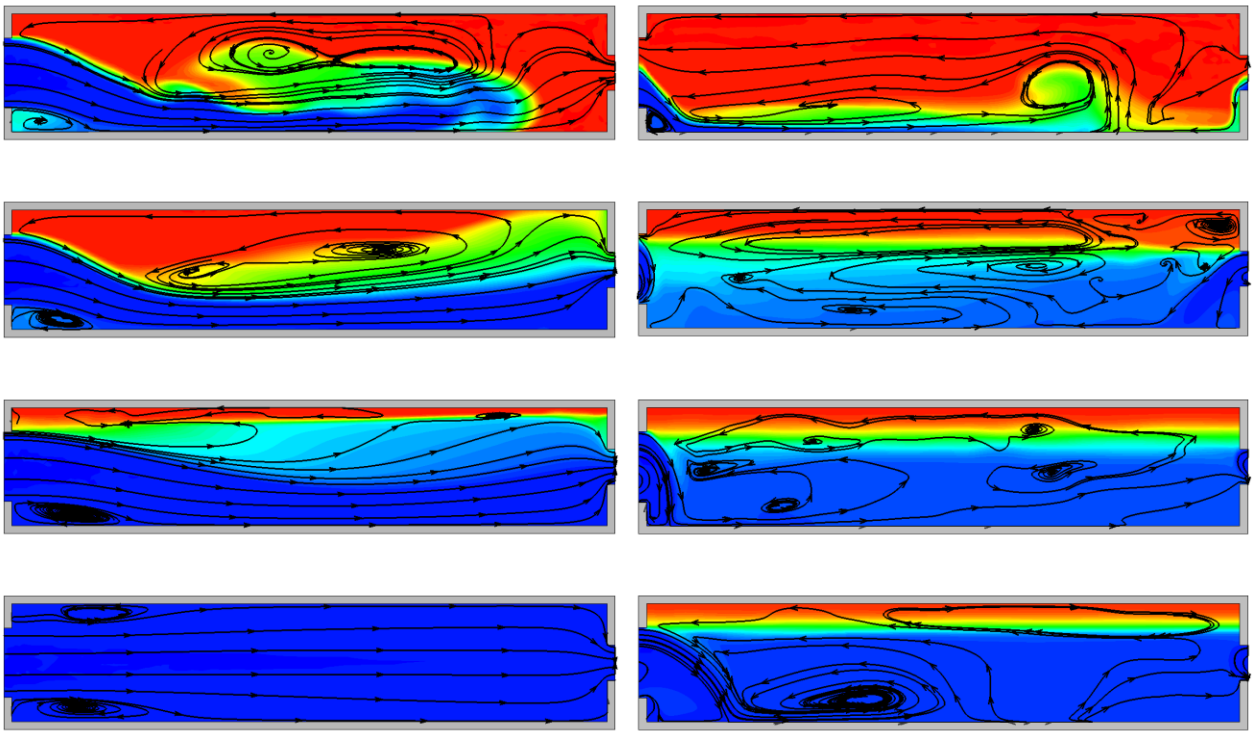

(a) Velocity inlet (b) Ambient pressure inlet

Figure 4.10. Time sequence of passive cooling represented with temperature contours and streamlines for Room 1.2.

In Room 1.2 at steady state, shown in Figure 4.11a, the flow moves from the larger to the smaller opening. There is inflow and outflow at both openings, but the dominate flow is inflow from the large opening into the space, with mixing downstream. A large eddy reaches approximately halfway into the space from the larger opening. The maximum velocity is approximately 0.35 m/s and occurs at the inlet. The second half of the space, near the small opening, has very low moving air and air exchange in this region is predominately due to mixing.

Room 1.3, which has equal sized openings, is effectively split into two different sections at the mid-plane in the x-direction by vertical streamlines, shown in Figure 4.11b. The flow patterns are the same in each half. Each opening has equal inflow and outflow and there is no exchange between the windows or the two halves of the room. A large recirculation zone exists in

each half, with air moving in from the top of the opening towards the lower portion of the room. The inflow moves up the center of the room and recirculates throughout one-half. The room has no pressure difference between the two openings, leading to no exchange between the two sides in the x-axis. Without the pressure difference between the openings, each half of the room is effectively ventilated with single-sided ventilation and only one opening. The case with no pressure difference assumes stagnant air on both sides, no temperature difference between openings, and no pressure difference due to turbulence effects or any other effects. The case can be referred to as the limiting case.

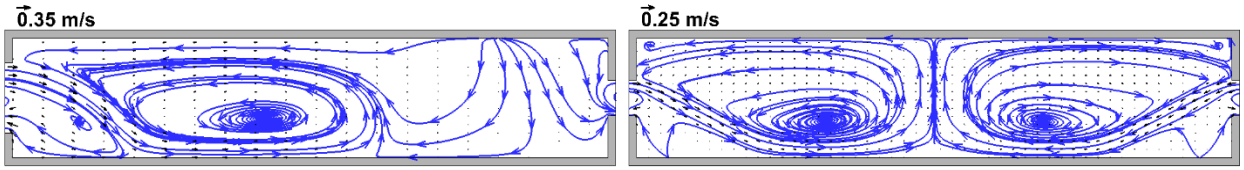

(a) Room 1.2 (b) Room 1.3

Figure 4.11. Steady-state flow fields represented with streamlines and vectors.

4.4 Investigation of the Rules of thumb

The rules of thumb were investigated by comparing the results of two rooms with depth-to-height ratios (DH) of 5 and of 7. The 7:1 ratio is larger than the recommended size of a room where cross-ventilation is reported to be effective. Comparing the two cases for Room 1.2 (refer to Figure 4.11a for DH = 5), the flow patterns for a DH = 7 are very similar and can be viewed in Figure 4.12. The main difference is in the extended region, where the area is dominated by a low velocity field and ventilation is due mostly to mixing. The extended section includes a larger region where the air exchange between the ambient air and the interior air is low. The larger low velocity region has the potential to have air that is less fresh than the rest of the room, but does not show any other major difference when the rule of thumb is broken.

DH = 7

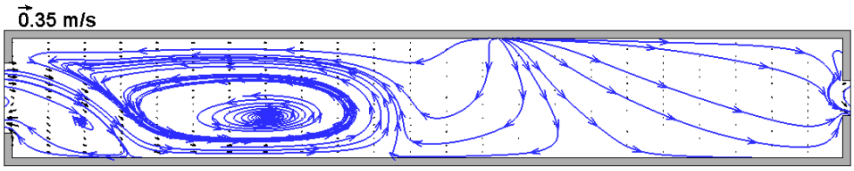

Figure 4.12. Steady-state flow fields represented by streamlines and vectors in Room 1.2.

The resulting flow patterns in Room 1.3 in the two rooms with a DH = 5 (Figure 4.11b) and 7, shown Figure 4.13, are very similar as well. In these cases, the difference between the flow patterns is the eddy that forms on either side of the room is extended in the larger room. The focus of the eddy is at approximately the same location. The flow extends towards the center of the room, but does not cross that location. The air velocity within the room is the same in both sized rooms. The region in the middle section of the room has very low speed air in the larger structure and leads to a larger area where mixing is dominate.

DH = 7

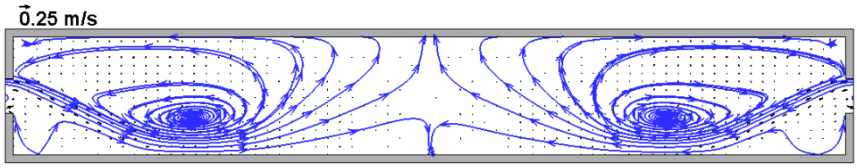

Figure 4.13. Steady-state flow fields represented by streamlines and vectors in Room 1.3.

The ACH is used to compare the overall air exchange rates in the rooms. As previously discussed, air quality is acceptable if the room has an ACH above 0.35, while heat removal is predicted to be sufficient with an ACH above 2. Both Room 1.2 (DH = 5 and 7) and Room 1.3 (DH = 5) have inflow and outflow at both openings, presented in Figure 4.14 Figure 4.15. The volumetric flow rate was determined using the inflow at both openings, where the sum of the inflow corresponds to the volumetric flow rate into the structure. The velocity was assumed to have a constant profile across the opening. The integral of the velocity profile into the room was multiplied by the area where the inflow occurs. Room 1.3 had equal inflow at both openings and

the total volume flow rate is twice one opening. The velocity profile is shown in Figure 4.15 for Room 1.3.

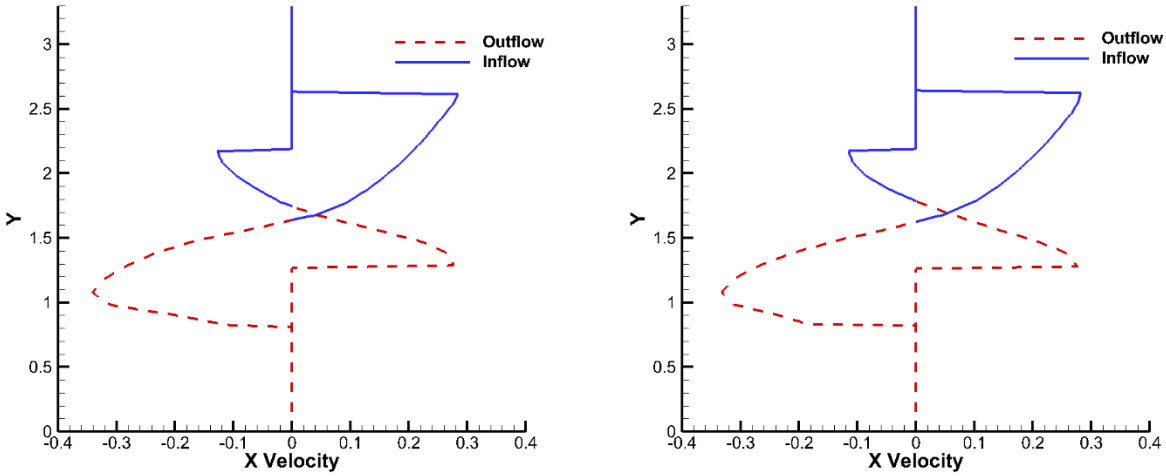

(a) DH = 5 (b) DH = 7

Figure 4.14. Flow patterns at the inlet and outlet for Room 1.2.

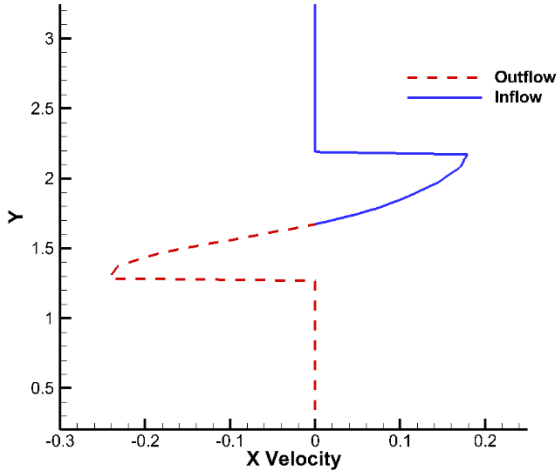

Figure 4.15. Flow patterns at the inlet for Room 1.3. DH = 5

The calculated ACH is shown in Table 4.3. In Room 1.2, both room sizes have adequate air exchange. The room experiences cross-ventilation even without forced air at either opening.

The flow is due to the pressure difference between openings and the temperature difference. The flow rate for both size structures is nearly equal and the difference between the ACH is due to the larger volume. The ACH for the room with a DH = 5 and 7 for Room 1.2 are 9.7 and 8.0, respectively. The air exchange in these rooms is high enough to adequately remove heat and to have fresh air. In Room 1.3, there is no pressure difference between the openings and the exchange is due to the initial temperature difference. Without a pressure difference between the openings, the air flow does not exchange between halves of the room. The overall ACH for DH of 5 and 7 are 1.8 and 1 respectively. While these values are high enough to maintain air quality, they are not high enough to remove heat adequately. Heat from any heat loads in the room would be expected to remain in the occupied space and would lower thermal comfort conditions in the room.

Table 4.3. ACH for cross-ventilation with pressure boundaries

Room	Room 1.2		Room 1.3	
Room ratio, DH	5:1	7:1	5:1	7:1
Volumetric Flow Rate (m^3/hr)	1368	1368	252	208
Volume (m^3)	141	171	141	171
ACH	9.7	8	1.8	1

Chapter 5 Single-Sided Ventilation

Single-sided ventilation is one method that is used to ventilate a space. In this chapter, a simple room with two windows on one wall will be used to simulate single-sided ventilation. Two configurations will be used. The first has windows near the ceiling and the floor and the second has windows in the middle of the wall vertically. A representation of human in the form of a rectangular cuboid with a heat flux on its surface will be used to observe the effects a human heat load has on single-sided ventilation. The simulations for single-sided ventilation show the flow patterns and the heat transfer in a room that uses single-sided ventilation.

5.1 Geometry and Conditions

Air flow patterns and heat transfer in a room that is expected to be naturally ventilated using single-sided ventilation (SSV) with two openings is modeled in the rooms shown in Figure 5.1. The two geometries are 3 m x 3 m x 7.5 m, which matches the depth and height corresponding to the rule of thumb, which is a DH = 2.5. The window placements are h_1=0.3 m, h_2=1.85 m, h_3=0.3 m, and h_3=1.075 m. Two rooms are modeled; the first has windows near the top and bottom walls (Room 2.1), and the second has both windows near the center of the wall (Room 2.2).

Passive cooling was modeled using the lower opening as a velocity inlet at 1 m/s and an initial temperature difference of 4 °C. The velocity was chosen as an upper limit of comfort. The lower opening was used as the inlet initially to model cool air entering the lower opening when the exterior air is cooler than the internal temperature so that hot air moves out the top opening. Pressure boundaries are also modeled to simulate air flow patterns without specifying an inlet.

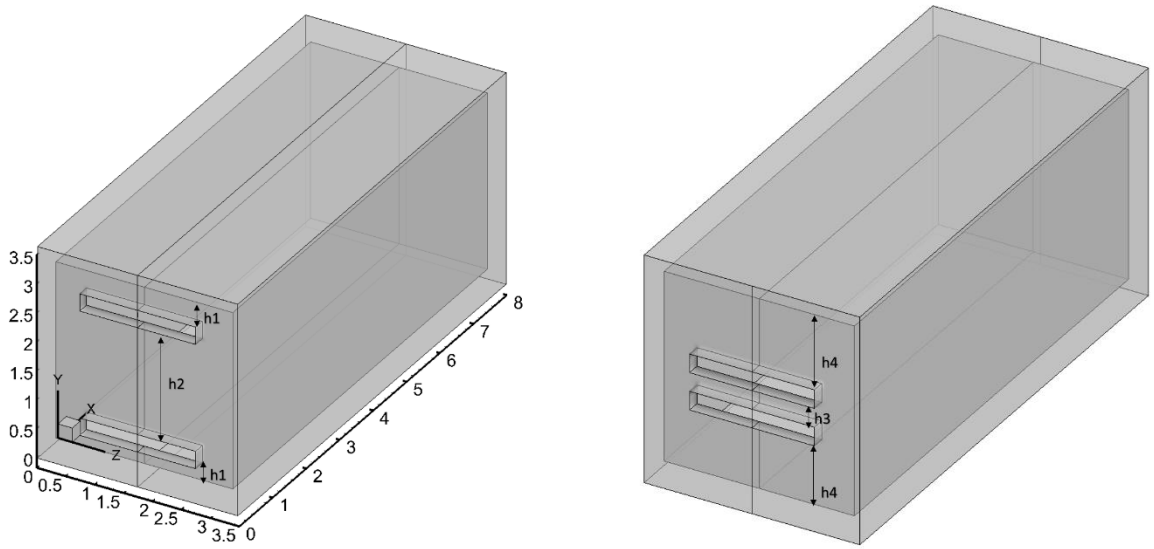

(a) Room 2.1 (b) Room 2.2

Figure 5.1. Rooms modeled with single-sided ventilation.

5.2 Results for Passive Cooling Simulations

Instantaneous passive cooling results are shown in Figure 5.2 with temperature contours and streamlines for Room 2.1. In Figure 5.2a, the flow moves in and along the bottom wall and recirculates through the entire room. As the incoming flow reaches the far wall presented in Figure 5.2b, a large eddy forms in the lower region of the room, with a smaller eddy above the incoming flow. The lower eddy continues to grow over time and remains at steady state as a large recirculation zone (Figure 5.2d), while the incoming flow moves from the inlet to the outlet. The smaller eddy near the outlet persists over time (Figure 5.2b, Figure 5.2c) but diminishes at steady state (Figure 5.2d) and flow is able to move smoothly from one opening to the other. The room cools fairly quickly and is at a nearly uniform temperature after only 5 minutes. The flow patterns are steady after 7.5 minutes and there is a uniform temperature and a large recirculation zone in the room.

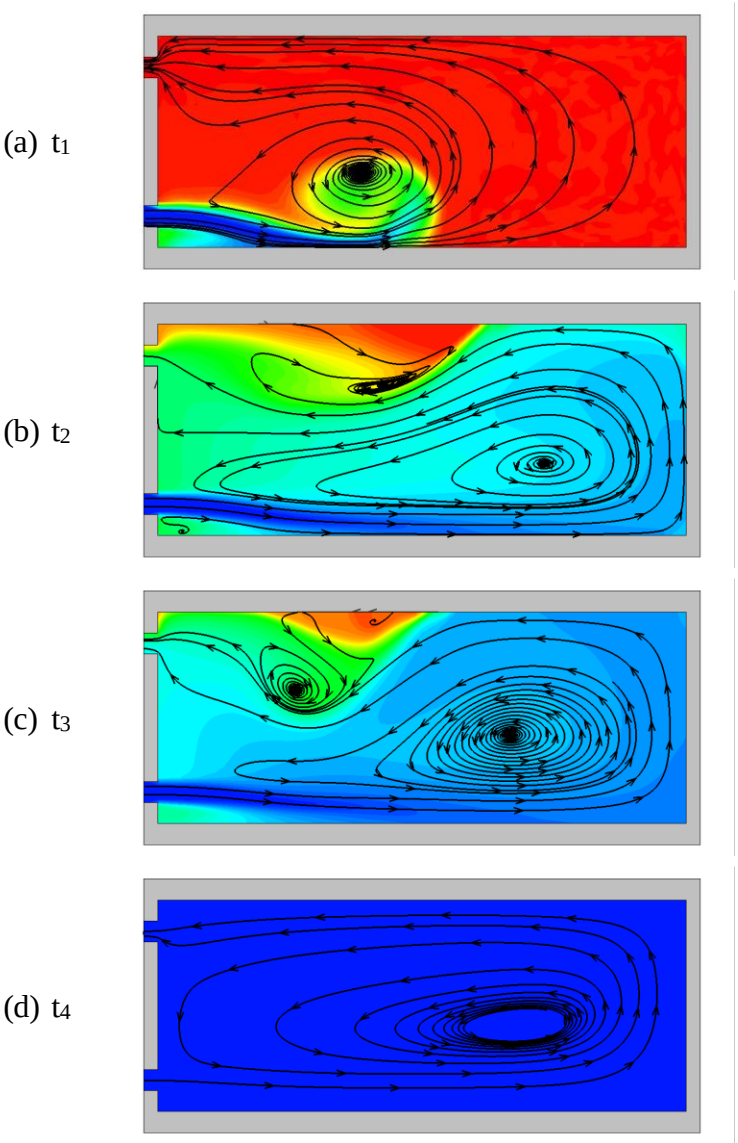

Figure 5.2. Instantaneous temperature contours for passive cooling with overlaying streamlines for Room 2.1

Passive cooling over time is represented with contours and streamlines for Room 2.2, shown in Figure 5.3. The cool air moves through the center of the room and initially cools the middle and far region of the lower half of the room (Figure 5.3a), while a pocket of warm air remains near the inlet. Over time the flow is represented by three recirculation zones (Figure 5.3b), two small ones near the inflow and a large eddy at the far wall. The large eddy reduces over time and the lower recirculation zone becomes the dominant flow in the room. The flow is represented by two small eddies above and below the incoming

flow (Figure 5.3c). As the temperature gradient in the room reduces, the cool inflow no longer attaches to the lower region of the room, but moves from the lower opening up and into the larger recirculation zone (Figure 5.3d). At steady state a small eddy persists near the outlet. When comparing the flow patterns of Room 2.1 (Figure 5.2) and Room 2.2 (Figure 5.3), this small eddy near the outlet appears to reduce the effectiveness of natural ventilation in the room.

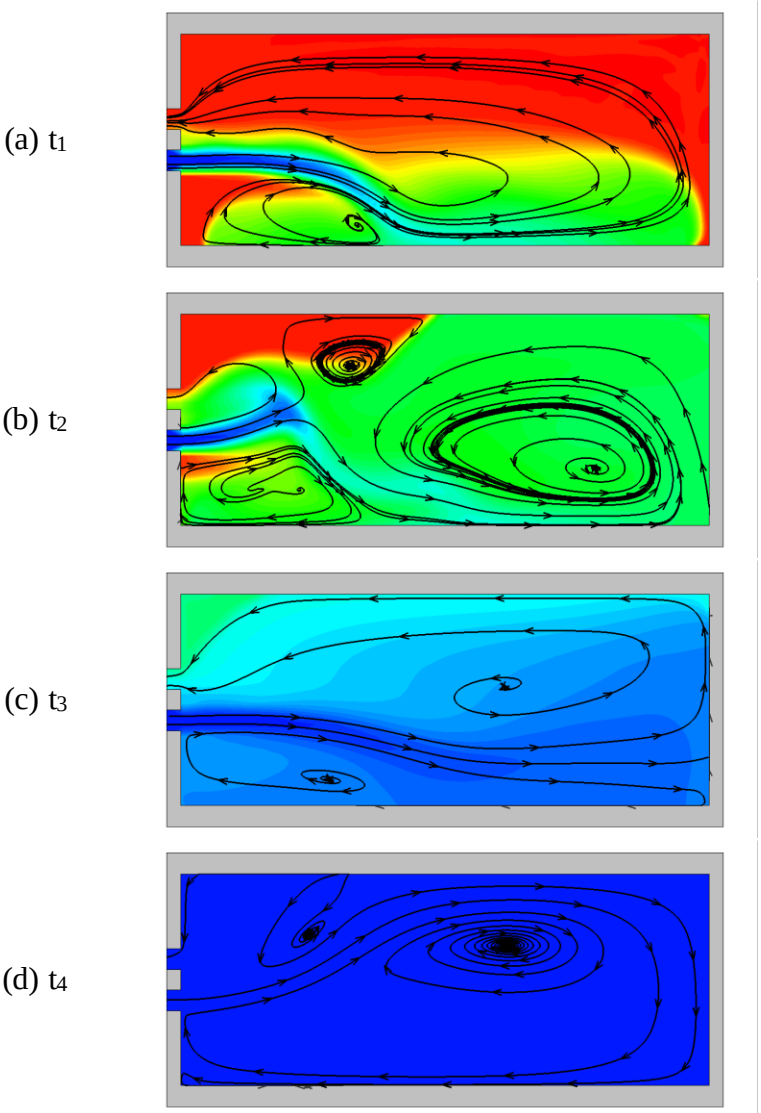

Figure 5.3. Instantaneous temperature contours and streamlines for passive cooling in Room 2.2.

The steady state flow is shown in Figure 5.4 for Room 2.1 and Room 2.2, represented with velocity vectors and streamlines. In Room 2.1, with the openings that are farther away, the flow is

characterized by a large eddy above the incoming flow. The incoming flow moves from inlet to outlet, and recirculates through the entire room. The majority of the flow is characterized by smooth low speed flow from inlet to outlet. In Room 2.2, where the openings are close together, the incoming flow moves toward the upper part of the room and is entrained into the large eddy. The majority of the room has low speed flow moving into the large eddy except for a small eddy that forms above the main flow. The room with windows farther apart has smoother flow form the lower opening to the upper opening, which presumably leads to more fresh air and less regions where stale will exist.

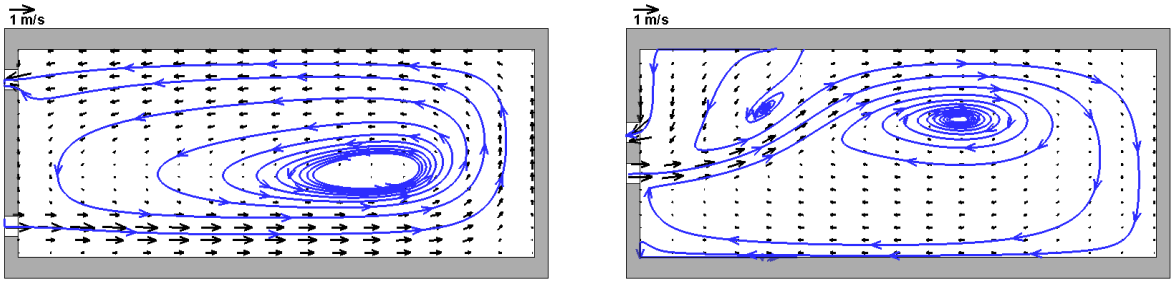

(a) Room 2.1 (b) Room 2.2

Figure 5.4. Steady state flow represented by velocity vectors and streamlines.

5.3 Investigation of the Effect of Different Boundary Conditions

The time sequence can be viewed in Figure 5.5 for Room 2.1 with ambient pressure specified at both openings to allow the flow to naturally develop without a prescribed inflow velocity. Initially, the cool air moves in to the lower opening and begins to fill the lower region of the room with cool air (Figure 5.5a). The temperature in the room is stratified throughout in Figure 5.5b, with low temperatures near the lower region of the room, medium temperatures in the center, and high temperatures at the upper region. As the cool region increases, the openings both have inflow and outflow and it becomes difficult to differentiate the inlet and outlet. As the temperature gradient reduces, and the hot air is confined to the upper region of the room, the inflow is from the

upper opening, as cold air moves in and towards the lower region of the room (Figure 5.5c). A large eddy forms and as the temperature in the room becomes uniform, and the flow patterns match that of the previous case (Figure 5.4a), with one large eddy. The flow pattern is essentially flipped from the velocity inlet case, and flow moves from the upper to the lower opening shown in Figure 5.5d.

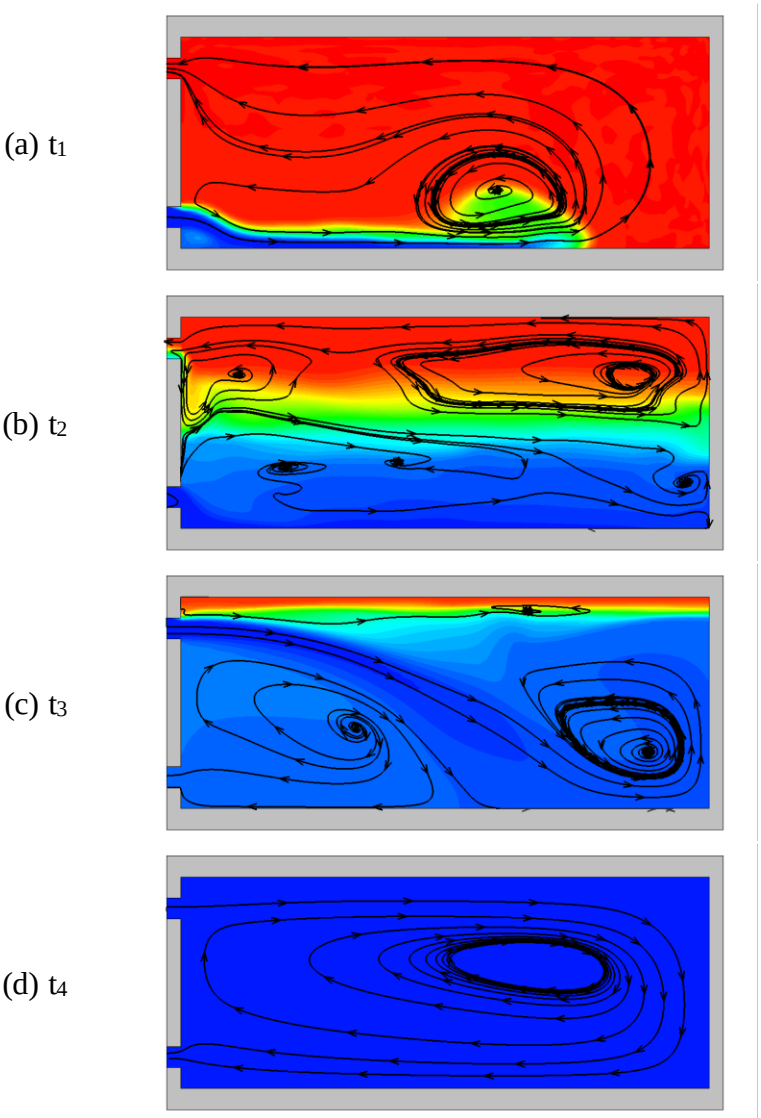

Figure 5.5. Instantaneous passive cooling modeled with ambient pressure at the openings represented with streamlines overlaying temperature contours in Room 2.1.

The cooling sequence is also shown in Figure 5.6 for Room 2.2. Cool air moves in through the lower opening initially and begins to fill the room from the bottom to the top (Figure 5.6a). The temperature stratification is less pronounced than in Room 2.1, as cooling is more reliant on mixing than forced air. The hot regions of air disappear more quickly, but the overall average temperature in the room is still higher and the flow into the room is lower (Figure 5.6b). Once the room has reached an effectively uniform temperature shown in Figure 5.6c, the flow pattern is represented by a large eddy from the inflow, and a small eddy that leads to the outflow. The inflow is from the upper opening and the outflow is at the lower opening. The flow patterns are effectively flipped from the velocity inlet conditions (refer to Figure 5.2).

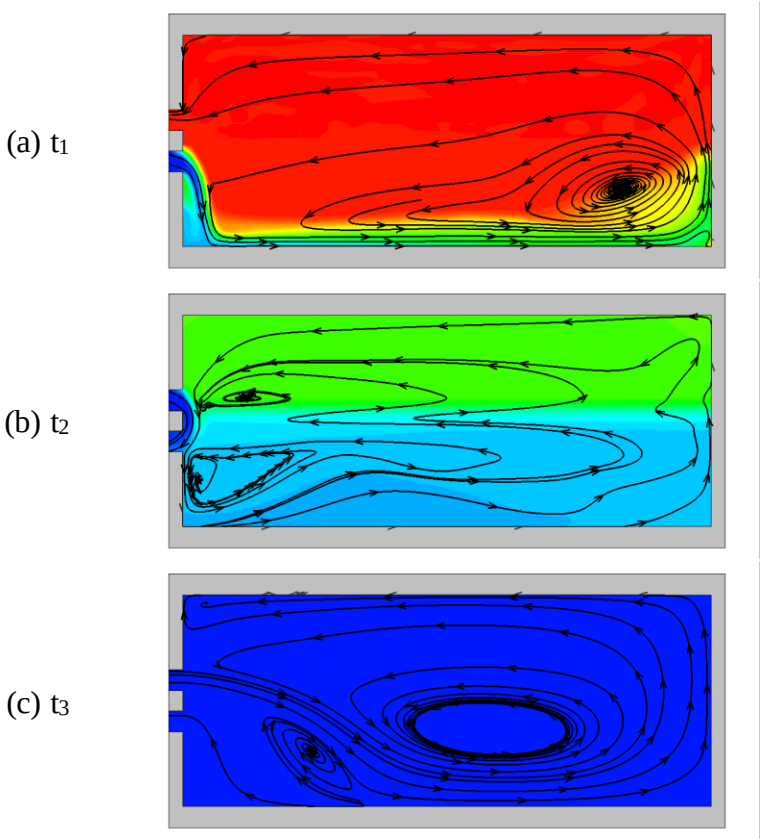

Figure 5.6. Instantaneous passive cooling modeled with ambient pressure at the openings represented with streamlines overlaying temperature contours in Room 2.2.

The steady state flow patterns for Room 2.1 and Room 2.2 are compared in Figure 5.7. The flow patterns are opposite of those in Figure 5.4 when a velocity inlet was specified. The flow in Room 2.1 appears to be more effective in cooling the room and also maintaining air overall quality. In Room 2.2, the inflow reaches near the center of the room and is entrained into a large eddy, but is accompanied by another small eddy near the outlet. The air speed in Room 2.2 is also about 50% of the air speed in Room 2.1, which leads to less inflow and a lower ACH. The lower air flow results in a longer time to remove heat and implies lower air quality.

The ACH for each case is shown in Table 5.1. A velocity of 1 m/s corresponds to an ACH of 30.59, much higher than the recommended comfort level. Using pressure boundaries, the ACH for both Room 2.1 and 2.2 is within a sufficient level, at 10 and 5 respectively. These values represent the lowest expected flow into the structure, as the driving force is the temperature difference and the pressure difference due to the distance between openings. An increase in pressure due to wind or turbulence at the openings would lead to a higher ACH and more effective cooling.

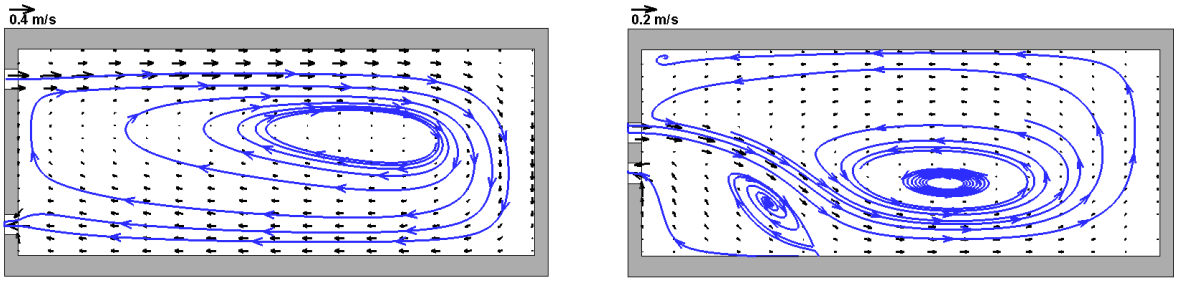

(a) Room 2.1 (b) Room 2.2

Figure 5.7. Steady state flow patterns represented by streamlines overlaying velocity.

Table 5.1. ACH for cases of single-sided ventilation.

	Velocity Inlet	Pressure Inlet	
Room	2.1, 2.2	2.1	2.2
Volumetric Flow Rate (m^3/hr)	2160	725.1	349.5
Volume (m^3)	70.60	70.60	70.60
ACH	30	10	5

The relationship Gr/Re^2 for SSV indicates the dominant effects between buoyancy and forced air, shown in Table 5.2. With a specified velocity, the conditions of the room are dominated by the forced air at the opening and buoyancy forces are very weak, which is evident in the flow patterns when comparing the cases with the specified velocity (Figure 5.4) and the cases with pressure boundaries (Figure 5.7), as the flow patterns are opposite. When pressure boundaries are specified, Gr/Re^2 = 0.32 and 1.76 for Room 2.1 and Room 2.2, respectively. The velocity at the openings is much lower with pressure boundaries, leading to a weaker effect due to the forced air, and a larger buoyancy contribution to the flow patterns.

Table 5.2. Reynolds number, Grashof Number, and the relationship Gr/Re^2 for 4 different cases

	Room	Re	Gr	Gr/Re^2
Specified Velocity	2.1	1.9×10^4	1.5×10^7	0.04
	2.2	1.9×10^4	1.5×10^7	0.04
Pressure Boundaries	2.1	6.7×10^3	1.5×10^7	0.32
	2.2	2.9×10^3	1.5×10^7	1.76

The difference in Reynolds number between Room 2.1 and Room 2.2 with pressure boundaries is due to the lower velocity at the opening for Room 2.2. As the temperature difference is equal in both cases, the velocity difference is due to the pressure difference created by the distance between the openings. A larger height between openings creates a larger pressure difference and in turn a higher volume flow rate, leading to a higher ACH, and presumably the room is ventilated better by removing heat quicker and raising the expected air quality in the overall room.

5.4 Analytical Results vs. Simulation Results

The volume flow rate determined from the simulations was compared to the analytical volume flow rate. The equation is derived from Bernoulli's theory for a buoyancy-driven flow [24]. The volume flow rate is calculated for single-side ventilation with two openings as a function of temperature and the height between openings:

$$\dot{V} = C_d A \sqrt{g h \Delta T / T_\infty} \tag{5.1}$$

where ΔT is the temperature between the interior and ambient temperature (T_∞), A is the opening area (assuming equal area), h is the height between openings, and C_d is the discharge coefficient (0.6) [24].

The analytical volume flow rates and simulated volume flow rates for Room 2.1 and Room 2.2 are shown in Table 5.3. The error between the results is approximately 5% and can be attributed to the discharge coefficient, where $C_d = 0.6$ is the value used when modeling flow through a doorway. The analytical and simulated results are in good agreement and validate the use of

pressure boundaries. The flow in these cases are driven by the initial temperature difference between the ambient and internal temperatures.

Table 5.3. Analytical and Simulated volume flow rate (m^3/s)

	Analytical	Simulation
Room 2.1	0.192	0.201
Room 2.2	0.102	0.097

5.5 Investigation into the Rules of Thumb for Single-Sided Ventilation

The rule of thumb for single-sided ventilation with two openings is DH=2.5. A room with a ratio of 3:1 is modeled for both far and close window configurations to predict the flow patterns that develop in the larger room and the corresponding ACH. The flow patterns for DH = 3 are shown in Figure 5.8 and refer to Figure 5.7 for DH = 2.5. In Room 2.1, the large eddy in the center of the room encompasses the entire room for both room sizes. The flow moves from the top to the lower opening with a large eddy forming towards the room center. The velocity in both room sizes are very similar and the volume flow rates are nearly equal. The only major difference is the increased volume in the larger room, which leads to a lower ACH shown in Table 5.4.

In Room 2.2, both rooms (DH=2.5 and 3) have a large eddy near the lower section of the room about 4 meters into the room. This eddy originates from the inflow and is elongated in the larger room and circulates through the entire room. Other than the elongation of the eddy, the flow patterns and velocities are very similar.

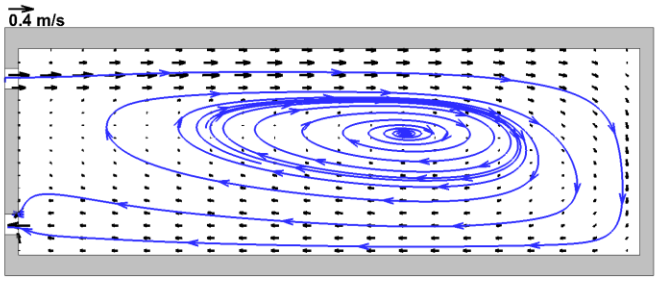

(a) Room 2.1

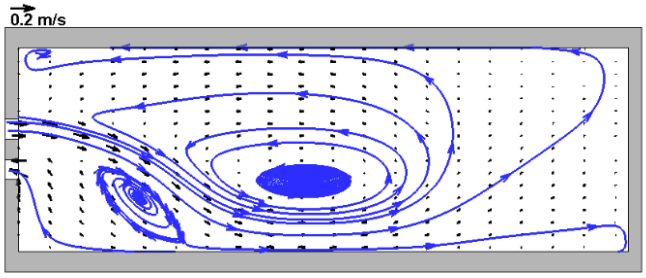

(b) Room 2.2

Figure 5.8. Steady state flow patterns represented with streamlines and vectors for a DH = 3.

The volume flow rate for the different sized rooms have a difference under 2%. The flow into the room is very similar, independent of the room length. The change in the ACH and subsequent air quality in the rooms, shown in Table 5.4, is due to the larger volume of the bigger room. Even though the ACH is decreased in the larger room, the ACH is still adequate to remove heat and to maintain proper air quality. An increase above DH = 2.5 did not lead to any discernible flow pattern differences or an unacceptable ACH value.

Table 5.4. ACH for single-sided ventilation with a DH = 3.

Room	Room 2.1	Room 2.2
Volumetric Flow Rate (m^3/hr)	712.7	352.08
Volume (m^3)	84.95	84.95
ACH	8.39	4.14

5.6 Effects of a Human Heat Load in Single-Sided Ventilation

The effect of a human heat load is simulated using the same geometry, room setup, and conditions for single-sided ventilation using pressure boundaries and a DH = 2.5 (Section 5.1) with a rectangular cuboid included to represent an average sized person. The geometry is shown in Figure 5.9. The model has a height of 1.7 m, a shoulder to shoulder width of 0.3 m, and a depth of 0.25 m. The total surface area is 1.92 m^3. The heat gain from the model is approximated to be 75 W, which is similar to the heat gain from people in conditioned spaces found in [16]. The activity modeled is standing, light work, and the sensible heat is modeled. In Fluent, a heat flux of 38.5 W/m^2 was applied at the surfaces representing the skin of the rectangular figure.

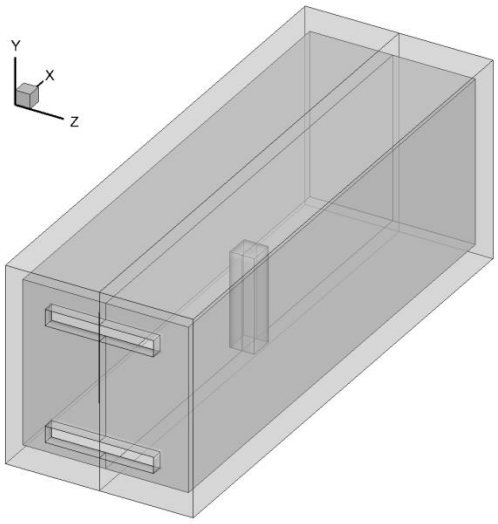

Figure 5.9. Geometry for single-sided ventilation with a rectangular cuboid representing a person

A steady state solution is reached to simulate the effect the human heat load has on ventilation in the room. Initially a steady state solution was simulated. If the residuals did not converge, the simulation is switched to a transient solution. A steady state is reached when the volume flow rate is constant or periodic, in which case a time-averaged solution is used. Symmetry was used in the z-plane and adiabatic walls are modeled to decrease computation time.

Temperature contours and velocity vectors are shown in Figure 5.10 at a plane through the center of the room in the z-axis, which is also the center of the rectangular figure. The region directly surrounding the figure is at an elevated temperature than the ambient temperature, but the temperature is only increased by approximately only 0.5 to 1 °C, a reasonable increase in temperature and within the thermal comfort range. The maximum air velocity in the room is comparable to the simulations for single-sided ventilation (refer to Figure 5.7a**)** 0.4 m/s, also in the comfort range. The cool ambient air circulates in the front half of the room near the openings and the opposite half is represented by low speed flow. The entire plane is characterized by vectors of significant size, as air is flowing through the entire room. The air flow throughout the room presumably keeps areas of stale or stagnant air to a minimum.

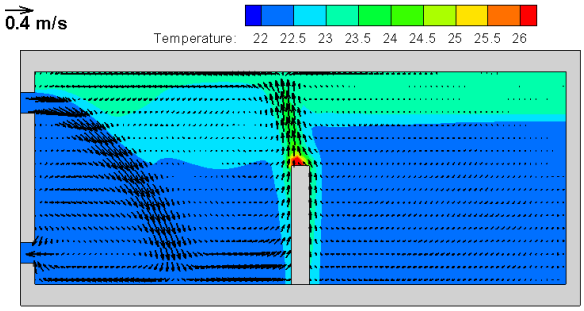

Figure 5.10. Temperature contour and velocity vectors for passive cooling with a room ventilated using single-sided ventilation with a human model inside

The thermal stratification in the room can be clearly seen in Figure 5.10. The contour has very few levels between the minimum and maximum temperatures, so that each 0.5 °C level can clearly be seen. Aside from the region of air directly above the human model, the temperature in the occupied region is between 22 and 22.5 °C, a deviation of 0 to 0.5 °C from the external air. The occupied region of the room is at a temperature comparable to the external temperature, whereas the added heat due to the model in the room is contained to the upper region, allowing the space to be within the comfort zone of the occupant.

The flow patterns in the room have changed from the original case (Section 5.2) due to the obstruction in the center of the room and the thermal plume above the figure. The flow patterns are shown in Figure 5.11with streamlines overlaying a temperature contour. The ambient air flows in the top opening and towards the floor. As it reaches the lower section, it branches off into two separate flows. The lower half moves towards the outlet and leaves the room. The upper half flows towards the model and up and into the plume that is created by the heat load. The flow reaches the ceiling and recirculates through the front half of the room. Above the model, the air mixes with the air from the second half of the room. In the upper portion of the room on the half that is farther away from the openings, the air from the inflow, above the model, and the far half is entrained into a recirculation zone out of the occupied space.

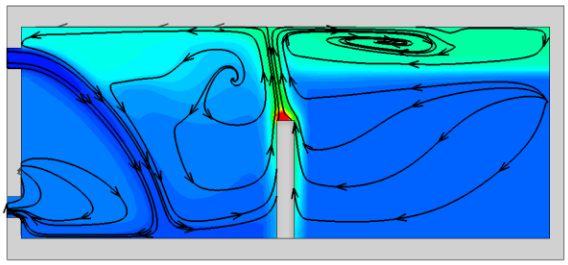

Figure 5.11. Flow patterns and thermal stratification in Room 2.1 represented with temperature contours with overlaying streamlines

A second plane, shown in Figure 5.12, which is 1.15 m from the wall and midway between the model and the wall, shows the effect of the heat load on a region of the room where the occupant is not currently in. The air flow patterns are similar to that of the mid-plane through the occupant, but a larger amount of air from the inflow reaches farther into the room and is entrained into a recirculation zone. The air flows from other regions of the room, including the upper region and the far half of the room, into the recirculation zone. The outflow is mainly from the air trapped underneath the inflow in a region that is at a slightly higher temperature than the inflow and the

majority of the room. It can also be seen that the warmer air, which in this case is closer to 23 to 23.5 °C, is contained to the upper portion of the room and out of the occupied space. The air flow patterns, combined with the slow moving air and temperature in the occupied zone, represent a space that is within comfort levels. The presence of a heat load does not lead to a room that is overheated or filled with zones of stagnant air.

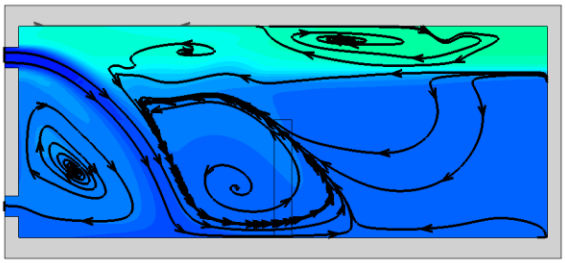

Figure 5.12. Temperature contour and overlaying streamlines at a plane 1.15 m from the wall

A plane through the center of the x-axis, which is also through the center of the rectangular mode, shows the overall thermal stratification in the entire z plane in the center of the room and is shown in Figure 5.13. The plane shows the effect the heat load has in the region closest to the rectangular figure. The zone directly adjacent to the rectangular figure is at an elevated temperature at about 24 °C, which is about 2 °C above the ambient air. The thermal plume begins at the bottom of the figure and increases in size as it moves up the boundary of the rectangular model. The vectors show that the air is moving away from the body and towards the ceiling. Besides the adjacent region to the model, the overall air temperature in the room is near the ambient temperature. The hot air is contained to the uppermost region of the room, keeping it above the occupied zone. The air flow moves up and along the boundary of the model and when it reaches the ceiling, the flow moves towards the corners and is entrained in the corners. Overall, there is presumably good airflow throughout the room, as air circulates from the lower portion into the upper region of the room.

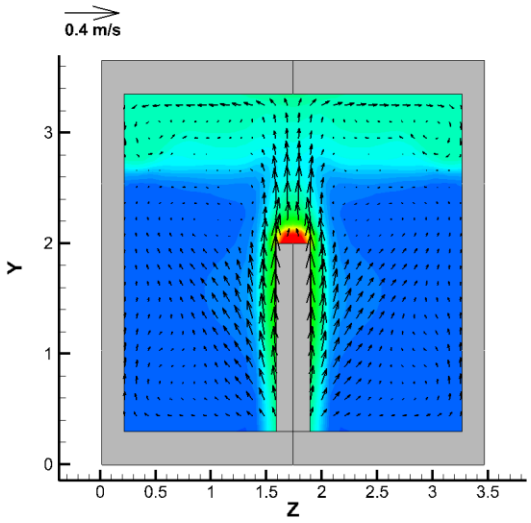

Figure 5.13. Temperature contour and velocity vectors through the center of the x-axis through the rectangular model

Figure 5.14 shows the air flow patterns in a room with a DH = 3. When comparing the overall flow patterns to the room with a DH = 2.5, the flow patterns are extremely similar. A large eddy is located in the upper region where the flow from the region far from the window meets the flow above the rectangular figure. Inflow moves into the room and is split into two parts. The upper part moves along the ground and up towards the rectangular model and the second part flows out the lower opening. The overall patterns and thermal stratification is very similar to the smaller room, and the size does not appear to have negatively influenced the flow patterns or the temperature of the occupied space.

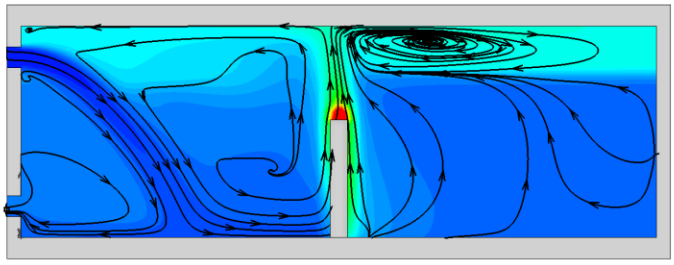

Figure 5.14. Temperature contour with overlaying streamline in Room 2.1 with a DH = 3

The ACH is shown in Table 5.5 for a DH = 2.5 and 3. The volume flow rate is comparable for both size rooms, with a difference of only 2 m^3/hr. The ACH is 8.4 and 7.0 for a DH = 2.5 and 3, respectively. The difference in ACH is due to the increased volume in the larger room, and while it is lower, it indicates that the room is adequately ventilated according to the recommended minimum ACH to remove heat. Overall, both rooms are expected to be adequately ventilated.

Table 5.5. ACH and volume flow rate for single-sided ventilation with a human model

DH	2.5	3
Volumetric Flow Rate (m^3/hr)	590.6	592.78
Volume (m^3)	70.60	84.95
ACH	8.4	7.0

Chapter 6 Casa Giuliana

The Casa Giuliana apartment in Como, Italy, which was built in 1939-1940 [25], is the first full-scale building modeled. Passive cooling is modeled in one apartment in the building. The apartment has an open layout and is located in a region with a mild climate. It utilizes a cross-ventilation with large deck doors and small windows on the walls opposing. The air exits the small windows and moves through an interior space that is in between hallways that serve the complex. Two different scenarios are simulated. The first has a volume flow rate based on the ambient conditions during the summer season, while the second has a flow rate that leads to an ACH close to the minimum recommended value. The apartment building represents a design that allows cross-ventilation to be utilized.

6.1 Apartment Background and Simulation Setup

Casa Giuliana is a building located near the southern tip of a lake in the valley of the Lago di Como. The model of an apartment in the building is shown in Figure 6.1. The CAD drawing was provided by Prof. Ulrike Passe and Suncica Jasarovic of Iowa State University. The apartment is well designed for natural ventilation, with an open layout in the apartment and deck openings that are wind facing with smaller openings on the opposing side. The apartment has two large rooms at the deck openings: a bedroom and living room. In the center of the back section of the apartment is a small room that can be used as a den or dining room and a larger bathroom. On either side of the small room is a bathroom and a kitchen. The kitchen and the small bathroom have windows that are used as outlets for cross ventilation.

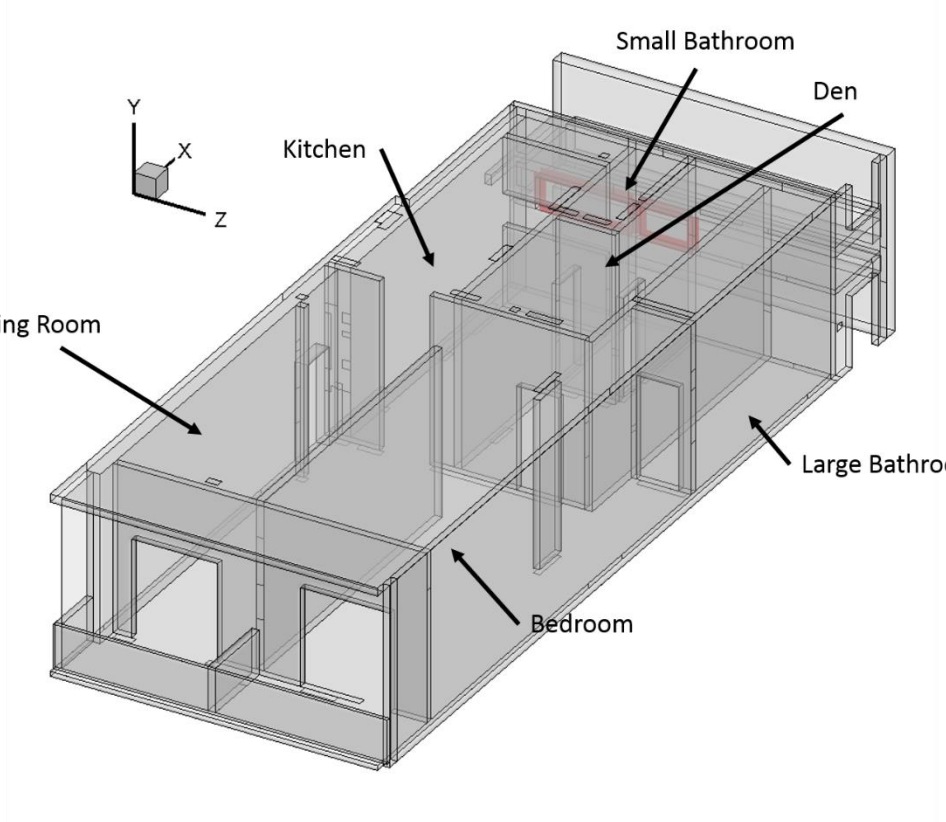

Figure 6.1. Geometry representing Casa Giuliana. Windows are outlined in red.

A closer look at the outlet windows is shown in Figure 6.2 as the red regions. There is one larger window to the left in the kitchen and a smaller window in the small bathroom. These windows are adjacent to a narrow region, similar to an air duct, between the floor and ceiling of the hallway corridors of the apartment complex. This small region between the windows and the exterior air is more isolated from the ambient conditions, which keeps the leeward pressure at the outlet windows lower, allowing the ambient conditions on the deck side of the apartment to drive the flow [25].

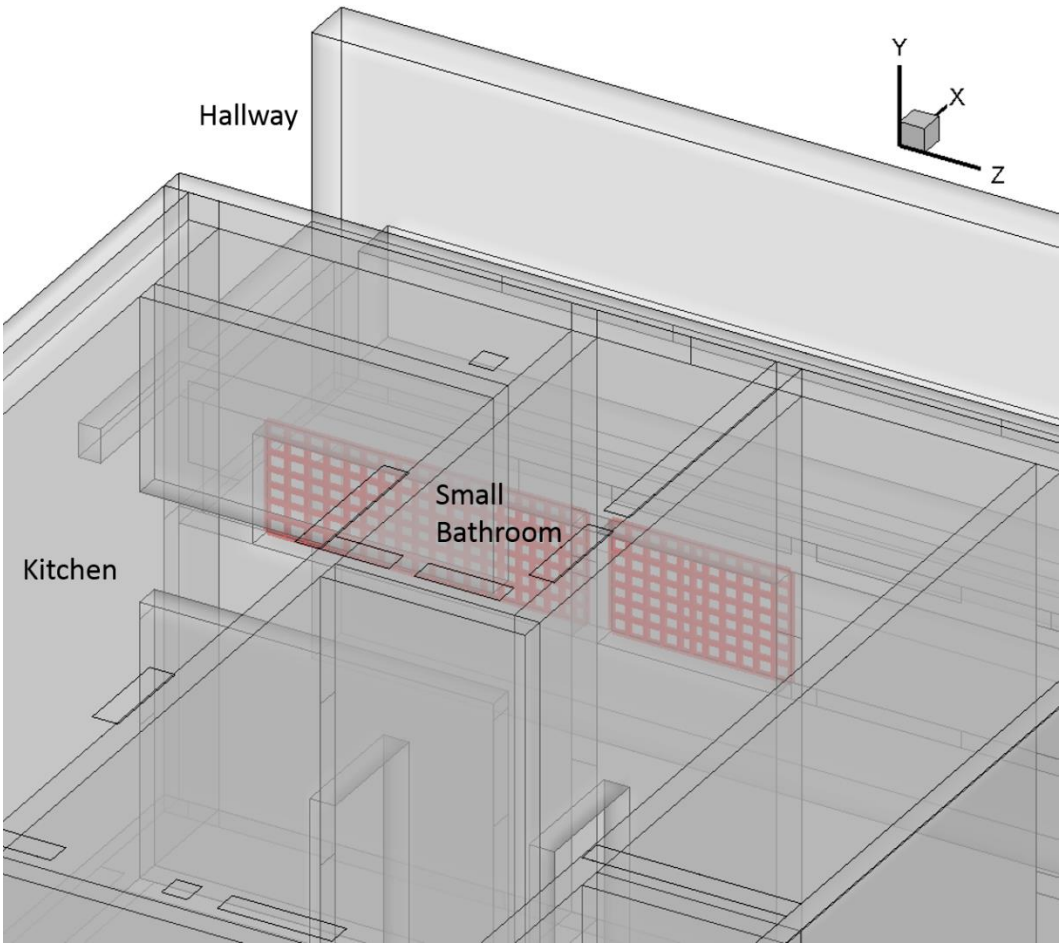

Figure 6.2. Enlarged view of the outlet windows

The section outside of the apartment, but interior to the building and adjacent to the apartment windows is shown in Figure 6.3. This region acts similarly to an air duct, as the air exiting the apartment moves through the windows (outlined in red), through this space, and out the exterior windows (outlined in black). This keeps the air immediately adjacent to the apartment isolated from the outside and insulated from ambient conditions with the hallways, which are located above and below this section.

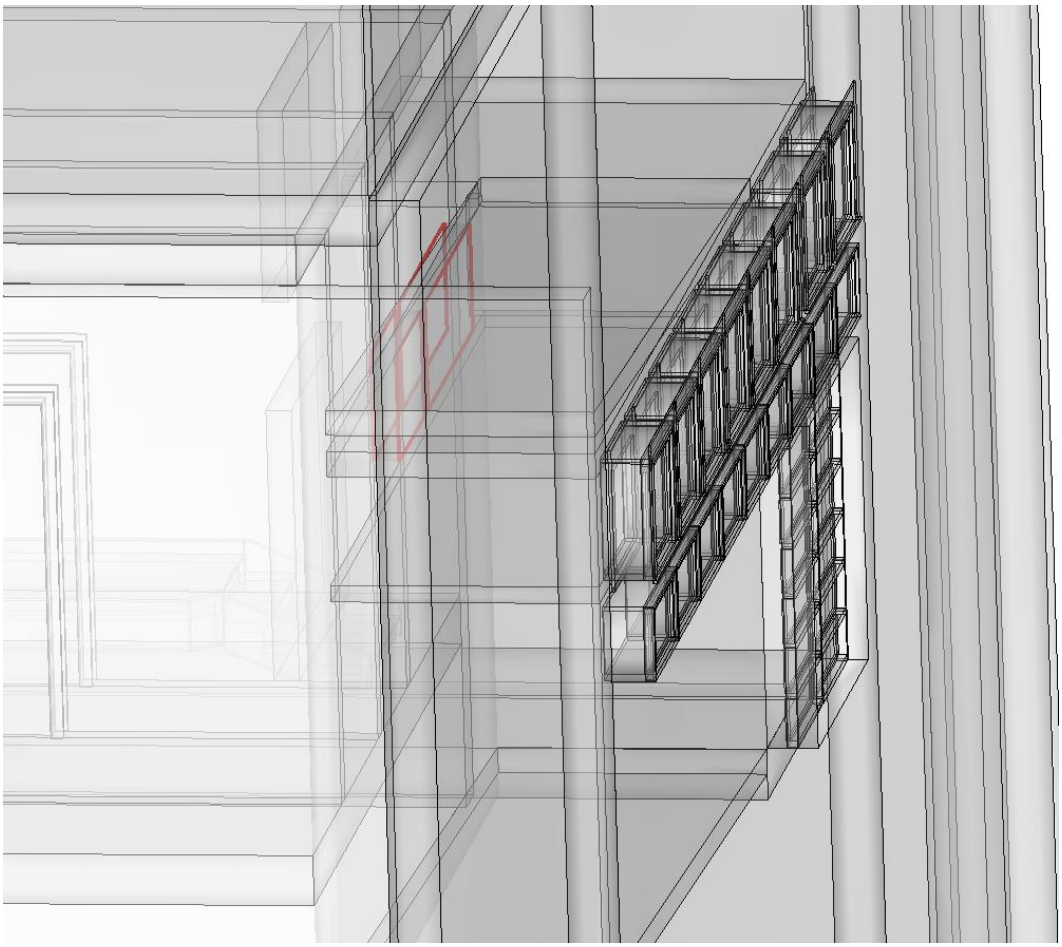

Figure 6.3. View of the region between the apartment windows and exterior windows

The mesh is shown in Figure 6.4, displayed with a front view in Figure 6.4a and a rear view in Figure 6.4b. The apartment is 16 m long from the deck to the apartment's outlet windows, 3.4 m from the floor to the ceiling, and 6.7 m wide. The high ceilings and long apartment contributes to a volume more than 350 m^3, which makes adding compression to the mesh computationally expensive. Due to the large interior volume, the intent of building a mesh was to have an average cell size of 10 cm. 10 cm was found to be sufficient to accurately depict the overall profile of the flows and the temperature profiles. Due to the complexity of the blocking and the large volume of the interior fluid, an average cell length of 12 cm was obtained when the mesh was built. The interior fluid volume has a total of 300000 cells. Computation time is reduced by modeling

adiabatic walls. A side view of the mesh is shown in Figure 6.5, which shows a good representation of the average cell size.

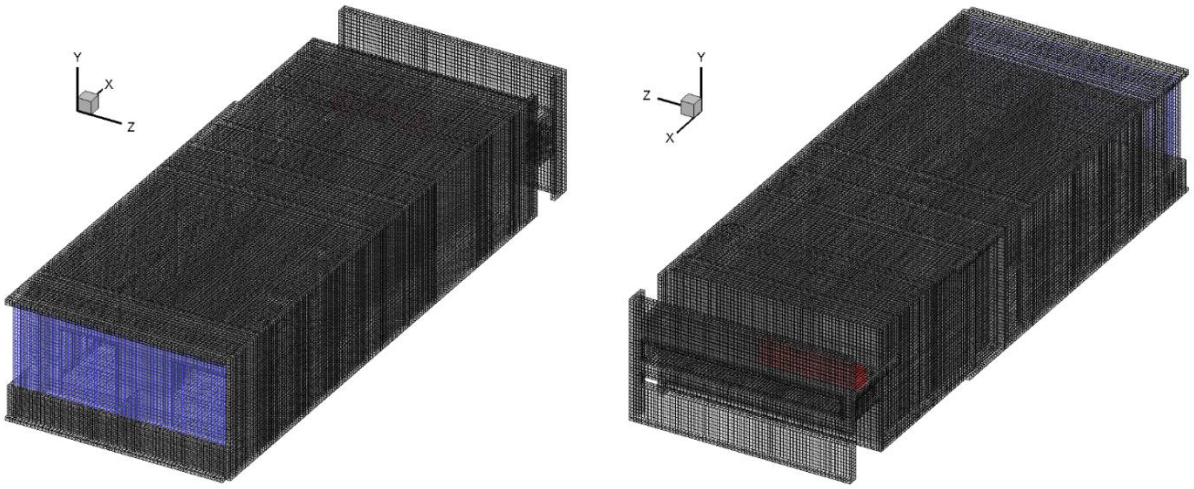

(a) (a)

Figure 6.4. Overall mesh for Casa Giuliana. (a) Front View (b) Rear View

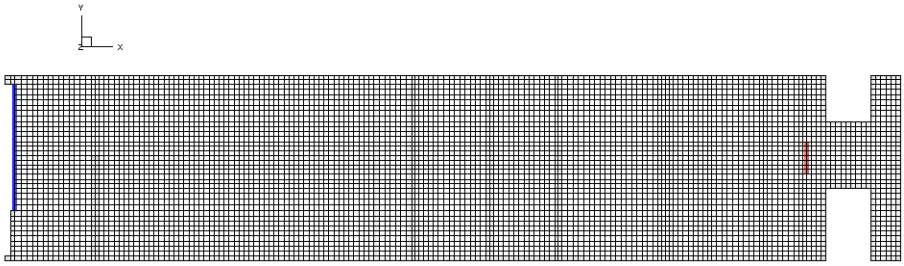

Figure 6.5. Side view of the mesh for Casa Giuliana

Physical obstructions and heat loads are added to the apartment to simulate their effects on ventilation, and the geometry with these objects is shown in Figure 6.6. In the bedroom, a bed and a cabinet are added. In the living room, a couch with a person sitting on it and a television on a stand are added. A high level of heat loads are added to the kitchen. A refrigerator and stovetop are located along the far wall with cabinets on the opposing wall. A person is included in the

middle of the room. A desk, computer chair, computer, monitor, and a person are included in the den. The furniture and heat loads are included to represent a normal apartment at a time in the day when the heat load is presumably at its highest, when food is being cooked and electronics are also being used. The heat loads and corresponding heat fluxes that are simulated at the surfaces of the furniture and people are shown in Table 6.1. Small surfaces that represent the approximate location of heat loss for the electronics and fridge are used as a portion of the overall geometry and not the entire surface. The people are modeled similarly to the model in Chapter 5 for single-sided ventilation are designed as a rectangular cuboid. The standing person is 1.7 m tall, which is also used as the height of the occupied zone in this study. For the stovetop, two separate square sections representing a "hot" stovetop are used as hot surfaces.

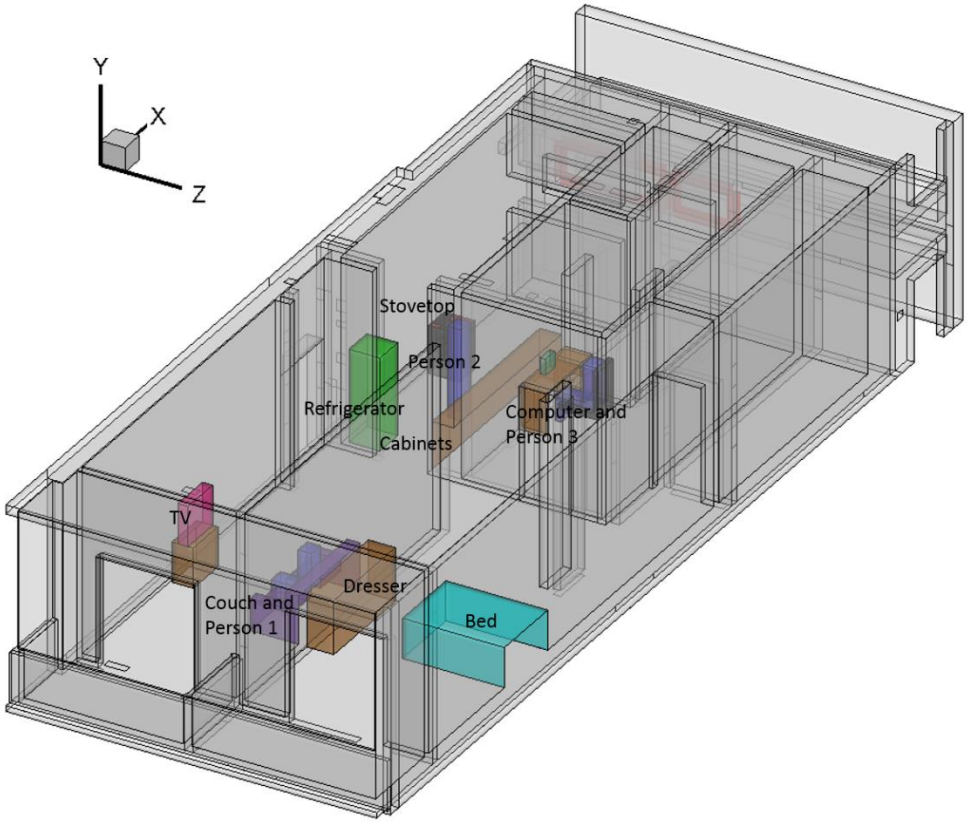

Figure 6.6. Geometry representing Casa Giuliana including furniture and models representing people

Table 6.1. Furniture/Person and its accompanying heat flux and heat load

Furniture/Person	Heat Flux (W/m^2)	Heat Load (W)
People (3)	38.5	75
Fridge [26]	4000	725
TV [27]	60	35
Monitor [27]	390	35
Computer	600	70
Range (2) [28]	25000	1125

The conditions simulated represent a cool breeze after a hot day, with an initial interior temperature of 28.5 °C and an ambient temperature of 24 °C at the windows. The wind direction and speed are 45 degrees from the north at 2.23 m/s (5 mph). The direction of the wind is flowing at an angle of 45 degrees into the apartment in the positive x and z direction [25]. A schematic of the expected flow is shown in Figure 6.7 as a reference.

The blue surface in Figure 6.4 is specified as a velocity inlet and the red surfaces are ambient pressure. The blue surface is not a physical boundary, such as a wall or window, but is a representation of a location in space that is affected by the ambient conditions. Two different conditions are simulated in the apartment. The first scenario has a velocity specified at the inlet that is estimated to be 10% of the external wind speed. The decrease is used to better estimate the actual air speed at the deck opening. The conditions correspond to an ACH of 32, well above the minimum recommended value to remove heat. In the second scenario, the velocity specified at the inlet is designed to have an ACH of 5, a value much closer to the minimum recommended value to remove heat (2).

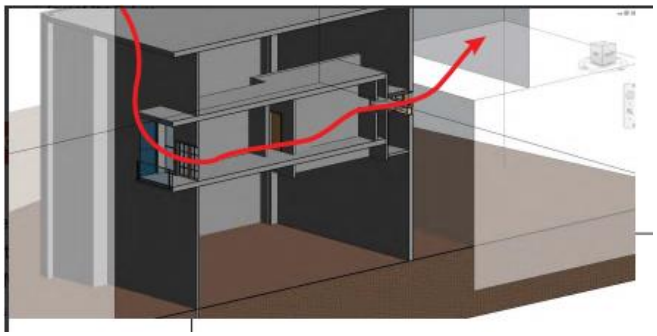

Figure 6.7. Representation of the expected flow through the apartment. Used with kind permission of Ulrike Passe, 2014.

6.2 Results Based on Ambient Conditions

The Casa Giuliana apartment is used to compare passive cooling without and with heat loads. The results from the first scenario described in section 6.1 are shown in Figure 6.8, using

temperature contours. In the empty apartment, the entire apartment is cooled very quickly. At one minute, the rooms near the deck have begun to cool substantially, with the initial high temperature air moving up and out of the occupied space, into the duct between the hallway corridors. The same conditions are shown in the apartment that includes furniture and people. At one minute, there is little difference between the empty apartment and the apartment with furniture and people. At 3 minutes, there are noticeably higher temperatures in the upper region of the kitchen near the rear windows. The kitchen experiences high heat loads when furniture and people are included and remains warmer than the empty apartment. The kitchen is also adjacent to the open windows, and receives a substantial amount of the inflow, as cross-ventilation from the large deck doors to the small rear windows drives flow. As a point of reference, the DH for the apartment is below 5, within the size constraints of the rule of thumb for cross-ventilation. The two rear rooms that do not have windows remain noticeably warmer in both simulations over time due to the lack of cross-flow in these sections, as they are isolated from any type of cross-flow and do not have a high driving pressure difference. The two rooms remain at a higher temperature than the rest of the apartment even as the overall temperature decreases towards the ambient temperature.

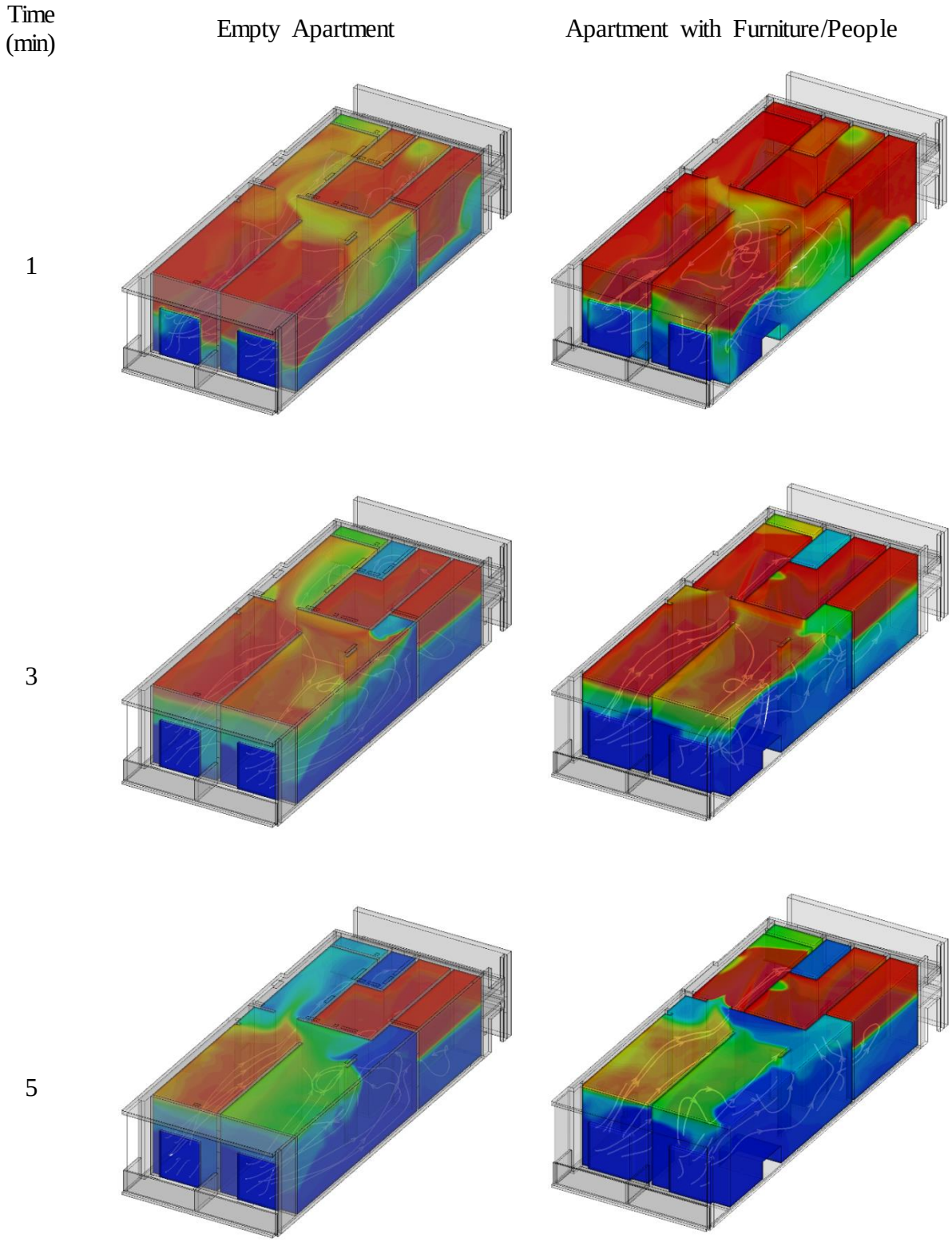

Figure 6.8. Temperature contours for passive cooling in Casa Giuliana over time.

Temperature contours with overlaying streamlines show passive cooling and the flow patterns in the apartment in Figure 6.9. The cross ventilation from the inflow at the deck doors through the kitchen and the outflow through the windows is visible in the far plane at each time step. Even with the obstructions in the apartment, there is a visible cross-flow through the entire apartment, which ventilates the left side of the apartment very well. The second plane, through the middle of the apartment, has a large eddy at the wall opposite of the inflow. The cool inflow reaches the back wall and cools the region, but is less effective than the section with cross-flow. Although it stays warmer than the other plane, the hot air is contained to the upper region of the apartment. When the heat loads are included, the cross-flow through the kitchen is unable to cool the entire kitchen to the ambient temperature, but the hot air is contained to a zone above the occupied zone. The room with the computer and person has higher temperatures within the occupied space, as the hot initial air and the generated heat from the electronics and the person are trapped in the room and do not flow out of the room as well as in the kitchen, where there is an opening. The room would presumably be better ventilated if the far wall had a window, as cross-flow would force the hot air directly out of the room without recirculating through the room before it flows out one of the other doors.

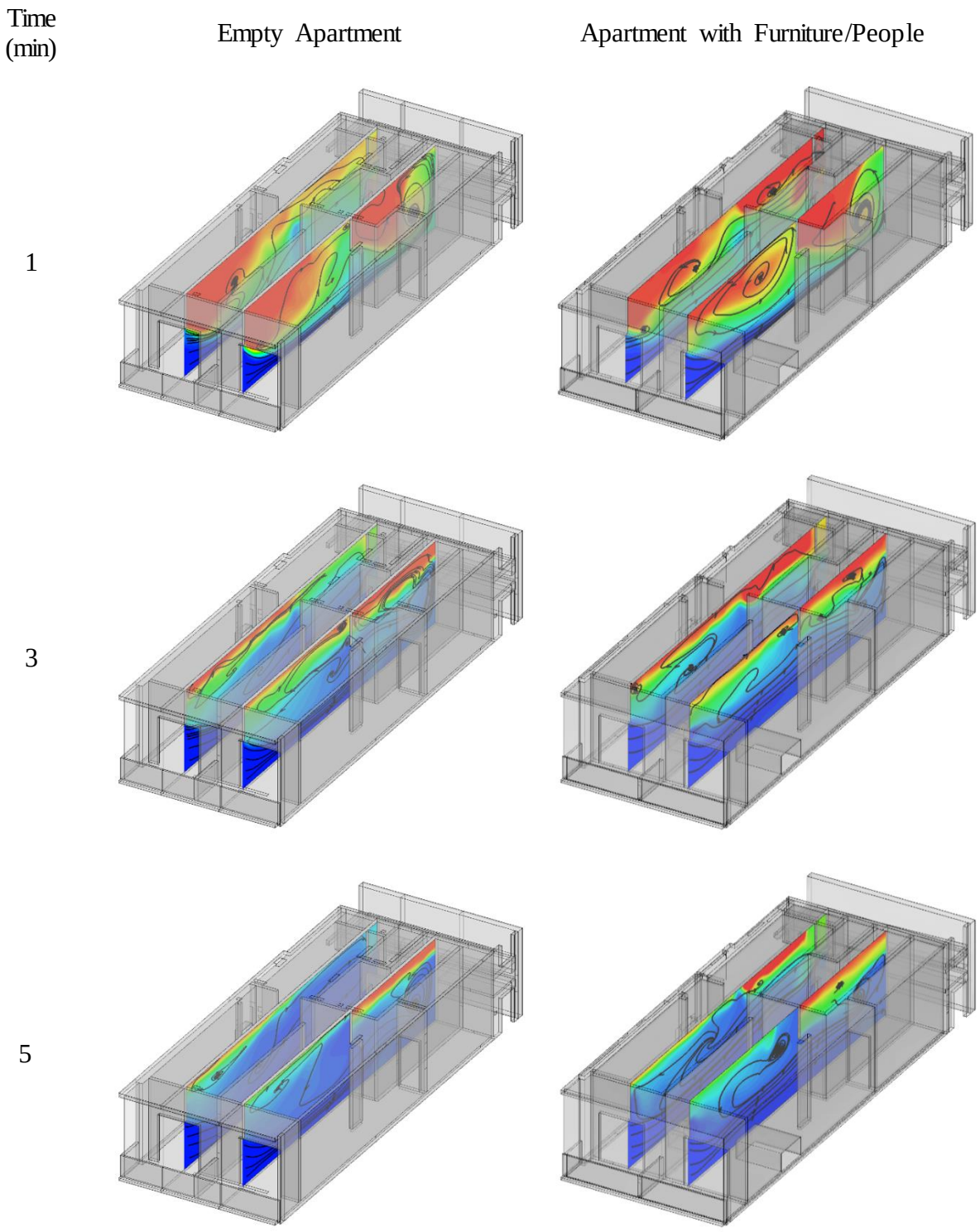

Figure 6.9. Temperature contours with overlaying streamlines at two different planes through the entire domain

Temperature contours and streamlines at two additional planes are shown in Figure 6.10. The cooling rate in both the empty apartment and the apartment with furniture and people are similar. Neither of the two planes in Figure 6.10 intersect a room at the far end of the apartment with a window. The plane closest to the side wall of the apartment shows the temperature contour in a room with only a door and no other opening to induce cross-flow. The upper region of that room is hotter than the average domain temperature at later time steps, indicating that heat is not being removed efficiently from that room. Overall, the two planes show that passive cooling has adequately removed heat from the majority of the apartment aside from the upper region of the far bathroom. Adequate air flow at the deck doors has removed heat from the majority of the occupied space after only 5 minutes. The cooling patterns in the planes of Figure 6.10 have similar patterns from the previous planes in Figure 6.9. The rooms that receive cross-flow have cooled significantly faster than the rooms that do not have a window, where heat is trapped in the upper portion or along the wall opposite of any inlet.

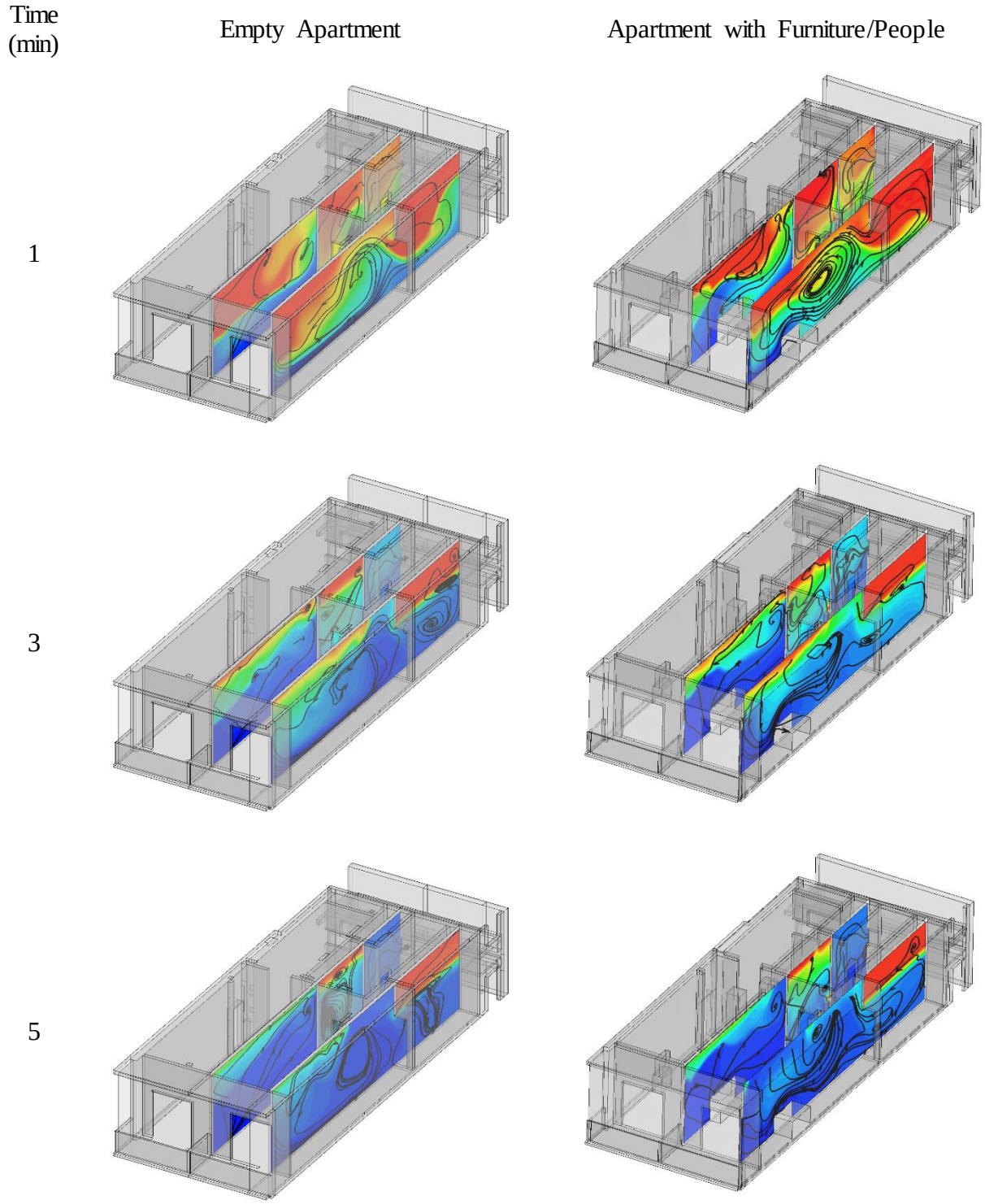

Figure 6.10. Temperature contours with overlaying streamlines at two additional planes through the entire domain.

Figure 6.11 shows temperature contours at planes through two of the human figures modeled as rectangular cuboids. The view through the models shows the location of the higher temperature region of air relative to the people. The temperature contours in the empty apartment at 5 minutes are in the second row and the bottom row shows the apartment with people and furniture. The kitchen is at the left room. Without furniture, the kitchen has nearly completely cooled to the ambient temperature, as it receives a significant cross-flow and the hot air moves out the rear windows. The middle room and far room are at elevated temperatures, but the hot region of air is above the occupied zone despite the low amount of flow into and out of those rooms. The apartment with people and furniture is at a higher overall temperature than the empty apartment. While this is the case, the higher temperature region is mainly isolated to a region above the person in the kitchen. The heat is isolated to the upper region even with a very high heat load in the kitchen: the refrigerator, the person, and the stovetop. The heat load in the kitchen is representative of a time when the heat load would be at its peak and is combined with an initially high temperature. However, passive cooling efficiently removes heat from the occupied region of the kitchen and the rooms that receive inflow. In the middle room, the empty apartment has reached a temperature near the average of the initial temperature and the ambient temperature. It is not ventilated as well as the kitchen. The higher temperatures are made worse when heat loads are added due to minimal ventilation. With the person, a computer, and a computer monitor in the room, the heated air remains throughout the majority of the room. It has not completely been removed from the occupied space and would presumably be at an uncomfortable temperature for occupants, while it is still within the ASHRAE standards for thermal comfort. This occurs even though the average temperature of the apartment is within 0.5 °C of the ambient temperature. It is very likely that this room would remain at an elevated temperature due to the heat loads because

the heat becomes trapped in the room and does not flow as well from the deck doors to the windows.

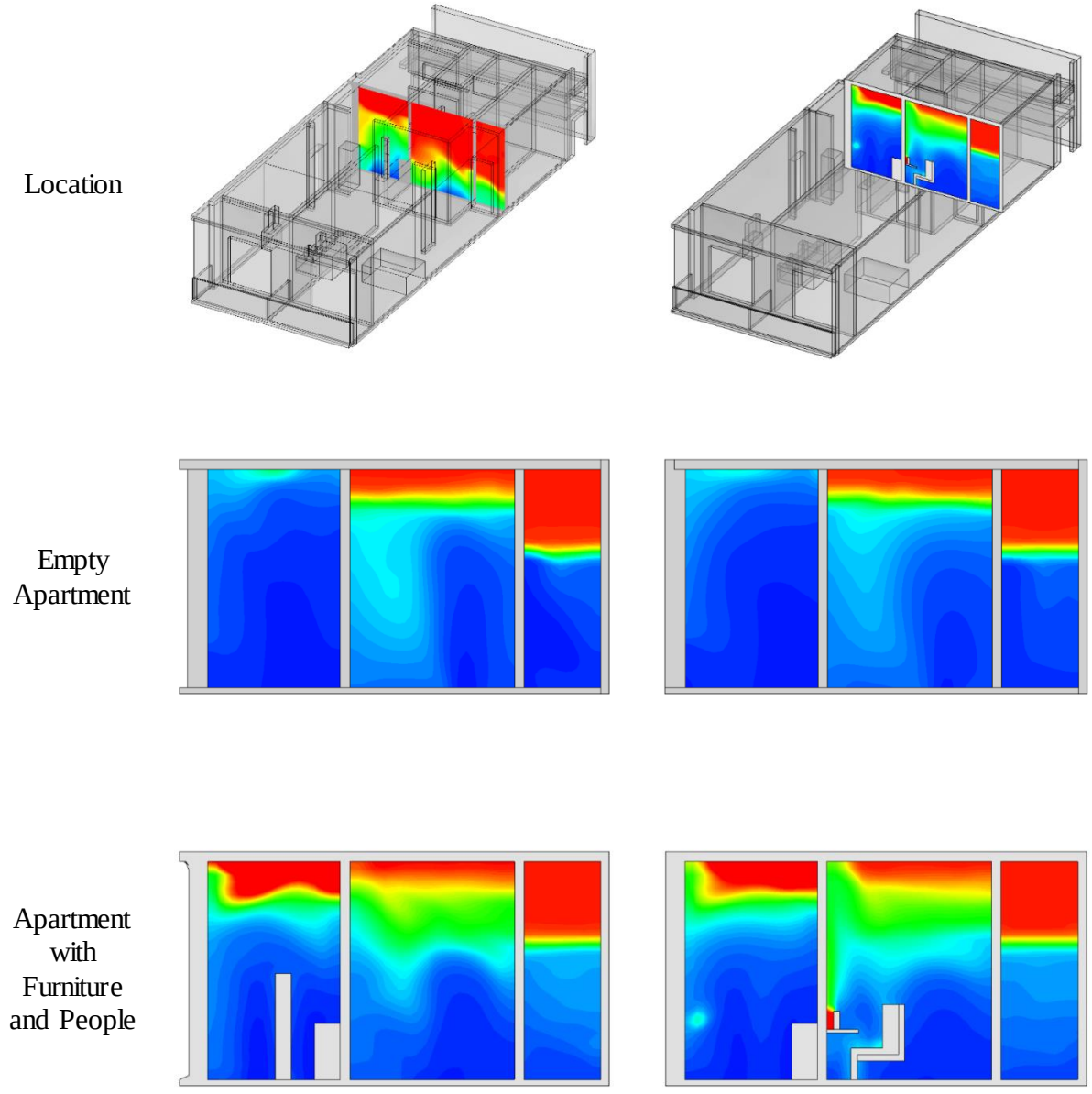

Figure 6.11. Temperature contours at planes through human models at 5 minutes.

The average temperature of the entire apartment and the average temperature at a height of 1.7 m is shown over time in Figure 6.12 and Figure 6.13, respectively. Both the average temperature overall and at 1.7 m follow the same overall path. After a steady decrease, they

begin to approach an asymptote. The empty apartment is approaching the ambient temperature at steady state. There is an increase of 0.5 °C in the apartment with heat loads as the temperatures approach their steady state. Based on the high heat loads, this is a very small increase in temperature over time. Using the external wind conditions as a basis for inlet conditions leads to an exaggeration of the actual ventilation of the space.

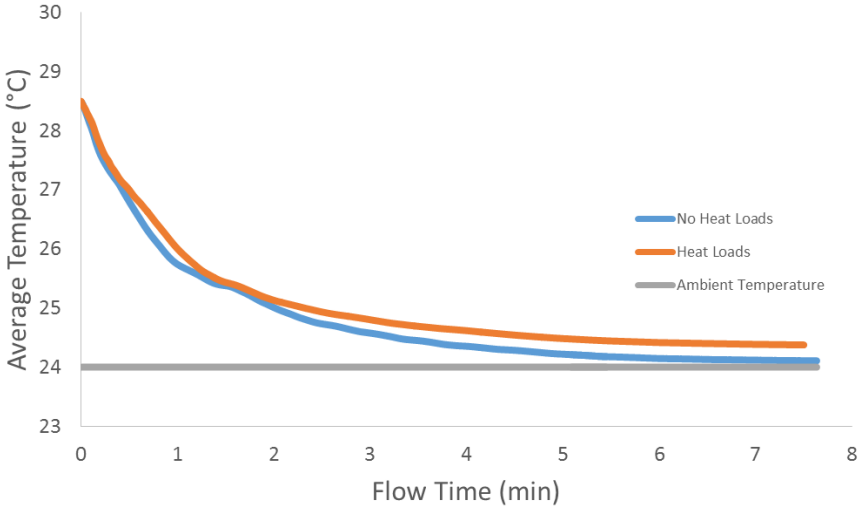

Figure 6.12. Average temperature versus time for the simulation of an empty apartment and the simulation for an apartment with heat loads

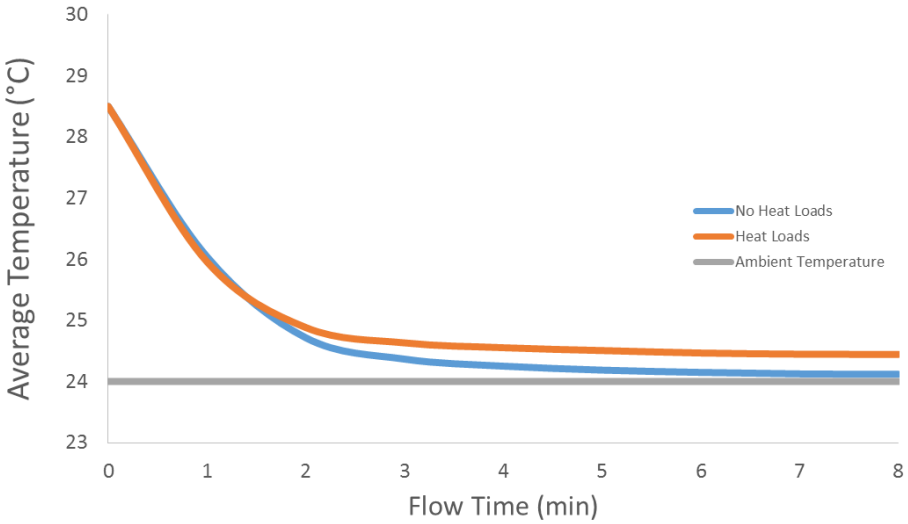

Figure 6.13. Average temperature at y = 1.7 m versus time for the simulation of an empty apartment and an apartment with heat loads

6.3 Results Based on a Low ACH

Inlet conditions are specified to achieve an ACH of 5, much lower than the ambient conditions discussed in Section 6.2, but much closer to the minimum ACH that is recommended to remove heat adequately. The conditions within the apartment have not changed and are displayed in Table 6.1 and described in Section 6.1.

The temperature contours at the center of the plane through the three human figures are shown in Figure 6.14. Initially, the high temperature air becomes confined to the upper portion of the apartment and above of the height of the human figures, which remains over time. At 5 minutes, the occupied zone has decreased in temperature in all three planes. In plane 1, the closest to the deck and in the living room, which has the lowest heat load of the rooms with included heat loads, the room initially begins to cool and the cool ambient temperature begins to appear in the lower region of the plane. The cool ambient air is reduced at 45 minutes, as the effect of the thermal plume above the human figure begins to emerge as the temperature begins to steady in the apartment. The heat loads in the living room hold the temperature noticeably above the ambient conditions. While the occupied zone remains at an elevated temperature above the ambient conditions, the high temperature air remains above and outside of the occupied zone. A steady state temperature near the ambient conditions, similar to the profile in Figure 6.12, is not possible. The low ACH is unable to remove heat due to the person and the television.

In plane 2 (Figure 6.14) which intersects a standing person in the kitchen, similar conditions from plane 1 exist. The high heat zone remains above the occupied zone throughout time, from five minutes to 45 minutes. At 10 minutes and 20 minutes, the lower region begins to cool to temperatures near the ambient conditions, but at 45 minutes the air temperature rises again. The thermal plume in plane 2 is not visible, as the top of the human model is at the lower portion

of the high temperature zone. A taller person (>1.7 m), who would stand above the expected occupied zone, would be in the high heat zone. These conditions would presumably exceed the occupants' comfort zone. At 45 minutes, the overall temperature has reached a steady temperature, and the temperature around the human model has persisted at a temperature noticeably above ambient conditions. The high heat load in the apartment has begun affected the room on the far right in the plane, which does not have any type of heat load in it. The far room was initially cooled to a comparable temperature to the ambient conditions, but at the latest time step it has begun to increase in temperature. As there are only two windows in the kitchen and the rest of the rooms do not have access to windows, the warm air has begun to circulate throughout the apartment, and through mixing has increased the temperature in regions without heat loads.

The third plane (Figure 6.14) shows similar conditions as the previous two planes. The human model is sitting in a zone that is at an elevated temperature from the ambient conditions, but is below the high temperature region. The computer contributes to a high temperature zone close to the wall that remains hot throughout time. The height at which the high temperature region begins is constant through the three planes. As noted previously, the high temperatures in this region would exceed an average person's comfort level. In this simulation, the warmest air begins at a height just above 1.7 m, which is a low height for such high temperatures, and with an ACH of 5, the ventilation of the apartment would be inadequate to remove heat and maintain thermal comfort for 80% of occupants.

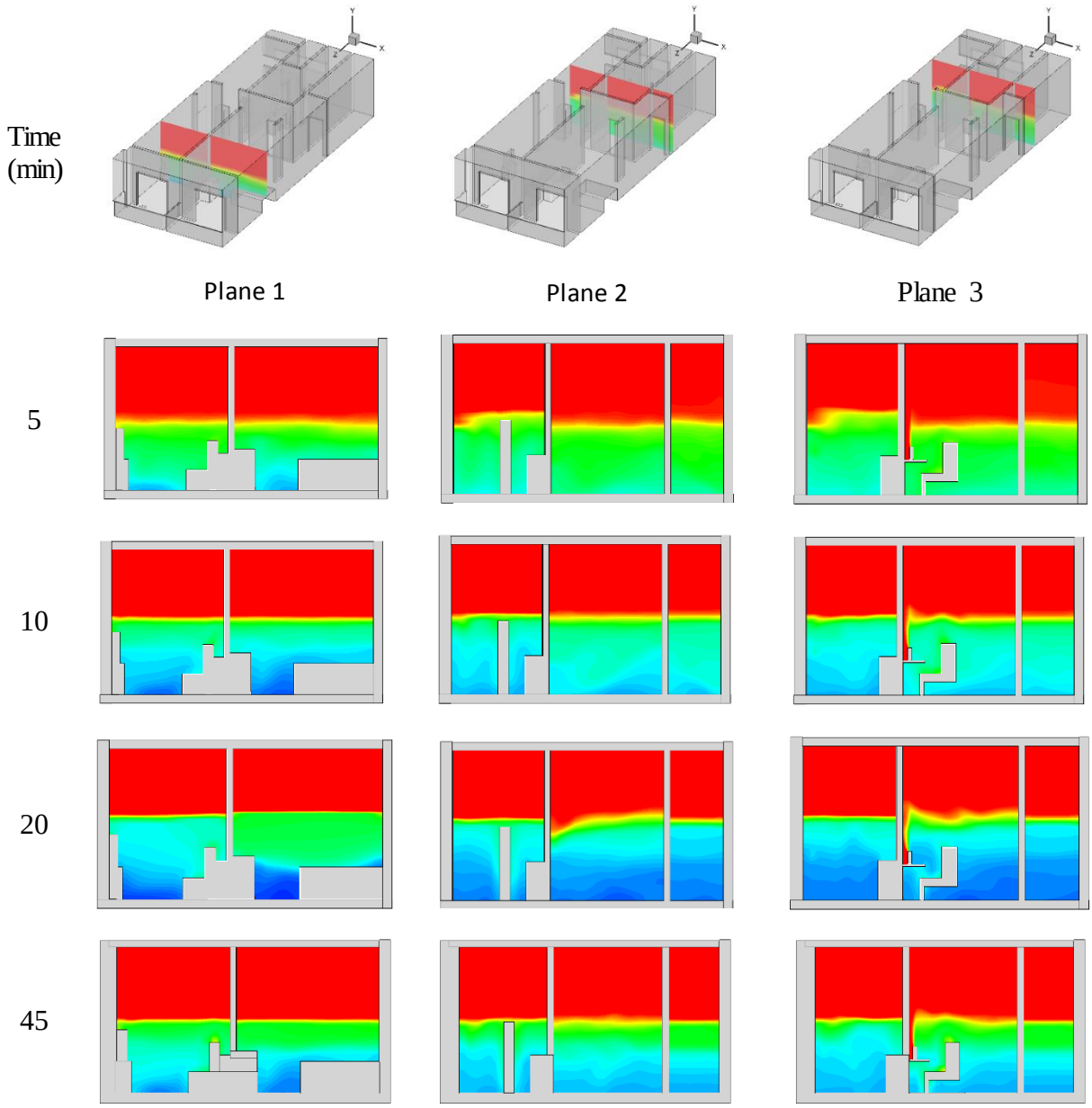

Figure 6.14. Temperature contours through the center plane of the human models.

The average temperature for the entire apartment and the average temperature at 1.7 m for the simulation with a low ACH of 5 are shown in Figure 6.15 and Figure 6.16, respectively. Without heat loads, the temperature in the apartment decreases towards the ambient temperature as expected, similar to the previous case with the higher ACH based on the ambient wind conditions. The time it takes for the temperature to begin to reach the ambient temperature is

longer, as expected, but the trend is similar. With heat loads added, the temperature of the overall apartment is increased above the ambient temperature. The average temperature in the apartment is increased above 27.75 °C, which is only a decrease of 0.75 °C from the initial conditions. The temperature stratification from Figure 6.14 in all three planes at later time steps shows the upper portion of the apartment is at or above 28.5 °C, increasing the average. The temperature at the upper portion of the occupied zone, shown in Figure 6.16 gives a representation of presumably the hottest portion where people would reside. The temperature at 1.7 m is also above the ambient temperature, at approximately 27.5 °C, a decrease of only 1°C from the initial conditions. From 0-20 min, it appears that the overall temperature decreases toward a slightly elevated temperature from the ambient conditions, but the high heat load of the apartment begins to increase the overall temperature until a steady state at about 35 min. At 45 min, the temperature had not changed for over 10 min, and presumably the apartment will stay at the elevated temperature without any decrease in the heat loads or increase in flow rate. The conditions of the apartment are not ideal for living spaces. According to ASHRAE standard 55, shown in Chapter 1 Table 1.1, when included into entire paper, the elevated temperature of the entire apartment would not be acceptable to more than 90% of the occupants but it would be acceptable to more than 80%, based on an external temperature of 24 °C. Passive cooling in this case would be narrowly acceptable for the occupants, but a reduction in the flow rate, potentially due to low wind conditions outside the apartment, would presumably lead to a living space where the thermal conditions create an uncomfortable environment.

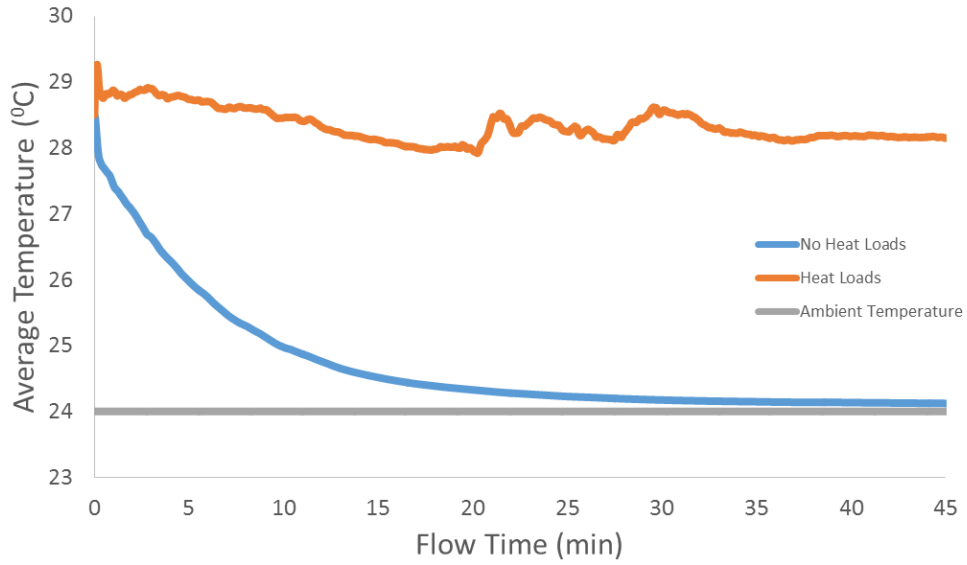

Figure 6.15. Average temperature versus time for the simulation of an empty apartment and the simulation for an apartment with heat loads and a low ACH

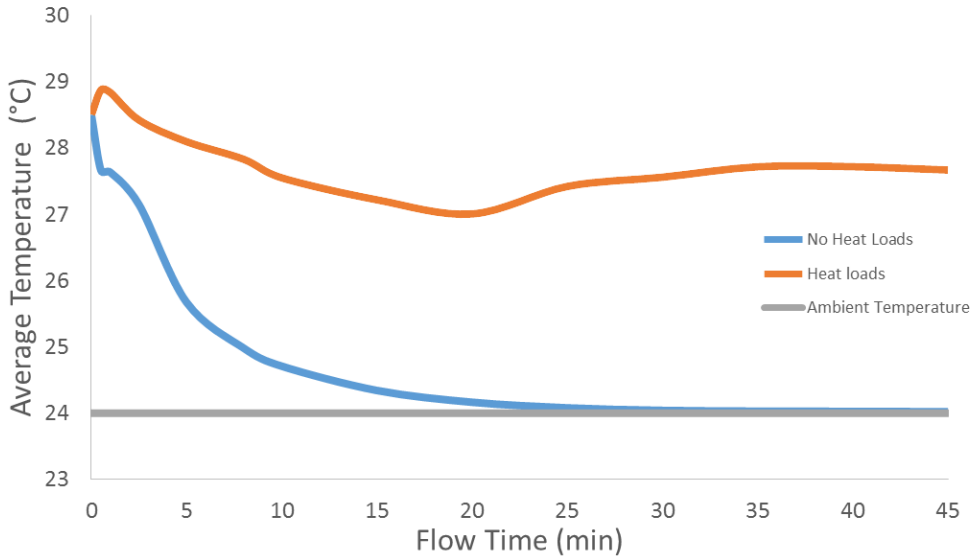

Figure 6.16. Average temperature at 1.7 m versus time for the simulation of an empty apartment and the simulation for an apartment with heat loads and a low ACH

Chapter 7 Affleck House

The Affleck house was designed by Frank Lloyd Wright and is located in Michigan. The home took advantage of its surroundings in its design for cooling, heating, and ventilation. The main living space has an open layout and multiple skylights that are used for solar heating. An unorthodox method to cool the house uses a window in the floor to entrain the cool wind under the home in an exterior basement into the home. Passive cooling will be simulated in this chapter, modeling flow under the house and using windows and doors in the house to create a pressure difference, drawing the cool air underneath the house into the home. The conditions for the simulation are from the summer month of August, when overheating is likely to occur.

7.1 Home Background and Simulation Setup

The Affleck house, shown in Figure 7.1, was designed to take advantage of its location and the terrain where it is located. The CAD drawing was provided by Prof. Ulrike Passe and Suncica Jasarovic of Iowa State University. The ground slopes from the northwest, allowing for an exterior basement below the house. The exterior basement is utilized to ventilate the home using a window in the floor above the main living area. The house was designed by Frank Lloyd Wright as an usonian home, which was designed to be located in places where the lot is unique where normal homes of the time would not belocated. Usonian homes were designed be cost-efficient and had open living spaces and were made with natural material [29]. Contrary to the customary homes of the era, the usonian homes were usually one floor and utilized solar heating with skylights and natural cooling. The Affleck house uses multiple skylights above the main living section for solar heating and the window in the floor for cooling [25].

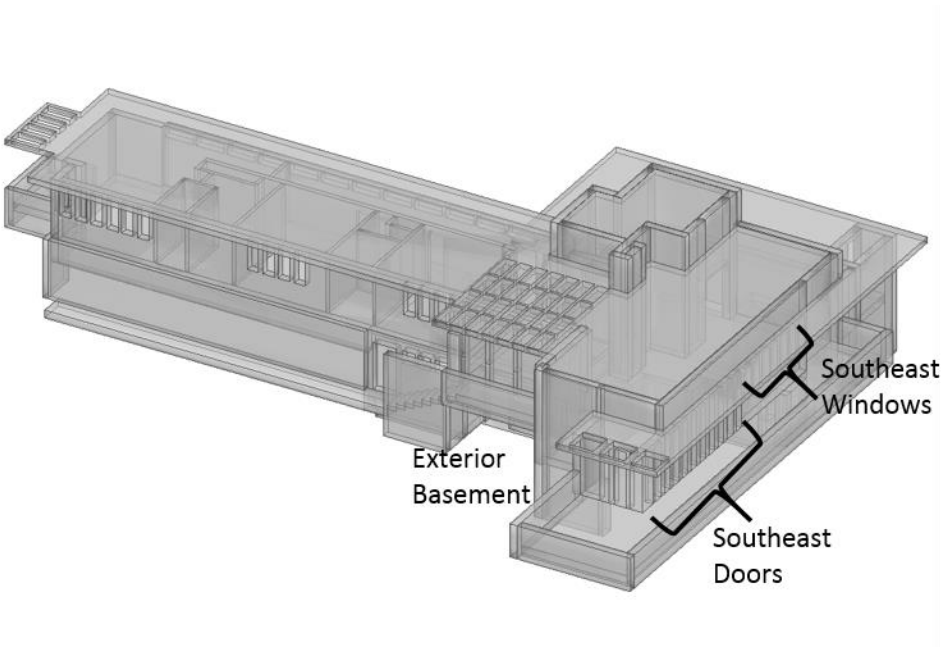

Figure 7.1. Geometry representing the Affleck House

The mesh for the Affleck house was built by "blocking" the interior of the structure to best represent the interior fluid domain and where average cell size is approximately 10 cm due to the complexity of the geometry and the large domain size. An overview of the mesh can be viewed in Figure 7.2 and a side view that shows the individual cells is shown in Figure 7.1. A cell size of 10 cm was appropriate to represent the overall flow patterns and temperature profile in the domain. A smaller cell size or compression along the walls, which was used for the smaller domains in Chapters 4 and 5, increases computation time and is not an efficient way to simulate conditions in a large building such as the Affleck house.

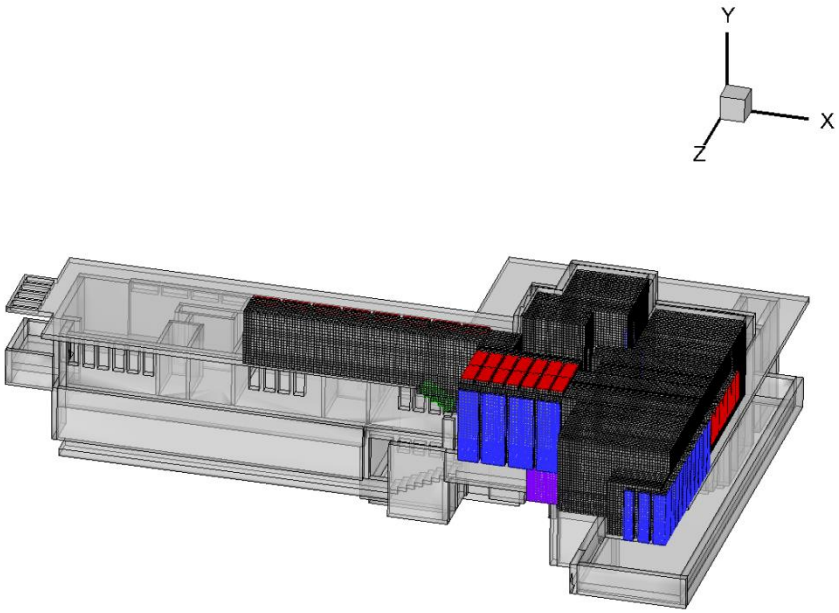

Figure 7.2. Overview of the mesh for the Affleck house. Doors are shown in blue, windows in red, "false surface inlet" in purple, and stairs in green

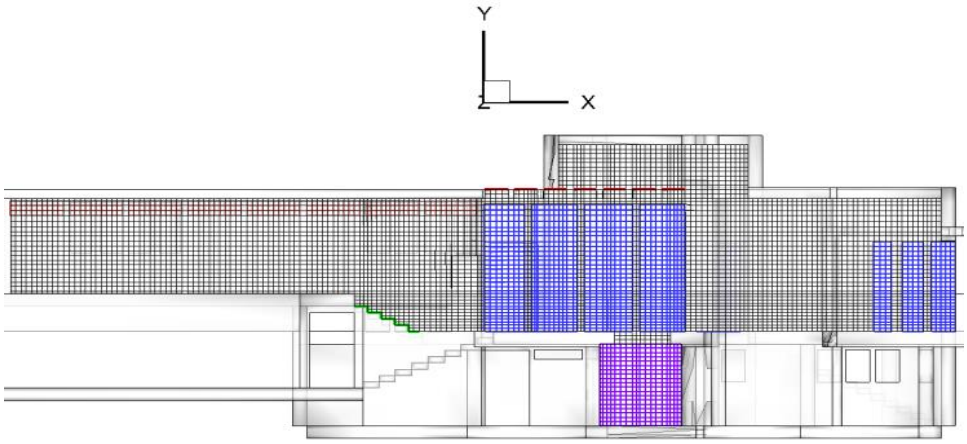

Figure 7.3. Partial side view of the meshed domain. Doors are shown in blue, windows in red, "false surface inlet" in purple, and stairs in green

A schematic of the home viewed from above is in Figure 7.4**.** The wind moves in from the southwest at an average velocity of 3.5 m/s. The average exterior temperature is 27 °C. These conditions are for the summer month of August, when overheating is most likely to occur. The

conditions simulated are shown in Table 7.1 [30]. A high initial temperature of 32 °C is used to model a high heat load during the day and a cool ambient temperature at night.

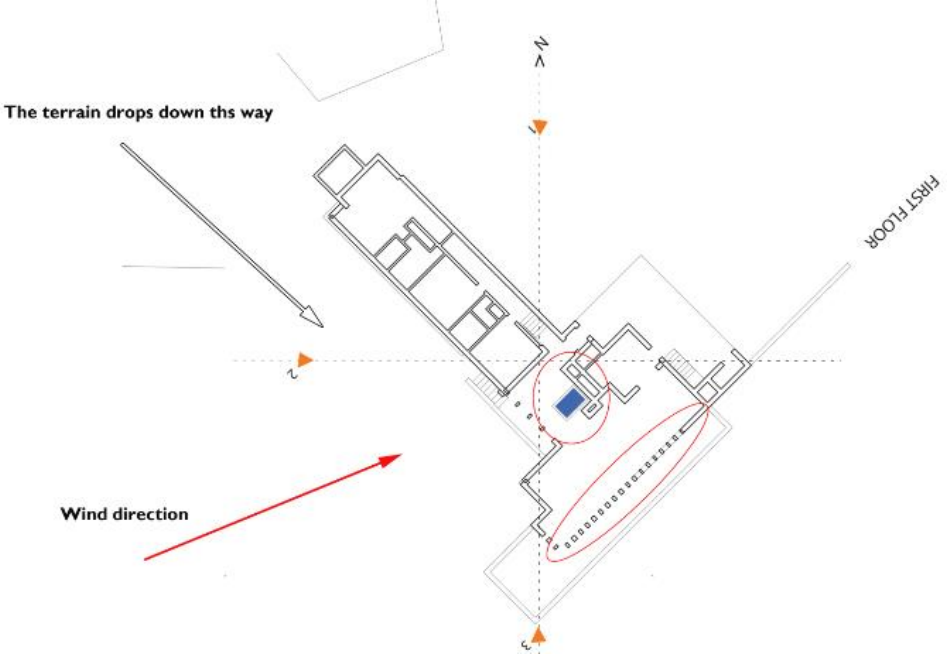

Figure 7.4. Overview of the Affleck house viewed from above.

Table 7.1. Ambient conditions at the Affleck house location for the month of August

	Metric
Initial Temperature	32 C
Ambient Temperature	27 C
Wind Speed	3.5 m/s
Wind Direction	WSW

As discussed in Chapter 6 for the Casa Giuliana modeling, a more realistic way to model ambient conditions associated with wind was to define a false surface. The surface creates a "boundary" that can have a prescribed velocity, which allows flow to move naturally into an opening and move through the house. The same approach is employed in the Affleck House, where

the exterior conditions below the home are simulated using a false surface. The false surface is located under the home in the exterior basement positioned in a small nook under the window in the floor. The false surfaces and house walls within the exterior basement are represented in Figure 7.5. The domain under the home has physical walls and two false surfaces representing locations under the home.

The first false surface, shown in blue in Figure 7.5, is perpendicular to the wind direction and is specified as an inlet. The ambient conditions are designated at the false surface, with 10% of the average wind speed specified in Table 7.1. The decrease in wind speed is used to model more realistic conditions under the home, as a constant wind speed of 3.5 m/s is unlikely to occur constantly over the entire surface over a long period of time. The second false surface is a pressure boundary. The pressure boundary is used so that the entire flow at the inlet is not directly forced up and into the home. The use of a false surface under the home gives the ACH value a meaningful number that is not directly controlled by the conditions specified at the inlet, allowing for an analysis of the overall air quality of the home.

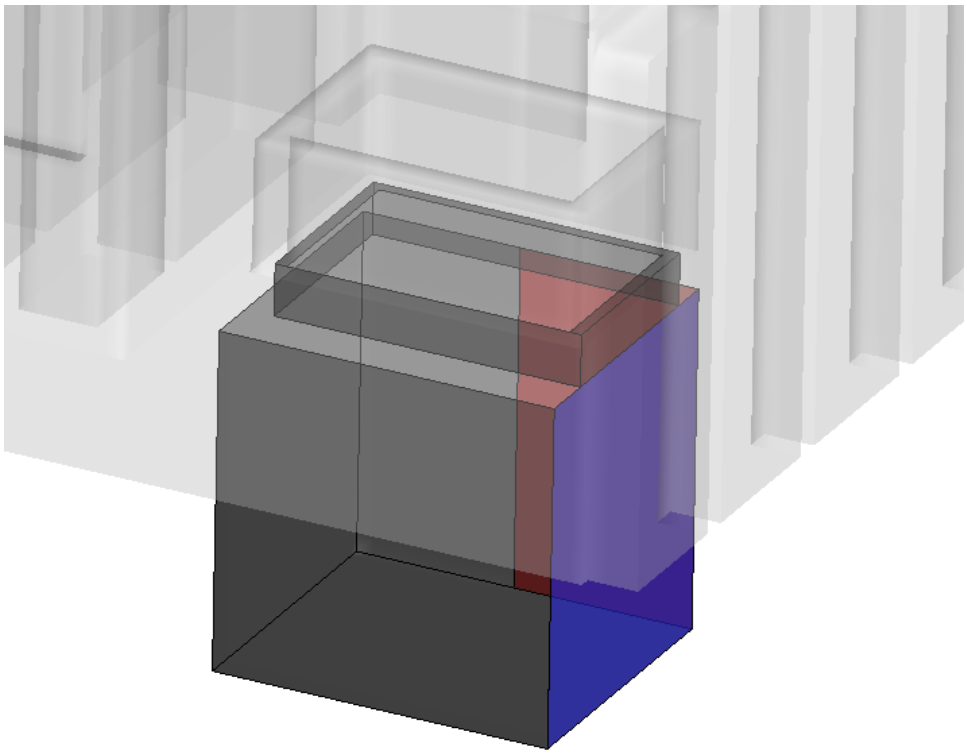

Figure 7.5. Surfaces underneath the home in the exterior basement. Blue represent the inlet (false surface), red represents a pressure boundary (false surface), and black represent the walls underneath the structure.

Two different cases were simulated. The first simulation modeled all windows and doors open that are located at the southeast side of. The corresponding boundary condition for the openings specified ambient pressure. The second simulation modeled the doors closed and the windows open at the southeast side. The open doors and windows create a pressure difference to the window in the floor, allowing the interior air to be ventilated through a majority of the living section. The living section has an open layout with high ceiling and many glass windows and doors to regulate air flow.

7.2 Passive Cooling Results

Passive cooling was simulated using the conditions from Section 7.1. The air flow moves up and through the window in the floor and circulates throughout the main living section. It cools the home evenly and forces the hot air above the cool inflow and out of the occupied space. While the hall and the area with the high ceiling do not receive significant air flow, the lower and mid-section of those two areas are still cooled. The majority of the incoming air through the floor-window moves upward to the southeast doors and windows.

Instantaneous temperature contours with streamlines at one minute, five minutes, and ten minutes are shown in Figure 7.6 for both cases. At each time step, streamlines clearly show that ambient air moves from below the house into the main living section. The cool air circulates throughout most of the house. At one minute, the region above floor-window and near the open windows and doors has begun to cool, with the lower region at a temperature at or near the ambient temperature. The streamlines show most of the incoming air circulates in the area near the floor-window and towards the open windows and doors. At five minutes, the main living section has cooled significantly and the ambient air is circulating throughout. The hallway at the northwest end, which does not have any openings, is beginning to cool due to the inflow from the floor-window. The cooling occurs primarily at low air speeds as inflow is mostly entrained towards the open windows and doors. At ten minutes, the majority of the house has significantly cooled, and the hot air is mostly contained to the region above the height of the doors, out of the occupied space.

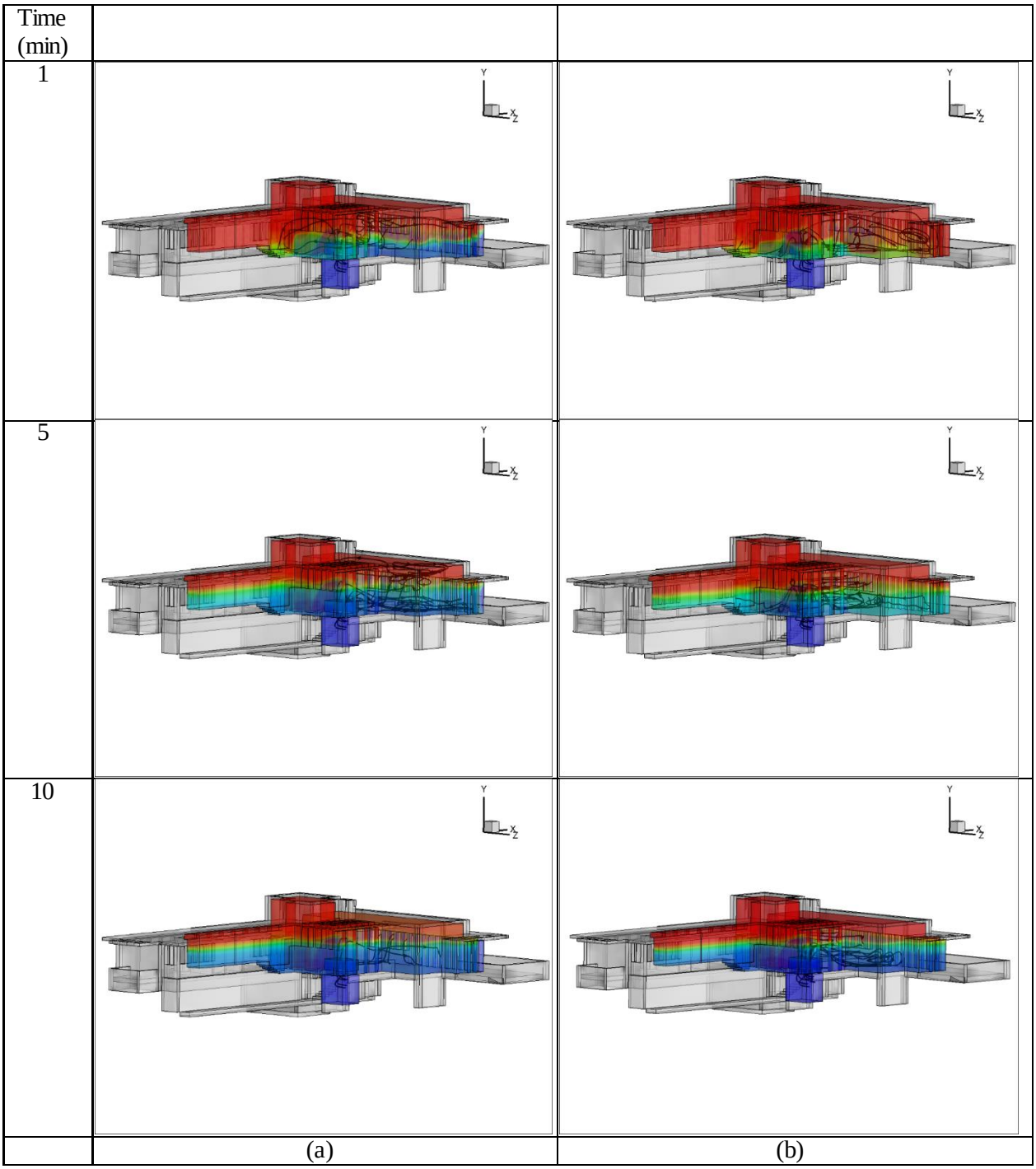

Figure 7.6. Passive cooling results represented with temperature contours and streamlines. (a) Windows and doors open (b) Windows open

The results for the case with only the southeast windows open are shown in Figure 7.6b represented with temperature contours and streamlines. The cooling patterns and air flow patterns are similar to the case with doors and windows open (Figure 7.6a), but the cooling is slower overall.

The cooling trends can be viewed in Figure 7.7 at a plane near the center of the main living section. The temperature contours show the cool air filling the lower region of the house at one minute. With both the windows and doors open, the middle of the room is significantly cooler than with only the windows open. Overall, both cases cool significantly over time.

In a plane through the main living section, shown in Figure 7.7a, the cool ambient air can clearly be seen at the lower region of the room. In Figure 7.7b, the room modeled with just the windows open, does not cool at the same rate. This trend continues over time, as cooling in the room with only the windows open lags behind the room with both the doors and windows open. At five minutes, the temperature in the room has begun to stratify, with cool air in the lower region, warm air in the middle region, and the hot air above. At ten minutes, the temperature in both rooms is mostly stratified, and the temperature comparable is to the ambient temperature. The hot air is contained close to the ceiling and does not directly impact occupants in the house. In the room with both windows and doors open, the upper region has begun to cool as well, and the hot air region has begun to decrease in temperature.

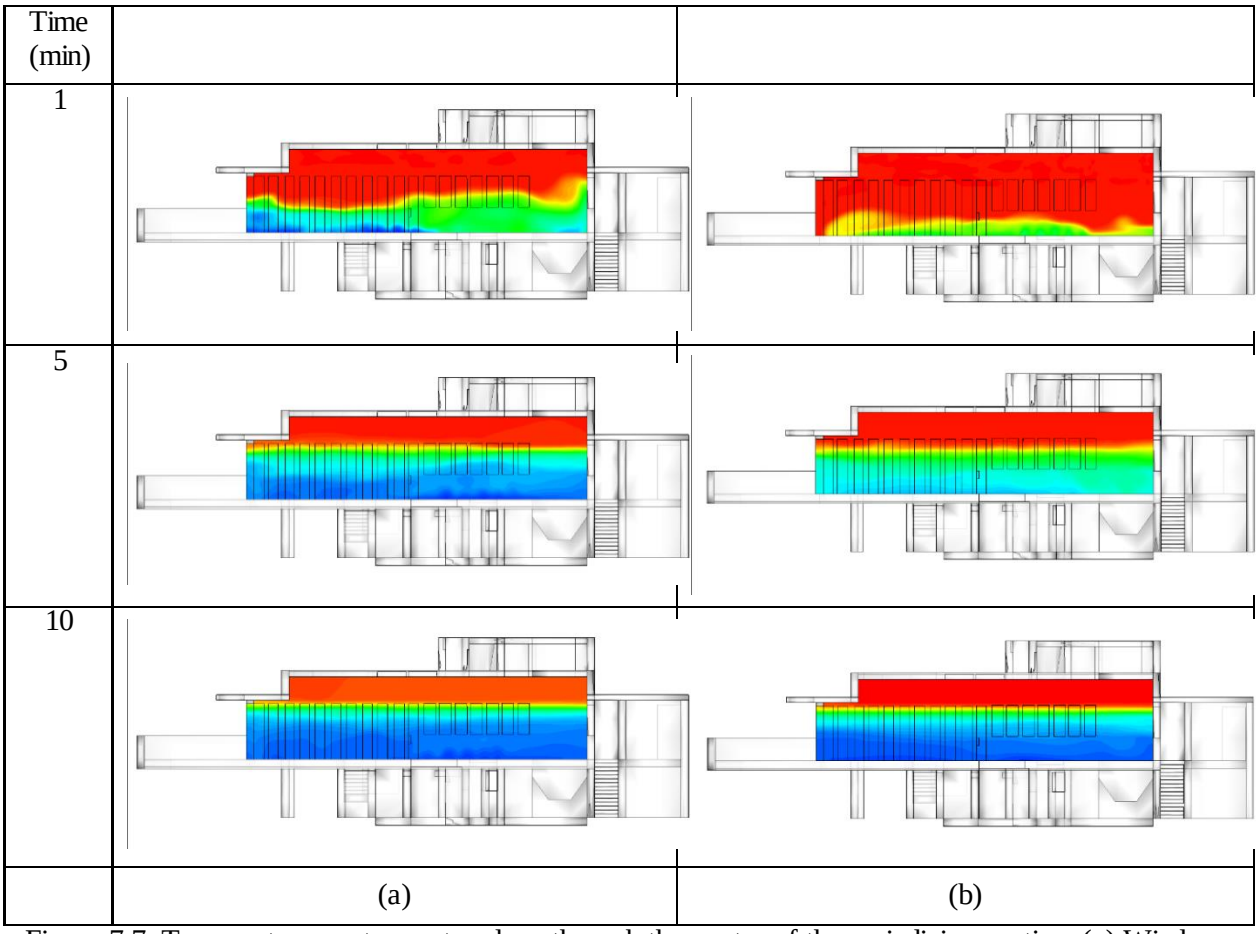

Figure 7.7. Temperature contours at a plane through the center of the main living section. (a) Windows and doors open (b) Windows open

The average temperature in the Affleck house for both cases is plotted in Figure 7.8 shown over time. Initially, there is a steep decline from the high initial room temperature. After one minute, the steep decline changes to a gradual decrease towards the ambient temperature. With only the windows open, the slope decreases at a slightly slower rate than with both the windows and doors open. Both cases do not have any heat sources, and it is expected that the steady state temperature is equal to the ambient temperature. The case with both windows and doors open has an average temperature approximately 0.5 °C lower than the case with only the windows open. The drop in temperature appears to originate at the beginning of the simulation, where the steep drop in temperature occurs. After the steep drop, the two slopes are similar besides an inflection

point at about five minutes. The slopes after the inflection point are nearly equivalent, and the temperature of the house begins to decrease at a similar pace up until ten minutes.

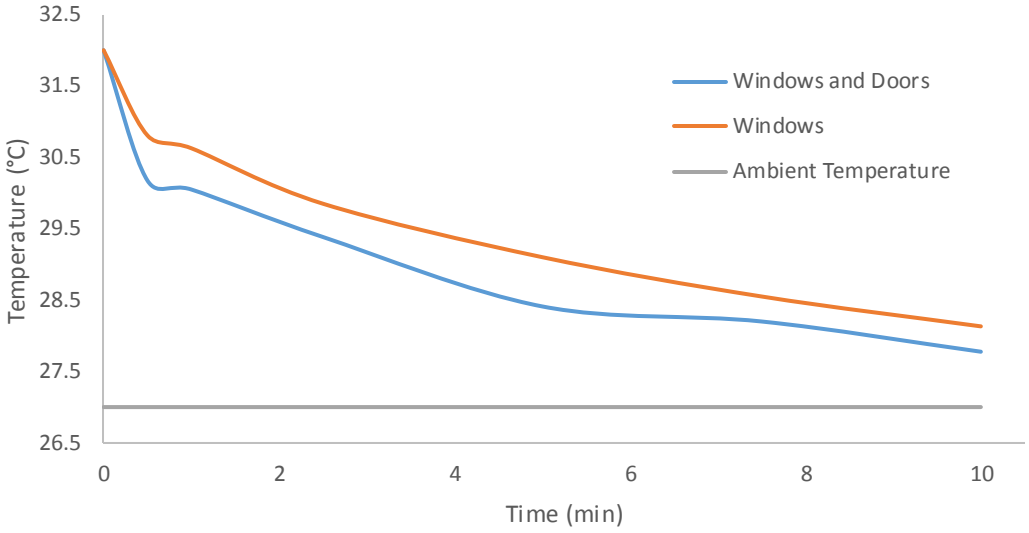

Figure 7.8. Average temperature in the Affleck house over time.

Chapter 8 Conclusions and Recommendations

8.1 Summary Conclusions

Designing buildings to be more ventilated more efficiently can help reduce the overall cost of energy. As the developed populations continue to grow, energy usage in buildings is expected to increase, as economically strong regions use 25 times more energy than impoverished regions. In the United States, energy usage to cool buildings is expected to increase during the next three decades due to migration to warmer southern climates [2]. Natural ventilation can be utilized to decrease the energy needed to cool and heat buildings. Even in cases when natural ventilation may not be the best option to maintain comfort for occupants, the principles can be applied to mechanically ventilated buildings to reduce energy usage.

CFD can be utilized during the building design phase by architects and designers to visualize the flow patterns and temperatures throughout a building. CFD gives full pictures of fluid volumes pressure, velocity, and heat transfer within a building. In this study, CFD was utilized to simulate natural ventilation in two small structures, an apartment, and a house. Ansys FLUENT 14.5 was used to model the flow using the three-dimensional Navier-Stokes equations. The Boussinesq approximation was used to include buoyancy effects for the incompressible flow field. Turbulence was modeled using the realizable k-ε model. The geometries were provided by colleagues at Iowa State University as .Sat files and imported into Ansys geometry tools. The mesh was created in Ansys ICEM and was built by blocking the interior volume and generating a mesh. The SIMPLE algorithm was used to couple pressure and velocity. Walls were modeled as adiabatic to reduce computation time.

The two small structures were used to simulate natural ventilation in rooms designed to utilize cross-ventilation and single-sided ventilation. The original models were designed to have a

depth-to-height (DH) ratio of 5:1 and 2.5:1 for cross-ventilation and single-sided ventilation, respectively. These ratios were used as they are the recommended maximum sizes the rooms should be to use cross-ventilation and single-sided ventilation. Passive cooling and heating were modeled with a 4 °C temperature difference between the initial internal temperature and the outdoor temperature. The air flow patterns, the air changes per hour (ACH), and the temperatures in the room are were used to analyze the overall ventilation of the rooms.

Cross-ventilation was modeled using two combinations of windows: two small openings and a large and small opening. A velocity inlet was used and two different velocities were specified, 0.5 m/s and 5 m/s. Both velocities corresponded to ACH values that were above the minimum recommended values to remove heat and maintain air quality. 5 m/s corresponds to interior velocities far outside of occupants' comfort levels, while 0.5 m/s is less than the maximum recommended air velocity for occupants. Results using a DH of 5 and all combinations of window sizes for a velocity of 0.5 m/s specified at the inlet and ambient pressure at the outlet are well ventilated and have flow patterns that presumably would keep regions of stagnant air at a minimum.

Simulations with a small inlet and large outlet matched the flow patterns and thermal stratification of simulations with a small inlet and small outlet. This similarity indicates that flow patterns are dominated by the size of the inlet and less so by the size of the outlet. As previously stated, the room with a larger opening at the inlet appeared to ventilate the room better. The better ventilation was again evident when both openings were specified as ambient pressure, a representation of motionless air around the building. In the room with a large opening and a small opening, flow patterns showed that air moves from one opening to the other, ventilating the entire room at an ACH above the recommendations. With equal size openings, both openings were

accompanied by regions where there was no air exchange between the halves of the room. With no pressure difference between the openings, the inflow was not high enough to adequately remove heat based on the recommendations. A pressure difference, in this case due to the opening size difference, drives cross-flow and was able to adequately ventilate a room in situation where the flow outside of the windows is still and there is a low amount of forced air into the building.

Passive cooling in single-sided ventilation was simulated in rooms that were equal to a DH of 2.5, the rule of thumb. Two window combinations were simulated, windows that were near the floor and ceiling on one wall and windows near the center of one wall above and below each other. With a velocity specified at the lower opening, air flow patterns and the ACH indicated a presumably well ventilated room. When ambient pressure was specified at both openings, the inflow comes from the top opening at later time steps and steady state. At steady state, the flow patterns were remarkably similar to results with a velocity inlet, but they are flipped. The overall indicator of ACH was above the minimum recommended value and the flow patterns did not indicate regions of stale or stagnant air and ventilation without any forced in the rooms is presumably adequate. The room with windows farther apart had a higher flow rate, leading to a higher ACH, due to the larger pressure difference between openings. Single-sided ventilation becomes more effective when there is a larger pressure difference between openings. In this case, as the openings both have the same specified conditions, the pressure difference is due to the increased height difference between windows. The pressure difference due to the height drives the flow at steady state.

The Casa Giuliana apartment is well-designed for natural ventilation. It is in a mild climate and receives a cool lake breeze. It utilizes cross ventilation, with a windward facing deck and large deck doors on one side, and isolated windows on the far side. The inflow into the apartment was

modeled with a false surface specifying a velocity in a space between the walls and the porch barriers, where the wind from the lake breeze would move into the apartment. A specified velocity based on $1/10^{th}$ of the exterior wind speed at the inlet led to conditions in the apartment where heat was removed quickly and the apartment was well-ventilated. The regions of the apartment that have windows (the kitchen and small bathroom) receive a higher amount of the inflow from the deck and the cross-flow removes heat in those sections quicker than in rooms, such as the den and large bathroom, which do not have windows and are ventilated with single-sided ventilation. In the Casa Giuliana simulations, heat loads due to people and electronics were included. In simulations with a specified velocity at the inlet based on the exterior conditions, there was only a 0.5 °C temperature difference between the average temperature of the apartment without heat loads and with. The low temperature difference was accompanied with velocities in the room that are below the maximum recommended velocities in ASHRAE standard 55 [5]. These simulation conditions would presumably be within occupants' comfort levels.

A low velocity case was simulated in the apartment to ensure that thermal conditions were adequate when the air flow into the apartment is low. The average temperature after a long period of time stabilized at an increased temperature above the ambient conditions but below the initial conditions. The interior temperature would not be decreased to the ambient conditions. The heat transfer from the people and electronics led to a high temperature region in the uppermost portion of the apartment. While most of the hot air was outside the occupied region (1.7 m and below), there are areas of high temperature regions within the occupied space such as the den, which does not have adequate cross-flow. The human model in the den was surrounded by a warm region of air. According to ASHRAE standard 55 [5], the conditions in the apartment would narrowly be within comfort standards. An increase in the apartments total heat load or a decrease in the flow

into the apartment would likely lead to conditions that are not within occupants' comfort levels. When designing buildings to utilize natural ventilation it is important to simulate conditions where natural ventilation may be inadequate and locate regions where ventilation can be improved, such as the den and large bathroom. Areas that receive cross-flow also receive a higher amount of inflow and heat is removed better.

Passive cooling was also simulated in the Affleck house. The Affleck house receives inflow from a window in the floor into the main section. Windows and doors are opened to create a pressure difference for the outflow. The setup was able to ventilate the main living section with the cool air under the house in the exterior basement. The flow was modeled with a false surface under the home, which allowed the simulation to better model the inflow into the house. A false surface not located at an opening allowed the flow into the house to be less controlled by the setup of the simulation and moves more naturally into the house. Using this setup, the flow from the false surface moved up and into the house and out of the open doors and windows. The actual inflow into the opening was difficult to model directly, but using this method a more natural inflow occurs. While the exterior conditions cannot be perfectly replicated, averages for each month can used to model a temperature and flow velocity. A false surface can be placed in strategically located positions and the inflow into the house does not have to be specified by the simulation. This is a more accurate representation of the conditions than using a velocity inlet at an opening.

8.2 Future Recommendations

The rule of thumb for cross-ventilation (DH=5) was challenged using a room with a DH=7. With ambient pressure boundaries, the flow patterns did not show any significant changes when increasing the room length. There were two minor differences in the ventilation of the room. First, there was a larger region where velocity vectors are very small, which indicates low velocity air

and ventilation is due predominately to mixing. Second, due to the larger volume, the ACH was decreased. Neither difference indicates that going beyond the rule of thumb leads to a decrease in the effectiveness of ventilation for the rooms. A designer and architect would have to be aware of the expected flow rate into the room and the volume of the room when cross-ventilation is the main tool to for ventilation. Although more work needs to be done to include heat loads and furniture into a room that uses cross-ventilation to model a more realistic situation, this study simulated cross-ventilation in a situation where low flow was expected. With a pressure difference between openings, the inflow was sufficient to remove heat and maintain air quality.

Using the results of the previous study, recommendations can be made for modeling structures for natural ventilation. For cross ventilation, the important design feature of the structure is that a pressure difference exists. The pressure difference can be due to opening size or height and/or wind around the building and temperature differences between openings. Without a pressure difference, cross-ventilation will not be achieved. When designing the structure, the building size (height, width, length) and its corresponding volume is more important to maintaining air quality than the rule of thumb (DH). The volume of the structure and the expected inflow into the structure should be used to determine the limiting case. In single-sided ventilation, higher amounts of air flow that leads to higher air quality are achieved when the openings are farther away from each other. The designer should use the maximum amount of practical space between openings when designing for single-sided ventilation. In the work for large structures, spaces that had larger amounts of cross-flow were better ventilated. In Casa Giuliana, the back two rooms without windows would be ventilated better if they did have windows, which allows for excess heat to be expelled better. In the Affleck house, openings in other regions of the house would allow for better flow into those sections and subsequently a higher amount of heat expelled.

References

[1] Ghiaus, Christian and Allard, Francis, eds., *Natural Ventilation in the Urban Environment*. London: James&James, 2005.

[2] U.S. Department of Energy. (2014) Annual Energy Review 2014. Washington, DC: Energy Information Administration

[3] Allocca, Camille, Chen, Qingyan, and Glicksman, Leon R. "Design analysis of single-sided natural ventilation," *Energy and Buildings*, 35, no. 8 (2003): 785-795

[4] Natural Ventilation in Non-Domestic Buildings, CIBSE Applications Manual. London: Chartered Institution of Building Services Engineers: Carbon Trust, 2005.

[5] ASHRAE. (2004). ASHRAE Standard 55-2004, Thermal Environment Standards for

Human Occupancy. Atlanta, GA.

[6] Park, David, "Numerical Simulations of Flow and Heat Transfer in a Room with a

Large Opening," M.S. Thesis, Virginia Tech, 2013.

[7] Asfour, Omar S. and Gadi, Mohammed B. (2008). "Using CFD to investigate ventilation characteristics of vaults as wind-inducing devices in buildings". *Applied Energy*, 85, no. 12 (2008): 1126−1140.

[8] Ayad, Samir S. "Computational study of natural ventilation." *Journal of Wind Engineering and Industrial Aerodynamics*, 82, nos. 1-3 (1999): 49-68.

[9] Stoakes, Preston, Passe, Ulrike and Battaglia, Francine, "Predicting Natural Ventilation Flows in Whole Buildings. Part 1: The Viipuri Library". *Building Simulation*, 4, no. 3 (2011): 263-276.

[10] Stoakes, Preston, Passe, Ulrike and Battaglia, Francine, "Predicting Natural Ventilation Flows in Whole Buildings. Part 2: The Esherick House". *Building Simulation*, 4, no. 4 (2011): 365-377.

[11] Heiselberg, P., Li, Y., Andersen, A., Bjerre, M. and Chen, Z., Experimental and CFD evidence of multiple solutions in a naturally ventilated building. *Indoor Air*, 14, no. 1 (2004): 43–54.

[12] Incropera, Frank and DeWitt, David. *Fundamentals of Heat and Mass Transfer*. 6th Ed. Hoboken, N.J., John Wiley & Sons.

[13] Linden, P. F.. "The Fluid Mechanics of Natural Ventilation." *Annual Review of Fluid Mechanics,* 31 (1999): 201-238.

[14] Craven, Brent and Settles, Gary. "A Computational and Experimental Investigation of the Human Thermal Plume." *Journal of Fluids Engineering*, 128, no. 6 (2006): 1251-1258.

[15] Stamou, A, and I Katsiris. "Verification of a CFD model for indoor airflow and heat transfer." *Building and Environment*, 41, no. 9 (2006): 1171-1181.

[16] Cengel, Yunus A., and Afshin J. Ghajar. "Heating and Cooling for Buildings." In *Heat and Mass Transfer: Fundamentals and Applications*. 4th ed. New York: McGraw Hill Higher Education, 2011.

[17] Edwards, C., 2000, "Design Rules of Thumb for Naturally Ventilated Office Buildings in Canada," B.Sc. Thesis, University of Waterloo, 2000.

[18] Walker, R.R, and M.K White. "Single-sided natural ventilation--How deep an office?" *Building Services Engineering Research and Technology*, 13, no.4 (1992): 231-236.

[19] Baker, N. "Natural ventilation: cross ventilation." Natural ventilation: cross ventilation. http://www.architecture.com/RIBA/Aboutus/SustainabilityHub/Designstrategies/Air/1-2-1-3-naturalventilation-crossventilation.aspx (accessed July 28, 2014).

[20] Fluent Incorporated (2012). FLUENT 14.5 User's Guide. Fluent Inc., Lebanon, New Hampshire.

[21] Lariani, A, H Nesreddine, and N Galanis. "Numerical and Experimental Study of 3D Turbulent Airflow in a Full Scale Heated Ventilated Room." *Engineering Applications of Computational Fluid Mechanics,* 3, no. 1 (2009): 1-14.

[22] Ferziger J.H., Peric M. *Computational Methods for Fluid Dynamics*. 3rd ed, Springer, 2002.

[23] ASHRAE. (2003). ASHRAE Standard 62-2001, Ventilation for Acceptable Indoor Air Quality. Atlanta, GA.

[24] Etheridge, D., and Sandberg, M., *Building Ventilation: Theory and Measurement*,

England: John Wiley and Sons, 1996.

[25] Passe, Ulrike and Battaglia, Francine. "Designing Spaces for Natural Ventilation: An Architect's Guide." Taylor & Francis Group, 2015.

[26] "Estimating Appliance and Home Electronic Energy Use." Energy.gov. Accessed August 1, 2014. http://energy.gov/energysaver/articles/estimating-appliance-and-home-electronic-energy-use.

[27] "TV Power Consumption Guide." TV.com. Accessed August 12, 2014. http://www.tv.com/news/tv-power-consumption-guide-3153/.

[28] "How Many Watts Does an Electric Range Pull?" Home Guides. Accessed August 1, 2014. http://homeguides.sfgate.com/many-watts-electric-range-pull-87939.html.

[29] "Frank Lloyd Wright's Usonian Vision." About. Accessed August 1, 2014. http://architecture.about.com/od/franklloydwright/g/usonian.htm.

[30] "Windfinder.com - Wind and Weather Statistic Detroit City Airport." Windfinder.com. Accessed August 1, 2014. http://www.windfinder.com/windstats/windstatistic_detroit_city_airport.htm.

Appendix A: Symmetry in Small Structures

The small structures for cross ventilation and single-sided ventilation were designed to have symmetry in the z-axis. The symmetry of the results are best viewed by viewing flow patterns from above, shown in Figure A.1. A geometry was designed to have symmetry at the center of the z-axis and passive cooling was simulated using this geometry. The results are compared in Figure A.2 and Figure A.3. The flow patterns and temperature contours are similar in Figure A.2. The velocity profile at locations along the plane are shown in Figure A.3

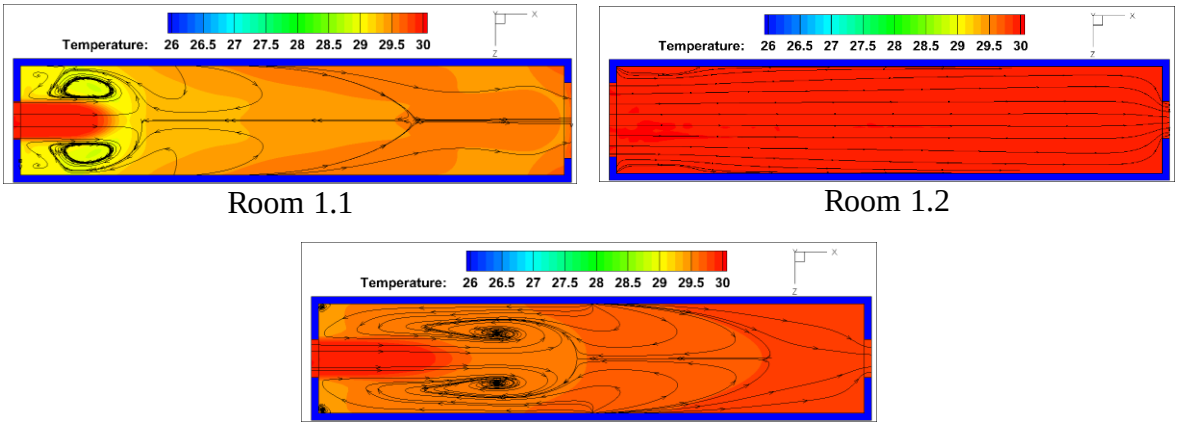

Room 1.1 Room 1.2

Room 1.3

Figure A.1. Symmetry in the z-axis viewed with streamlines and temperature contours for each room setup in cross-ventilation.

Full Geometry Half Geometry

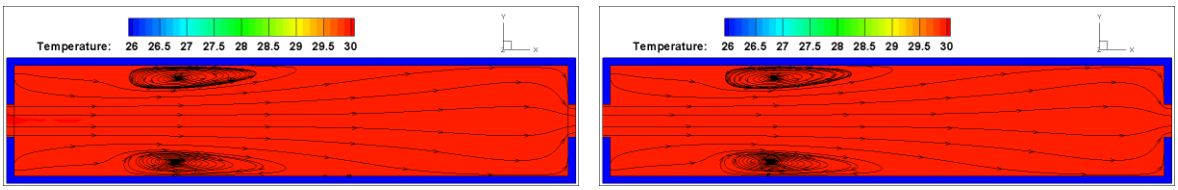

Figure A.2. Results shown with temperature contours and streamlines for the full geometry and a geometry with symmetry at the center of the z-axis.

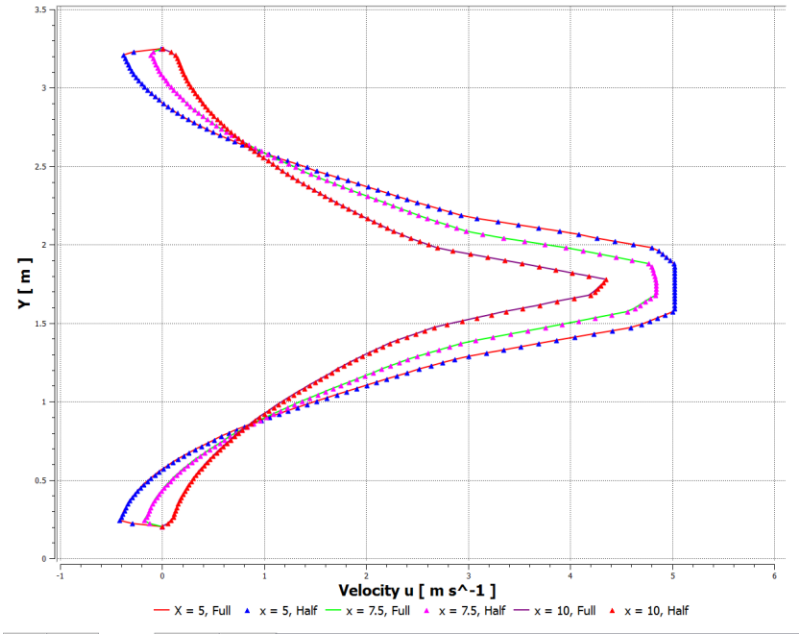

Figure A.3. Velocity profile at 5, 7.5, and 10 m along the midplane of the z-axis. The full geometry and half geometry profiles overlap.

Appendix B: Views of the Casa Giuliana Building

Accompanying the views of the Casa Giuliana apartment are views of the building. In Figure B.1. The front view, rear view, and a view of the corridors of the apartment building can be viewed. The deck doors are highlighted in blue, the rear wall and windows are highlighted in red, and the windows outside the space are shown in a bold black. The apartment modeled was the middle unit.

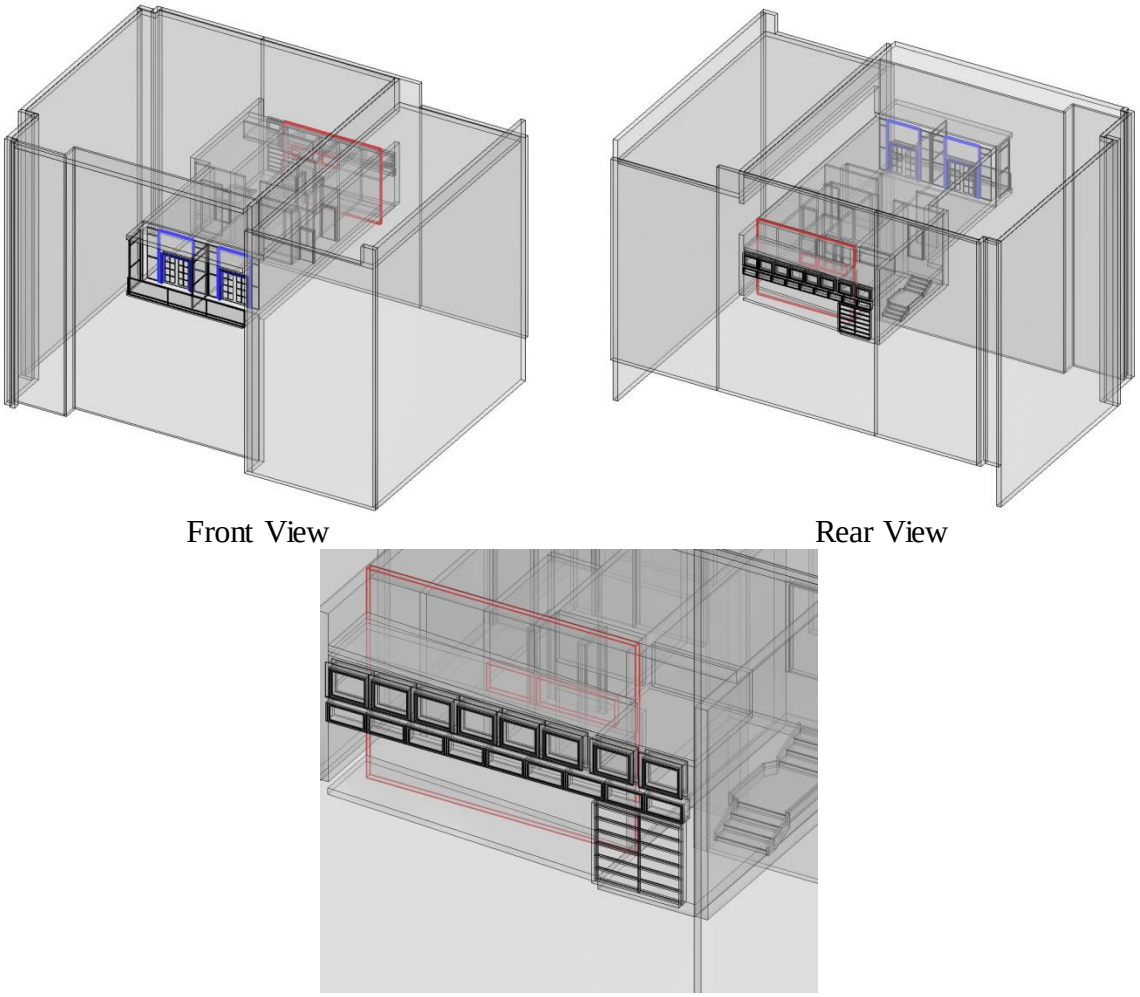

Front View

Rear View

Enlarged view of the corridors

Figure B.1. Views of the Casa Giuliana apartment building.